PERFORMANCE EVALUATION OF THE MIG GYRO FOR BALLISTIC MISSILE APPLICATION

R. B. Clark and B. H. Evans

29 JULY 1960

SPACE TECHNOLOGY LABORATORIES, INC.
P.O. Box 95001, Los Angeles 45, California

STL/TN-60-0000-09112

PERFORMANCE EVALUATION OF THE MIG GYRO FOR BALLISTIC MISSILE APPLICATIONS

by

R. B. Clark
B. H. Evans

29 July 1960

Approved L. K. Jensen
L. K. Jensen, Head
Inertial Components Laboratory

Approved G. A. Harter
G. A. Harter, Manager
Inertial Guidance Department

SPACE TECHNOLOGY LABORATORIES, INC.
P. O. Box 95001
Los Angeles 45, California

CLEARINGHOUSE FOR FEDERAL SCIENTIFIC AND TECHNICAL INFORMATION CFSTI
DOCUMENT MANAGEMENT BRANCH 410.11

LIMITATIONS IN REPRODUCTION QUALITY

ACCESSION # AD 607152

☑ 1. WE REGRET THAT LEGIBILITY OF THIS DOCUMENT IS IN PART UNSATISFACTORY. REPRODUCTION HAS BEEN MADE FROM BEST AVAILABLE COPY.

☐ 2. A PORTION OF THE ORIGINAL DOCUMENT CONTAINS FINE DETAIL WHICH MAY MAKE READING OF PHOTOCOPY DIFFICULT.

☐ 3. THE ORIGINAL DOCUMENT CONTAINS COLOR, BUT DISTRIBUTION COPIES ARE AVAILABLE IN BLACK-AND-WHITE REPRODUCTION ONLY.

☐ 4. THE INITIAL DISTRIBUTION COPIES CONTAIN COLOR WHICH WILL BE SHOWN IN BLACK-AND-WHITE WHEN IT IS NECESSARY TO REPRINT.

☐ 5. LIMITED SUPPLY ON HAND: WHEN EXHAUSTED, DOCUMENT WILL BE AVAILABLE IN MICROFICHE ONLY.

☐ 6. LIMITED SUPPLY ON HAND: WHEN EXHAUSTED DOCUMENT WILL NOT BE AVAILABLE.

☐ 7. DOCUMENT IS AVAILABLE IN MICROFICHE ONLY.

☐ 8. DOCUMENT AVAILABLE ON LOAN FROM CFSTI (TT DOCUMENTS ONLY).

☐ 9.

PROCESSOR: eah

TSL-107-10/64

ABSTRACT

This report describes a series of tests performed on two Minneapolis-Honeywell MIG gyros. Performance of gyros during the tests is given in detail, and the philosophy, procedures, and merits of each type of test are discussed. The test program had two objectives: to evaluate the gyros themselves, and to study and compare the various types of tests used in the program.

Both of the tested gyros performed within the manufacturer's specifications during the entire program, with the exception of a mass shift occurring in one gyro as a result of excessive vibration applied during a test. Results of different tests of the same gyro characteristics correlated, in most cases, within the expected consistency of gyro performance, indicating satisfactory reliability of the test procedures and equipment.

CONTENTS

ILLUSTRATIONS

ILLUSTRATIONS (Continued)

TABLES

I. INTRODUCTION

This report describes an extensive series of tests carried out on two Miniature Integrating Gyros (MIG's) and discusses the results of the tests. The test gyros, one of which is shown in Figure 1, were purchased from Minneapolis-Honeywell (M-H) and tested at STL with a dual purpose in mind. One purpose was to study the methodology and procedures of gyro testing, while the other purpose was to evaluate the performance of the two MIG's under test, with particular reference to the application of this model to ballistic missiles. The model designation of the two gyros tested was GG49D1; serial numbers were K-13 and K-14.

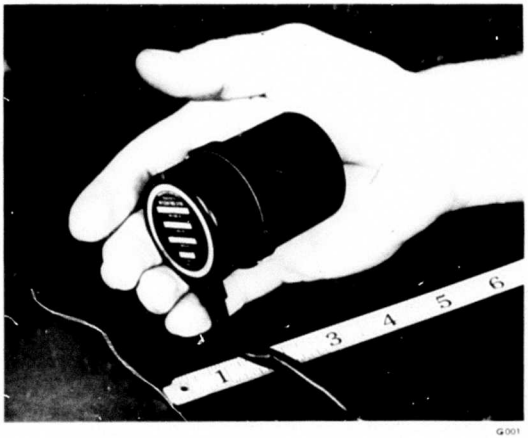

Figure 1. Photograph of GG49D1 Miniature Integrating Gyro.

The tests described in this report constituted a major part of a general study of gyro testing methodology conducted at STL.* This study compared the validity of different test procedures by applying them to the same gyro

*This study is included in the Inertial Components Studies laboratory project, Project Plan 165-18, supported under AFBMD Contract AF 04(647)-309.

and comparing the results. One objective of the study was to develop optimum and standard test procedures for the evaluation of gyros to be used in the guidance systems of ballistic missiles.

The work described in this report was limited to the study of test procedures for the evaluation of precision gyros used to control the stable platforms of inertial measurement units. More specifically, it consisted of laboratory-type tests designed primarily to measure drift rates as a function of time and acceleration. The gyros tested (Minneapolis-Honeywell Type GG-49) are considered representative of the type of gyro used for stable platform control.

In addition to presenting detailed results of tests performed, this report discusses the correlations obtained between tests, and presents the significant advantages and disadvantages of each of the various tests.

II. BACKGROUND

The selection of gyroscopic sensing instruments for use in inertial guidance systems is based on the results of performance tests. It is evident from industry surveys, however, that there are wide variations both in the procedures for such performance tests and in the methods of evaluating the resulting data. There is also considerable uncertainty regarding the interpretations to be attached to the data obtained, because significantly different results have been obtained by using different procedures for the same gyro.

For these reasons, it has been difficult to make reliable comparisons between gyros from different sources, since gyros from different suppliers are not tested in a uniform manner. It follows that there is a general lack of confidence in performance information presented by the various manufacturers. This study is part of an effort to establish generally acceptable uniform performance evaluation procedures and to make possible valid comparisons of data from different tests.

III. SUMMARY AND CONCLUSIONS

A. Testing Program

The series of tests made on the two gyros measured drift rates as a function of acceleration and time. Drift rates were measured in closed-loop servos, using both servo table feedback and torquer feedback The torquer feedback tests were made with both earth-fixed and tumbling attitude configurations. The cogging test was used to measure short-term repeatability, and the servo test to measure long-term repeatability. Torque generator characteristics were measured by means of a servo table, and extensive vibration tests were made to measure drift rates proportional to the square of the acceleration. Tests designed to measure the transfer function, the dynamics, or other similiar characteristics of the gyros were not conducted.

B. Gyro Performance

A summary of the results of the testing program is shown in Table 1. Examination of the table reveals that both gyros performed within the manufacturer's specification when received and that they continued to do so throughout the test program, with the exception of a large mass shift in K-13 resulting directly from excessive vibration applied during a test.

The results shown in Table 1 are averages of gyro performance over the entire testing period. Day-to day variations in drift coefficients were as high as 0.2 deg/hr for fixed drifts and 0.1 deg/hr-g for unbalance drifts when the gyro was not allowed to cool. When the gyro was cooled to room temperature, the variation increased by a factor of two or three. Some observed irregularities in performance were attributed to float pivot friction and to spin-axis mass shifts.

Table 1. Average Performance Characteristics for 200-Hour Running Time.

Characteristic	Manufacturer's Specification	Gyro K-13	Gyro K-14
Fixed Drift, deg/hr	2.0 max	0.5	1.0
Unbalance, $\frac{\text{deg/hr}}{\text{g}}$	2.0 max	3.5	0.5
Compliance, $\frac{\text{deg/hr}}{\text{g}^2}$	0.02 max	0.020	0.018
Torquer Linearity, percent full scale	0.5	0.4	0.25

C. Correlation of Test Results

Results of the various tests correlated, in most cases, within the anticipated consistency of gyro performance. However, there appeared to be a systematic difference in measurements of the fixed-drift term corresponding to the two sets of electronics used to excite the gyro. This difference, amounting to approximately 0.5 deg/hr, serves to illustrate the importance of careful application of excitation equipment.

D. Significance of the Individual Tests

1. Gimbal Mass Unbalance Test*

This test proved useful as a quick and simple measure of the fixed and unbalance torques acting on the float. Its accuracy may be limited by earth's rate input to the gyro, but this limitation is not severe

*Detailed test descriptions are presented in Appendixes D through H.

enough to degrade the usefulness of the test for quick production determinations, such as are required for balancing the float.

2. Tumbling Test

The continuous tumbling test demonstrated the possibility of accurate, automatic, and continuous drift coefficient measurement, minimizing the influence of human factors and yielding a complete set of data capable of reliable interpretation. Disadvantages are that the test time is relatively long (approximately 2 hours) and that the float suspension is subjected to abnormal loadings. These drawbacks are not serious and may be circumvented by making a discontinuous (or step) tumbling test. The performance irregularities mentioned in B above appeared in both continuous and discontinuous tumbling tests, causing a degradation of accuracy and confidence in the determination of the drift coefficients. They appeared as deviations from the normal sinusoidal characteristics of a continuous tumbling test or as increased "settling times" in the discontinuous tests.

3. Servo and Cogging Tests

These tests were found useful for determinations of the stability or uncertainty of the gyro because they provide the most precise measurement of angular rates and most closely simulate a platform application of the gyro. The cogging test is particularly satisfactory for measuring the short-term (minutes) uncertainties of the gyro and the servo test for measuring the long-term (days) uncertainties. However, neither test is satisfactory for coefficient determination since the 24-hour servo test consumes an excessive amount of time and the cogging test requires excessive manipulation of the gyro or test turntable.

4. Vibration Tests

Vibration tests were used with unexpected success, to measure compliances thus demonstrating the usefulness of vibration as a tool for evaluating precision gyros. The work done on this part of the

testing program is considered an advance of the state of the art. It made possible compliance coefficient measurements with uncertainties of $0.0015 \frac{\text{deg/hr}}{g^2}$.

5. Torquer Linearity Tests

The measurements of torquer linearity demonstrated the feasibility of making these measurements with an accuracy of 0.01 percent.

IV. THEORY AND NOMENCLATURE

The Minneapolis-Honeywell MIG gyro GG-49 is a floated, single-degree-of-freedom (SDF), rate integrating gyro. This type of gyro, one of the most widely used today, was originally developed under the direction of Dr. C. S. Draper at the MIT Instrumentation Laboratory some 15 years ago. Since then, it has been manufactured in production quantities by several companies.

The theory of the SDF gyro has been extensively described in the literature, and will be only summarily described here. Briefly, the SDF gyro consists of a spinning rotor mounted in a single gimbal whose pivot axis is perpendicular to the spin axis of the rotor. Figure 2 shows a cutaway view of the construction. The rotor, supported by ball bearings and hermetically sealed in a float which constitutes part of the gimbal, is driven by a polyphase electric motor. The float is surrounded by, and neutrally buoyant in, a heavy viscous fluid contained in the case of the instrument. The fluid serves the double purpose of supporting the float against acceleration, thus relieving the loading on the pivot bearings, and applying viscous damping torques to the gimbal. The output signal of the gyro is generated by a transducer which measures the rotation of the gimbal relative to the case.

Performance of the SDF gyro is described by the equation of motion of the gimbal relative to the case. A right-handed coordinate system is defined, fixed to the float, with axes OA, SA, and IA. OA, the output

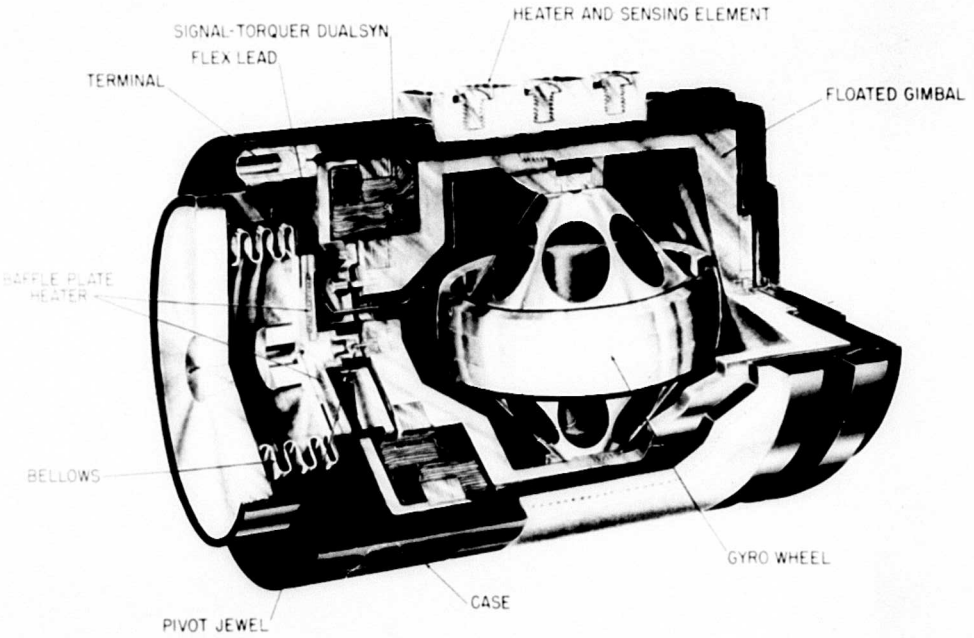

Figure 2. Cutaway View of Miniature Integrating Gyroscope.

axis, is the pivot axis of the gimbal; SA is the direction of the rotor spin axis; and IA, the input axis, is orthogonal to SA and OA. The gyro is principally sensitive to rotations about IA.

Since the relative motion of gimbal and case is confined to rotations about OA, the equation of motion may be written simply by summing the torques acting on the float about OA:

$$\Sigma T_{OA} = J\ddot{\theta}_{OA} + C\dot{\theta}_{OA} + k\theta_{OA} \qquad (1)$$

where

J is the float inertia

C is the viscous damping coefficient

k is the elastic restraint coefficient

T_{OA} is the torque acting on the float about OA

θ_{OA} is the angular deflection of the float.

T_{OA} includes the desired or signal torques, as well as the unwanted or drift torques. Signal torques consist of gyroscopic torques resulting from the angular rotation of the case about its input axis plus controlled torques applied to the float through an electromagnetic torque generator. Drift torques are of four kinds: 1) constant torques independent of acceleration, e.g., residual torques from the pick-off transducer and spin motor power leads; 2) unbalance torques proportional to the instantaneous linear acceleration of the gyro, resulting from lack of coincidence of the float center of gravity, center of buoyancy, and pivot axis; 3) compliance torques proportional to the product of accelerations along the principal axes of the float, resulting from the anisoelasticity of the gimbal structure; and 4) uncertainty torques resulting from other torques not specifically mentioned plus fluctuating components of any or all of the torques listed. The torques not specifically mentioned would include cross coupling torques that result from the rotation about the output and spin axes. The

fluctuating torques, also called "random" or "residual" torques, include torques due to pivot friction variation, mass shift effects, flotation fluid convection currents, etc.

Although Equation (1) may be expanded to provide a more complete dynamic response of the SDF gyro, for purposes of this report, which is concerned only with very small and essentially steady-state angular inputs, the component of gyroscopic torque about the output axis $(d\vec{H}/dt)_{OA}$ may be simplified to $\omega_{IA}H$, where ω_{IA} is the angular velocity of the gyro case about the gyro input axis and H is the angular momentum of the rotor. With good gyro design, this consideration also makes it possible to neglect the float inertia J and to relegate the elastic restraint coefficient k to a second-order effect.

Expanding Equation (1) to include all disturbance torques, rearranging, and expressing the torque coefficients in terms of their equivalent rate input yields

$$\dot{\theta}_{OA} = \frac{H}{C}\left[R + (U_I a_S - U_S a_I) + 2Ka_S a_I + \delta\omega - k\theta_{OA} + K_\omega i_c + \omega_{IA}\right] \quad (2)$$

where

R = fixed (constant) drift coefficient, deg/hr

U_I, U_S = unbalance drift coefficients along IA and SA respectively $\frac{\text{deg/hr}}{g}$

K = compliance drift coefficient * $\frac{\text{deg/hr}}{g^2}$

k = elastic restraint torque gradient, $\frac{\text{deg/hr}}{\text{deg}}$

K_ω = torque generator scale factor, $\frac{\text{deg/hr}}{\text{ma}}$

---

*K, as defined here, is the usual compliance coefficient. Specifically, $2K = m^2(K_{SS} - K_{II})$ where m is the equivalent mass of the compliant portion of the float, and K_{SS} and K_{II} are the principal compliance constants of the gimbal structure.

i_c = electrical input control current to the torque generator, ma

$\delta\omega$ = "random" drift rate of the gyro, deg/hr

ω_{IA} = input angular rate about IA, deg/hr

a_I, a_S = components of linear acceleration along IA and SA respectively, g

The relation of these terms to the torque terms listed previously is obvious. Since it is generally desirable to operate the gyro at null in order to eliminate the elastic restraint term as well as a number of other second-order effects, both θ_{OA} and $\dot{\theta}_{OA}$ must be zero. In testing they are made zero by a closed-loop servo that adjusts i_c or ω_{IA} to give a zero gyro output, i.e., $\dot{\theta}_{OA} = 0$. Either i_c or ω_{IA} is thus made equal and opposite to the total drift rate $-\omega_{IO}$ of the gyro, where

$$-\omega_{IO} = R + (U_I a_S - U_S a_I) + 2Ka_S a_I + \delta\omega \quad . \qquad (3)$$

The tests are called "torquer feedback" or "torquer servo" and "servo feedback" tests, respectively.

V. DETAILED TEST RESULTS

A. Gyro Performance

The principal result of the testing program with regard to the gyros tested was, as noted in Section III, the determination that both units met the manufacturer's specifications. Gyro K-14 continued to do so after more than 200 hours of testing, including 2 hours of vibration. K-13 exhibited high mass unbalance and stiction, but was still operating after 300 hours of spin-motor running time, including 3 hours of vibration. The departure of K-13 from specification occurred after about 1 hour of rather severe vibration testing on 18 and 19 August 1959.

History of the drift coefficients is presented graphically in Figures 3 and 4. Complete tabulations will be found in Appendix A. The data shown cover numerous cool-downs to room temperature, exposure to vibration, and ordinary handling. Figure 5 shows the consistency of coefficient determination when special precautions were taken, such as maintaining the temperature of the gyro and minimizing handling.

From the information presented in Figure 5, it can be seen that day-to-day variations in drift coefficients were as high as 0.20 deg/hr for reaction torque and 0.10 deg/hr for mass unbalance when the gyro was not allowed to cool. Under these conditions, the rms variation, on the average, was of the order of 0.1 deg/hr, while complete cool-downs raised this average variation to approximately 0.3 deg/hr.

Variations in reaction torque with gyro attitude* approached 0.10 deg/hr, with an average rms value of 0.04 deg/hr. The cogging tests yielded maximum and rms values of 0.3 and 0.1 deg/hr, respectively, but these values were disregarded because of the possibility of a testing error. It seems probable that any changes in the reaction torque result from variation in position of the gimbal within the pivot-to-jewel clearance, causing a magnetic gap variation in the dualsyn (pickoff-torquer combination).

Torque-generator scale factor and linearity of both gyros were within the value specified in the JPL specification (Reference 14) to which they were purchased. The specified linearity is ± 1 deg/hr from 0 to 200 deg/hr, and ± 10 deg/hr from 200 to 2000 deg/hr. The Minneapolis-Honeywell specification (Reference 3) calls for ± 0.5 percent of the actual unit scale factor over a range of ± 2000 deg/hr, and K-13 did not meet this requirement. Maximum linearity error found for K-13 was 0.77 percent, at approximately 700 deg/hr. Appendix E shows that the torque-generator error is always of the same sign, indicating that it is not principally a function of magnetic nonlinearities. The mechanism creating

*See Table 6 for details.

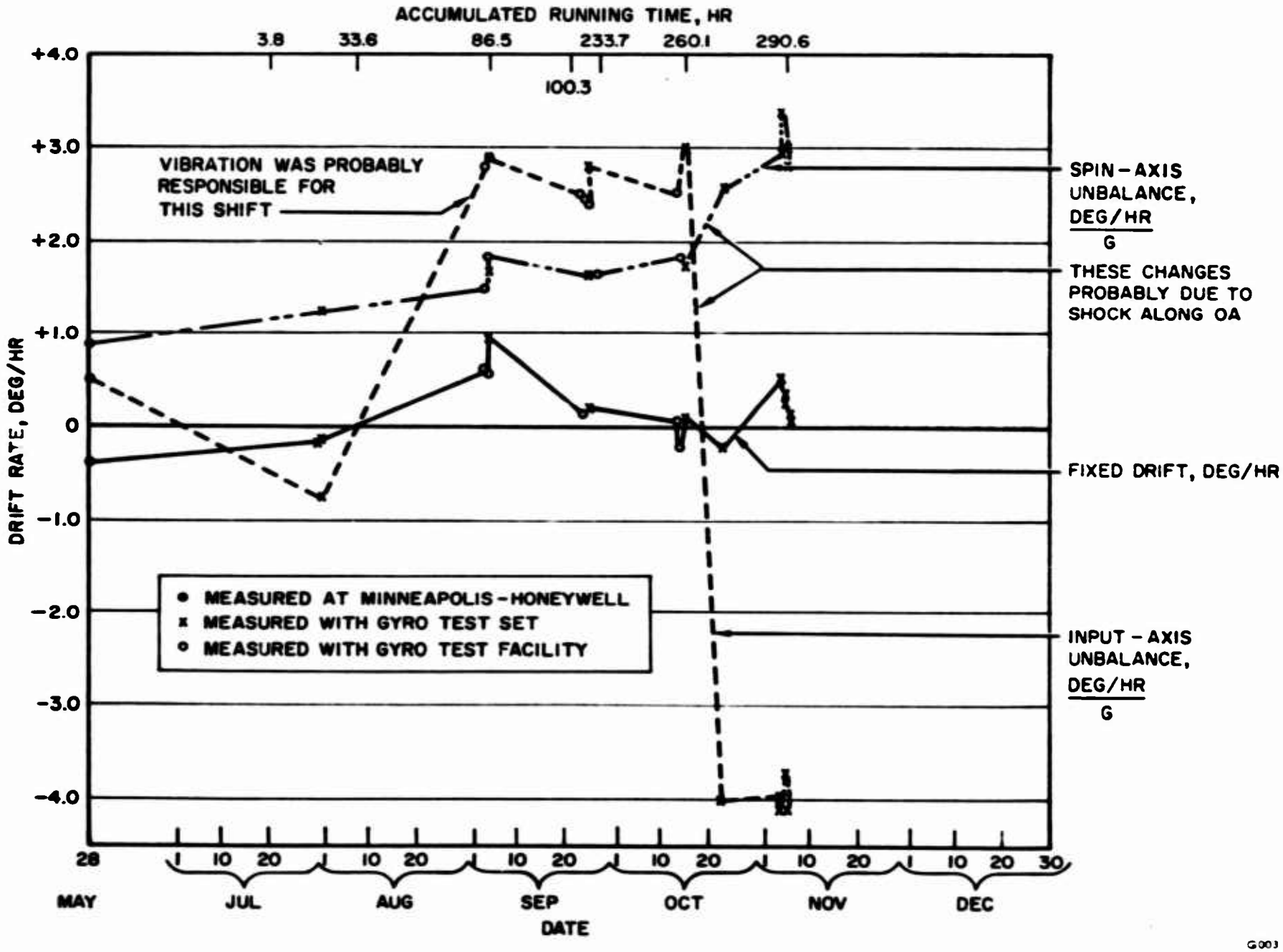

Figure 3. Performance Summary of Gyro K-13.

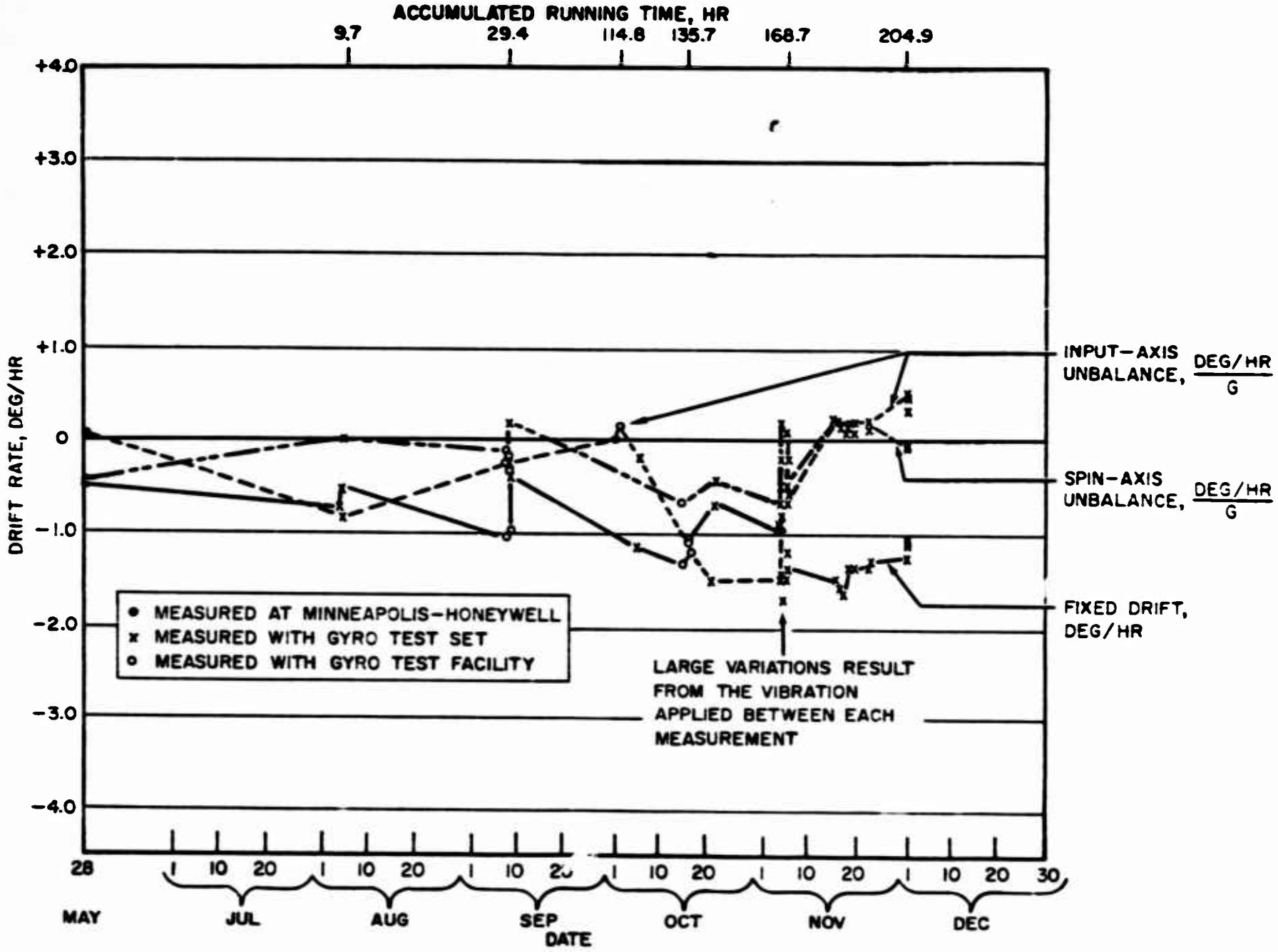

Figure 4. Performance Summary of Gyro K-14.

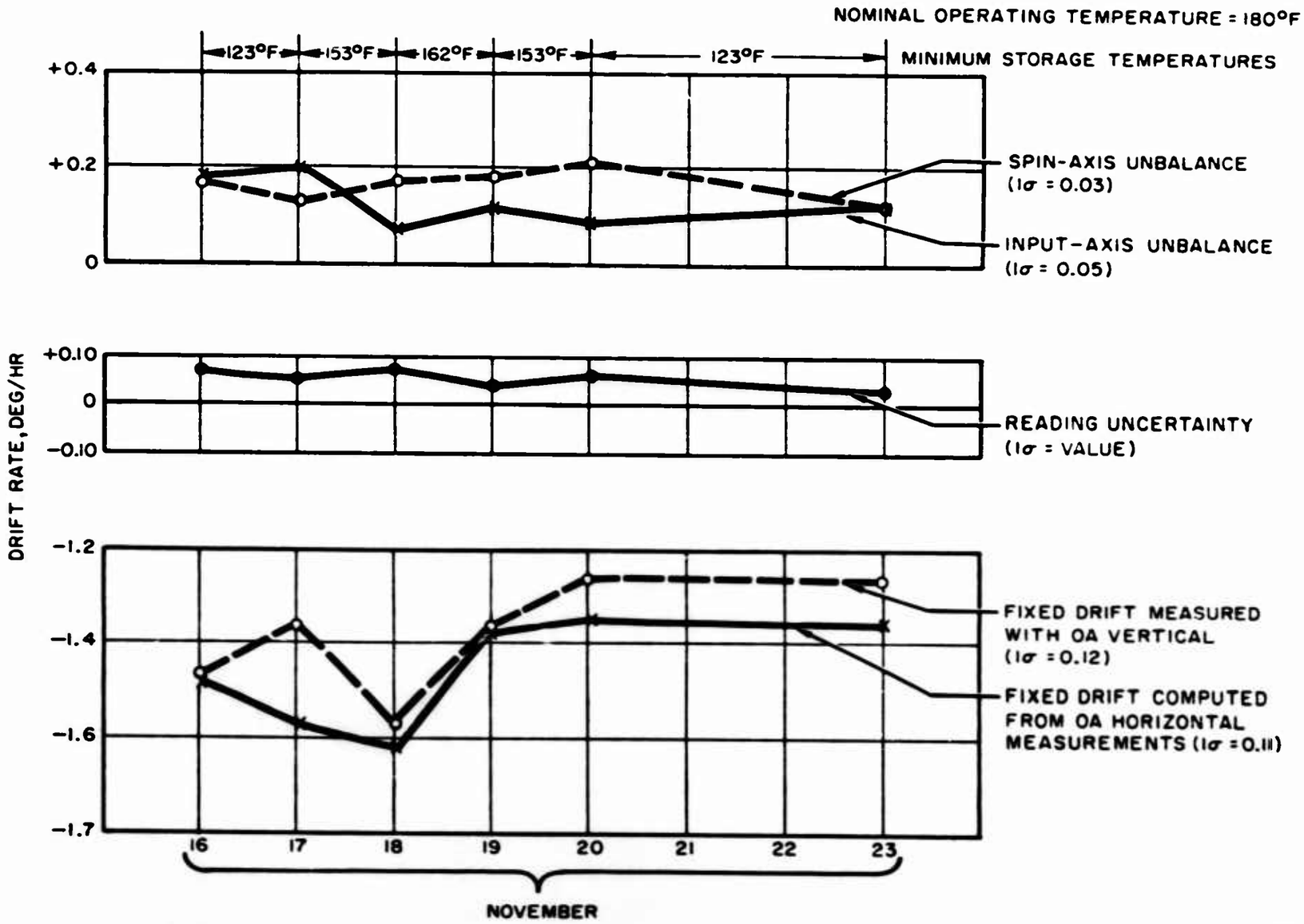

Figure 5. Coefficient Stability of Gyro K-14. Gyro maintained warm between measurements.

this linearity error is not understood; it may be induced circulating currents or some systematic phenomenon associated with torquer or gimbal torques. The test of torquer linearity was a severe one because various techniques, excitations, and circuits were used during the tests. The test variations account for some of the changing characteristics of the curves, and contribute to the uncertainty concerning the mechanism which is causing torquer errors. Additional testing would provide a better understanding of the torquer error and might possibly identify the responsible mechanism.

Results of random drift determination in six cogging tests, each test at a different gyro attitude, are summarized in Table 2. Note that the gyro performs fairly well in this test, which is representative of its application in stable platforms. Each entry in the table is the rms variation of the drift rates, based on fifteen 1-degree cogs.

Table 2. $\delta\omega_{rms}$ for Various Orientations in Cogging Test

Gyro Orientation		$\delta\omega_{rms}$, deg/hr	
		K-13	K-14
Output axis vertical	Up	0.009	0.010
	Down	0.019	0.004
Spin axis vertical	Up	0.011	0.006
	Down	0.012	0.023
Input axis vertical	Up	0.038	0.033
	Down	0.028	0.052

Table 2 indicates that unbalance uncertainties are the major problem, particularly along the spin axis. It should be noted that the test is sensitive to spin axis unbalance when the input axis is vertical. The increase in settling times appearing in stepwise tumbling tests as the spin axis approaches the horizontal, and the erratic data of continuous tumbling tests under the same conditions, reinforce this conclusion.

The combined $\delta\omega_{rms}$ for all runs was 0.022 deg/hr for K-13 and 0.027 deg/hr for K-14. These values are derived from 90 cogs for each gyro, 15 cogs in each of the six attitudes. Measurements were made over a 2-day period.

This summary of the performance of the two GG49D1 gyros would not be complete without adding that they were completely dependable in operation, simple to use, straightforward in their operation, and capable of withstanding considerable abuse.

B. Correlation of Test Results

The inertial components study program at STL has as one of its objectives the comparison and correlation of results from various tests. The series of tests described in this report was not particularly fruitful for correlation studies, chiefly because the uncertainties in the gyros were of the same order of magnitude as the expected test correlation.

Had the primary objective of the tests been to study correlation rather than testing methodology, it would have been possible to obtain results more useful for this purpose. The poor correlations appearing on some tests can be attributed to the new and untried test equipment, the lack of tried and proven test philosophy and techniques, and in general the lack of that knowledge which can be acquired only through experience in experimental work. Consideration is being given to additional tests which would stress the correlation aspect of the study.

Table 3 through 8 present, in summary form, the correlation of results from the various tests performed. Table 3 shows the correlation of drift measurements made at M-H and those made at STL. R and U_S correlate within the performance uncertainty to be expected under the conditions prevailing between tests. While the change in U_I is greater in both gyros than might be expected, it is known that large changes in U_I occurred in the earlier MIG gyros when they were subjected to vibration and cool-down at Minneapolis-Honeywell. It appears

Table 3. Comparison of M-H and STL Drift Coefficient Measurements.

Gyro	K-13			K-14		
Conditions Between Tests	2 months -- shipped to Los Angeles; 8 cool-downs			2 months -- shipped to Los Angeles; 2 cool-downs		
Test	M-H	STL	Change	M-H	STL	Change
Date	5/28	7/31		5/28	8/5	
R, deg/hr	-0.38	-0.13	+0.25	-0.51	-0.53	-0.02
U_I, $\frac{deg/hr}{g}$	+0.49	-0.72	-1.21	+0.06	-0.64	-0.70
U_S, $\frac{deg/hr}{g}$	+0.92	+1.26	+0.34	-0.02	+0.02	+0.47

Table 4. Comparison of Drift Coefficient Measurements From Tumbling and Mass Unbalance Tests.

Gyro	K-13			K-14		
Conditions Between Tests	3 hr of running -- moved to next lab--no cool down			3 hr of running -- moved to next lab--no cool down		
Test	Tumbling	Mass unbalance	Difference	Tumbling	Mass unbalance	Difference
Date	9/4	9/4		9/9	9/9	
R, deg/hr	+0.55	+0.93	+0.38	-1.01	-0.39	+0.62
U_I, $\frac{deg/hr}{g}$	+2.92	+2.88	+0.04	-0.35	-0.27	+0.08
U_S, $\frac{deg/hr}{g}$	+1.85	+1.67	-0.18	-0.17	+0.19	+0.36

Table 5. Comparison of Drift Coefficient Measurements From Cogging and Mass Unbalance Tests.

Gyro	K-13			K-14		
Conditions Between Tests	1 hr -- moved to next lab-- no cool-downs			5 days -- 20-hr running time -- moved to next lab -- 1 cool-down		
Test	Cogging	Mass unbalance	Difference	Cogging	Mass unbalance	Difference
Date	10/13 to 10/14	10/15		10/15 to 10/16	10/21	
R, deg/hr	-0.21	+0.10	+0.31	-1.30	-0.70	+0.60
U_I, $\frac{deg/hr}{g}$	+2.55	+3.00	+0.45	-1.13	-1.62	-0.49
U_S, $\frac{deg/hr}{g}$	+1.83	+1.74	-0.09	-0.68	-0.46	+0.22

Table 6. Reaction Torque Variation With Gyro Attitude, as Measured in Cogging Tests.

Table Axis Orientation	Gyro Orientation	Reaction Torque, deg/hr	
		K-13	K-14
Horizontal	OA up	+0.061	-1.046
	OA down	+0.052	-1.055
	SA vertical	+0.091	-1.129
	Average (of above readings)	+0.068	-1.073
Vertical	IA Vertical	-0.208	-1.295
Change (table axis horizontal to vertical)		-0.276	-0.222

Table 7. Comparison of Compliance Measurements From Tumbling and Vibration Tests.

Gyro	K-13		K-14	
Test	Tumbling	Vibration	Tumbling	Vibration
Date	9/4	9/21	9/9	11/6
K, $\frac{deg/hr}{g^2}$	0.22	0.02	0.03	0.018

Table 8. Comparison of M-H and STL Cogging Test Measurements of $\delta\omega_{rms}$ (IA Vertical).

Gyro	K-13			K-14		
Conditions Between Tests	5 months -- 260 hr of operation -- many cool-downs -- much handling			5 months -- 135 hr of operation -- many cool-downs -- much handling		
Test	M-H	STL	Change	M-H	STL	Change
Date	5/28	10/14		5/28	10/15	
$\delta\omega_{rms}$, deg/hr	0.027	0.038	+0.011	0.012	0.033	+0.019

probable that K-13 and K-14 were from this earlier group. Such an assumption is borne out by the STL tests, which consistently show larger gross changes in U_I than in U_S. It is noted, without explanation, that the unbalance shifts in both gyros were in the same direction and of roughly the same magnitude.

Table 4 and 5 show a comparison of drift coefficients derived from the tumbling and mass unbalance tests and from cogging and mass unbalance tests, respectively. The comparison is of particular interest because in each case, the tests used completely different sets of electronics for excitation. The same electronics was used for tumbling and cogging; a different set was used for mass unbalance. The differences between these two sets of equipment are noted in detail in Appendix B.

Both comparisons reveal, for each gyro, a similar shift in R in excess of the expected uncertainty. Such shifts could be caused by the electronics (e.g., by differences in loading or driving impedances, noise rectification effects, or bias shifts), by misalignment of the gyro to the table, or, in the tumbling test, by side loading of the pivots. Since nearly identical shifts occurred for both tumbling and cogging tests, it is concluded that a basic difference in electronics is the most probable cause.

Changes in U_S and U_I between the tests were either negligibly small or of the opposite sign, indicating a lack of systematic error in the measurement of unbalance coefficients caused by differences in the electronics.

Four independent values of R were obtained for each series of cogging tests, with considerable variation among the four values. The value of R shown in Table 5 was selected from those obtained with the input axis vertical, because the greatest confidence can be placed in this value and because a comparison of test results with test conditions indicated the possibility of a testing error. This possibility is presented in Table 6 which

shows the changes in reaction torque with gyro attitude during the cogging test. The systematic changes indicated between the table axis vertical and table axis horizontal tests could be accounted for by assuming that the table axis was misaligned by 1 to 1-1/2 degrees from either the vertical or horizontal position during the tests.

Table 7 shows the results of compliance determination from the tumbling test and the vibration test for both gyros. It is not possible to draw any inferences from a comparison of the results, since uncertainties in gyro performance have completely masked the low-valued compliance coefficient during the tumbling tests. However, vibration tests showed consistent results for both gyros.

The short-term random drift $\delta\omega_{rms}$ for each gyro was determined separately by Minneapolis-Honeywell and STL during cogging tests. A comparison of the results obtained by Minneapolis-Honeywell and STL appears in Table 8. All data is based on fifteen 1-degree cogs, with the input axis up. The decrease in repeatability is not surprising in view of the amount of running time, handling, and number of cool-downs occurring between the two tests.

In summary, it may be said that variations in gyro performance make it difficult to make valid correlations of results from one type of test to another. Test routines established for the specific purpose of correlating test results would eliminate certain ambiguities appearing in the above data.

VI EVALUATION OF THE TEST PROGRAM

A. Criteria for Test Evaluation

The following criteria may be used to judge the usefulness of a gyro test:

1) Importance of the performance characteristics measured

2) Accuracy of the measurement

3) Number of performance characteristics measured

4) Ability to separate the measured characteristics

5) Correspondence of test conditions to operational conditions

6) Ease and simplicity of test setup and procedure

7) Simplicity of data reduction and confidence in reduced data

8) Time required for equipment and personnel

9) Cost and reliability of required test equipment

10) Effect of test on component performance.

These various criteria must be assigned varying weights, depending on the purpose of the test (i.e., design evaluation, production, or acceptance). Although detailed numerical weights and ratings were not attempted, the above criteria served as a guide in judging the usefulness of the various tests, as discussed below. The procedures followed were largely those prescribed in Reference 1.*

B. Preliminary Tests

Continuity and impedance checks, along with other quality-control functions, are a necessary part of any complete production or acceptance test program, although they are perhaps not of great importance for the evaluation of performance characteristics. Polarity, phasing, and alignment tests are simple and basic to any test program, since no confidence can be placed in the subsequent data unless these parameters are established.

C. Bench Drift Tests

The bench drift tests followed the specifications of Reference 2. They constitute a major portion of the performance testing performed by Minneapolis-Honeywell on GG49 gyros. All the bench drift tests are torquer servo mode tests.

*References are listed at the end of Appendix H.

1. Null Repeatability

This is the least valuable of the bench drift tests. It provides a measure of the gyro's performance as a gyrocompass (which can easily be determined from other data) and a determination of spin-axis alignment much inferior to that described in Appendix C, Section II-C.

2. Gimbal Mass Unbalance

This is the most important of the bench drift tests, providing quick and simple determinations of reaction torque and mass unbalance along each axis. In addition, a measure of randomness is provided, depending on how the data is taken. This test is adequate for acceptance testing of drift coefficients for the less-accurate inertial platform gyros, and is extremely useful for making the final trim adjustments on all gyros.

A basic limitation of this test is its lack of resolution. The scale required for analog readout instrumentation is dictated by the vertical component of earth's rate, a signal much larger than the drift coefficient the test is to measure. This circumstance restricts the resolution of the measurement. Another limitation of this test is its dependence on the accuracy of the torque generator scale factor. An input signal much larger than the drift coefficient produces a proportionately larger error in the measurement of that coefficient.

As a tool for evaluation, the mass unbalance test may be overshadowed by the more sophisticated testing techniques, but it retains great advantages in speed and simplicity.

3. Torquer Calibration Test

This test is useful for a simple determination of the rate sensitivity of a gyro, using known components of earth's rate for an input. The accuracy is limited only by the randomness of the gyro. The torquer linearity test, described in detail in Appendix E, is preferable if high accuracy is required.

4. Reaction Torque Test

This test determines R with OA vertical, and while it is useful as a simple determination of the reaction torque, it must be kept in mind that the reaction torque measured in this way may vary from that measured with OA horizontal.

5. Elastic Restraint Test

This test is also conducted with OA vertical, and is useful for a quick and crude determination of elastic restraint. This characteristic need not be determined unless the gyro is to be operated with the gimbal very far from null.

In conclusion, it is felt that the bench drift tests described are useful for production tests requiring quick, but not precise, measurements of gyro performance.

D. Tumbling Tests

The tumbling test provided much interesting and unlooked-for information, but failed to provide a significant improvement over the much less complicated gimbal mass unbalance test with regard to measurement of drift coefficients. On the gyros tested in this program, it failed completely as a means of measuring anisoelastic coefficients because of the low value of the anisoelastic coefficient for the GG49 gyro. On larger gyros such as the MIT 2FBG, where the anisoelastic coefficient is more nearly comparable in magnitude to the mass unbalance and reaction torques, the tumbling test may provide a meaningful measurement of K.

Despite the complexity of the required equipment and data reduction, and the length of time required for the test, the tumbling test can be adapted to fairly large-scale production testing. It is automatic in its operation, requiring relatively little manpower expenditure, and the resulting data can be reduced by computer, thus further reducing man-hour requirements. AC Spark Plug has demonstrated the practicality of a production tumbling test by using such a test as the principal element in its 10FG production testing program for the Thor missile.

In the STL test program, the difficulty of carrying out accurate tumbling tests on the MIG gyro resulted chiefly from the failure of the gyro to conform to its ideal performance characteristics; i.e., the performance could not be adequately explained by the drift coefficients alone. These uncertainties made it difficult to measure accurately the predictable drift coefficients. It seems probable that they resulted from pivot friction, mass unbalance uncertainties (perhaps mostly from spin-bearing retainers), and reaction torque variations. It is expected that for gyros of greater precision the tumbling test will show a significant increase in accuracy over the mass unbalance test.

The stepwise tumbling tests described in Appendix F were developed in an effort to reduce the pivot friction torque and at the same time to reduce the time required for tumbling tests. The stepwise test is a combination of the gimbal mass unbalance test and the standard MIT-style tumbling test, and retains many of the advantages of both.

Many variations are possible with the stepwise tumbling tests, which can be looked upon as a new tool with characteristics somewhat different from those of the usual tumbling test. For example, a new and unexplained characteristic noted during stepwise tumbling was the variation of settling time with gyro attitude. (See Appendix F for detailed discussion.) The stepwise test, like the regular tumbling test, can be adapted to automatic operation and machine data reduction.

A serious drawback to any kind of tumbling test, and to servo tests as well, is the necessity of performing a harmonic analysis on the data in order to extract useful information. Much time has been spent at STL in programming the IBM 709 computer to perform this analysis, but the program had not been completed at the time of the test program described in this report. All data presented here was reduced by hand, with the use of desk calculators.

In general it is felt that tumbling type tests should be used as production tests for final and precise determination of detectable drift coefficients in precision gyros as is done at AC Spark Plug.

E. Servo and Cogging Tests

The servo and cogging tests are grouped for purposes of discussion, since both utilize the same equipment and operate the gyro in the same mode. The primary information obtained is the random drift rate, although it is possible to obtain drift coefficients by making several runs with the table and gyro in various orientations. Such a technique of obtaining drift coefficients is time consuming and inconvenient in general, and changes in the coefficients are likely to occur during the time required to make the multiple runs.

Servo tests made with continuous rotation of the servo table appear best suited for gyros intended for long-term guidance applications. The principal attractions are that they simulate applications of the gyro for long-term stabilization under constant or low-level variable accelerations, and that they offer the possibility of automatic operation and machine data reduction.

The servo table test mode inspires the greatest confidence in test results; it represents the way in which the gyro will perform in a stable platform system, and the measurements of angles and time can be very accurate.

For ballistic missile applications, the cogging test has the advantage that the time to "drift" 1 degree is usually comparable to the time of guided flight. A cogging test also provides the highest accuracy of any type of test, because multiple measurements can be made over the same angular increment, thus minimizing errors in the angular measurement.

On the basis of results obtained in the testing program, it is felt that the most significant repeatability data can be obtained with the cogging test for short-term (minutes or hours) repeatability and with the servo test for long-term (days) repeatability.

F. Vibration Tests

Vibration testing of gyros intended for ballistic missile use is important for two reasons. First, it indicates what degradation of performance, if any, is to be expected when the gyro is operated in the predicted vibration environment of the missile; and second, vibration can be used as a tool to measure compliance drift coefficients. A knowledge of compliance coefficients permits compensation of gyros intended for use in high linear acceleration fields, and contributes to a better understanding of the internal mechanisms of the gyro--an understanding which is requisite to good gyro design.

Vibration tests were used in the test program for both of the purposes mentioned. Performance degradation was determined by applying random and sinusoidal vibrations to the gyro while it was operating. Vibration tests of this kind are common and require no further comment in this report, except for the observation that they are necessary to a testing program. Results of these tests are presented in Appendix H.

The tests made to evaluate compliance coefficients were both significant and valuable, not only because of the information obtained, but because new techniques were developed for the purpose. While many companies make use of vibration exciters to determine the anisoelastic coefficient, it is felt that the unusual scope of the vibration tests performed for this program, together with the accuracy and consistency of the results, makes the testing reported here an extension of the state of the art. The accuracy of the measurements is quite comparable to that obtained with specialized precision machines of many times the cost of the equipment used in this study, and having much less flexibility (see Reference 12).

The vibration tests performed for this study were made by subjecting the gyro to vertical vibration while mounted on an angle block in such a way that the output axis of the gyro was parallel to the earth's

polar axis. The gyro was than rotated about its output axis in 16 discrete orientations and vibrated at 6-, 8-, and 10-g rms in each of these orientations. For each level of vibration, the torquer control current and the acceleration along each of the principal axes of the gyro were measured. The change in torquer control current was plotted as a function of acceleration squared, and the best straight line fitted to this set of data. The slope of this line was then used as one of 16 points in a Fourier analysis of the data.

Illustrations of the test equipment and a sample of the data reduction process will be found in Appendix H.

Additional tests using these techniques should be made, particularly to determine the results of using different frequencies. It should also be possible to eliminate effects of vibration table wobble through use of the STL horizontal vibration facility with the gyro input axis in a horizontal plane, and thus to perform tests at very low frequencies.

The vibration tests described in this report are suitable chiefly for performance evaluation. Vibration tests for production or acceptance could be greatly simplified, providing only for measurement of the major compliance term. Such a test might consist of applying excitations of 4-, 6-, 8-, and 10-g rms at a nonresonant frequency in the IA-SA plane. The vibration would be applied at an angle of 45 degrees with respect to IA and SA, for a short duration.

It is concluded that production testing should include vibration tests to evaluate the major compliance term, if the tumbling tests do not provide satisfactory data.

G. Torquer Linearity Tests

Torquer linearity tests are of considerable interest, particularly for ballistic missile "strap-down" applications. They establish the usefulness of the gyro as a rate measuring instrument. For most inertial

platform applications, the simple earth's rate calibration described in Appendix E is sufficient, while for more precise measurements (better than 1 percent) it was found necessary to apply precision torquing currents to a gyro stabilizing a servo test table. It appears from test results that torquer linearity measurements of 0.01 to 0.02 percent are possible.

APPENDIX A

TEST HISTORIES OF MIG GYRO GG49D1

Table A-1. Test History of MIG Gyro GG49D1, Serial No. K-13.

Date 1959	Cool to °F x Times		Test	R, deg/hr	U_I, deg/hr-g	U_S, deg/hr-g	K, deg/hr-g	$\delta\omega_{spread}$ deg/hr	$\delta\omega_{rms}$ deg/hr	Scale Factors and Miscellaneous	Accumulative Running Time, hr	Remarks
28 May			M-H performance data	-0.38						K_z = 2.04 deg/hr-ma^2		K computed from -1.77 deg/hr at +10 mr to +0.11 deg/hr at -10 mr. Note lack of symmetry about R
			Mass unbalance		+0.45	+0.92				K_I = 31.3 mv/mr		
			Null repeatability					0.031		K = 0.09 deg/hr-mr		
			Cogging, IA up						0.027	stops ±340 mv		
18, 20 Jul			Test set checkout								3.8	
27, 28 Jul	74	3	Phasing and axis alignment									
	74	2										
29 Jul	74	1	Null repeatability					0.070	0.03			I_p = 1 ma
30 Jul			Torquer calibration					0.36	0.107	K_w 20.1 deg/hr-ma		Standard deviation of K_w is 0.86%
			Reaction torque, elastic restraint	-0.14						K = 0.19 deg/hr-mr		IA east OA vertical
31 Jul	73	1	Mass unbalance	-0.13	-0.72	+1.26		0.50				
5 Aug	72	1	Elastic restraint							K = 0.07 deg/hr-mr		IA west K = +0.054, IA east K = 0.078, IA north K = 0.071, IA east error in K = 0.0125 deg/hr-mr due to earth's rate
7 Aug	71	1	Limit stops and null							Stops ±355 mv e_n 0.08 mv	33.6	
10, 18 Aug	72	1	Test equipment checkout									10-g rms, 100 cps, vib, 20 min for accel. calib.
19 Aug	72	2	Vibration, sinusoidal sweeps along IA, OA, SRA							U_r 2.3 deg/hr-g	50.9	5-g rms, 8 to 2000 cps, 0.5 oct/min, no significant gyro resonances
21 Aug	83	1	Attempt to use CIO shaker									Shaker field too strong, strong harmonics on vibration
22 Aug - 2 Sep	76	1	Mod D servo table checkout								76.6	
3 Sep	73	13	Tumbling Test OA//EA (No. 1)	+0.59	+2.80	+1.51	+0.21	1.05	0.23	A_2 +0.062 deg/hr		Obvious friction in gyro, worse in Test 2
			Tumbling Test OA//EA (No. 2)	+0.51	+2.67	+1.85	+0.21	1.84	0.37	A_2 +0.301 deg/hr		Gyro 100°F below normal operating temperature
4 Sep	72	1	Tumbling Test OA//EA (No. 3)	+0.55	+2.92	+1.85	+0.22	0.91	0.20	A_2 +0.358 deg/hr		Much friction still apparent
			Tumbling Test OA//EA (No. 4)	+0.65	+2.75	+1.41	-0.13	0.49	0.11	A_2 +0.029 deg/hr	86.5	Gyro 100°F above normal operating temperature
4 Sep	Op-15	1	Mass unbalance	+0.93	+2.88	+1.67		0.20				
16-21 Sep	74	2	Tumbling under vibration				+0.0027			$\frac{K_{SI}}{2}$ +0.0006 $\frac{K_{IS}}{2}$ -0.0016 $\frac{K_{IO}}{2}$ -0.0017 $\frac{K_{SO}}{2}$ +0.0002		10-g rms, 230 cps, total 1 hr OA//EA Vibration vertical, IA at 15-deg intervals about OA Standard deviation = 0.0204, spread = 0.0802 All units deg/hr-g^2
	72	5	Vibration to find $(K_{SS} \cdot K_{II})^{1/2}$				+0.0198		0.063	rms deviation = 0.0018 deg/hr-g^2	100.3	230 cps, 4, 6, 8, and 10-g rms, OA horizontal vibration 45° to IA and SRA

Table A-1. (Continued).

Date 1959	Cool to ^{o}F x Times		Test	R, deg/hr	$U_{I'}$ deg/hr-g	$U_{S'}$ deg/hr-g	K, deg/hr-g^2	$\delta\omega_{spread}$ deg/hr	$\delta\omega_{rms}$ deg/hr	Scale Factors and Miscellaneous	Accumulative Running Time, hr	Remarks
22-25 Sep			Servo test IA//EA(No. 11)	+0.20*	+2.52	+1.65*		1.01	0.161	A_2 = +0.041, B_2 = +0.110		*Assuming R = +0.20, then U_S = +1.65, i_p = 7.9 ma
			Servo test IA//EA(No. 12)	+0.20*	+2.49	+1.57*		3.16	0.494	A_2 = -0.173, B_2 = -0.28		*Assuming R = +0.20, then U_S = +1.57, i_p = 7.9 ma
			Servo test IA horizontal(No. 13)	+0.14	+2.43			4.66	0.708	A_z = -0.033, B_z = -0.211		i_p = 10 ma (standard)
25 Sep	Op-15	1	Mass unbalance	+0.20	+2.81	+1.63		0.20			177.1	
25-27 Sep	100	1	Servo test IA vertical (No. 14)	+0.92*		+1.63*		0.43	0.087	10^{0} data	233.7	*Assuming U_S = 1.63, then R = +0.92
	72	1										
13 Oct			Cogging, OA up (No. 22)	+0.061				0.029	0.009			Installed gyro in improved holding fixture
			Cogging, OA down (No. 23)	+0.052				0.063	0.019			Average R = -0.017 deg/hr
			Cogging, SRA up (No. 24	+0.091	+2.55			0.037	0.011			For all cogging tests combined, $\delta\omega_{rms}$ = 0.022
			Cogging, SRA down (No. 25)					0.058	0.012			Gyro overheated an undetermined amount between Tests 25 and 26
14 Oct	Op-5	2	Cogging, IA up (No. 26)	-0.208		+1.83		0.122	0.038			
			Cogging, IA down (No. 27)					0.088	0.028			
15 Oct	Op-5	1	Mass unbalance	+0.010	+3.00	+1.74		0.60			260.1	
21, 22 Oct	70	1	Torquer linearity (No. 36)	-0.05*		+2.54*				K_{nl} = 19,892 ±0.5% deg/hr-ma up to 300 deg/hr		*Assuming R = -0.05, then U_S = +2.54. Maximum error in K_{nl} = +0.77% up to 2417 deg/hr. R due to torquer with i_p = 10 ma is +0.12 deg/hr
23 Oct	Op-20	2	Torquer scale factor versus gimbal angle (No. 37)							θ to ±3 deg, ω_i = 600 deg/hr		Standard deviation = 0.07%. Can be improved by factor 3 or better
23 Oct	Op-7	1	Mass unbalance	-0.20	-4.01	+2.59		0.34			277.3	Large change in U_I probably due to shock along OA
3 Nov	70	1	Checkout with gyro on shaker	+0.50								
4 Nov	65	1	Mass unbalance, eight position	+0.34	-3.94	+2.95						
			Shaker equalization									1-g rms sinusoidal, 20 to 2000-cps sweeps, total 45 min
			Random vibration									20 to 2000 cps, 12-db rolloff 1000 to 2000 cps, 1, 2, and 5-g rms for 1 min each of IA, OA, SRA
			Mass unbalance, eight position	+0.23	-4.1	+3.4						Gyro overheated 16^{0}F during several readings
5 Nov	Op+3	1	Mass unbalance, eight position	+0.15	-3.7	+2.8						
			Random plus sinusoidal vibration									Random 2-g rms, sinusoidal 2-g rms swept 1 oct/min. Random and sinusoidal 20 to 2000 cps with 12-db rolloff 1000 to 2000 cps. Applied along OA, IA, SRA
			Mass unbalance, eight position	+0.10	-4.1	+3.0					290.6	

Table A-2. Test History of MIG Gyro GG49D1, Serial No. K-14.

Date 1959	Cool to °F	x Times	Test	R, deg/hr	U_1, deg/hr-g	U_2, deg/hr-g	K, deg/hr-g^2	$\delta\omega_{spread}$, deg/hr	$\delta\omega_{rms}$, deg/hr	Scale Factors and Miscellaneous	Accumulative Running Time, hr	Remarks
28 May (shipped)			MH performance data	-0.51						K_1 = 10.1 deg/hr-ma		
			Mass unbalance		+0.06	-0.45				K_2 = 29.5 mv/mr		K_2 probably a typographical error. 1.01 dyne cm/ma^2 = 20.8 deg/hr-ma
			Null repeatability					0.10		K = 0.008 deg/hr-mr		
			Cogging 1A up						0.012	stops +355 mv, -360 mv		
4 Aug			Phasing, null repeatability					0.105	0.036	stops +350 mv, -360 mv		Null voltage 0.18 mv, I_{bp} = 1 ma
			Torquer calibration					0.31	0.095	K_1 = 21.1 deg/hr-ma		Standard deviation of K_1 is 0.76%
			Reaction torque, elastic restraint	-0.72						K = +0.025 deg/hr-mr		1A east K = +0.037, 1A north K = +0.025, 1A west K = +0.013
5 Aug	71	1	Mass unbalance	-0.53	-0.64	+0.02		0.16	0.09		9.7	
8 Sep	72	2	Tumbling test (No. 6)	-1.06	-0.29	-0.12	+0.06	0.53	0.10	A_2 = -0.02 deg/hr		
	76	1	Tumbling test (No. 7)	-1.25	-0.01	+0.02	+0.05	1.19	0.21	A_2 = -0.02 deg/hr		100°F below operating temperature
9 Sep			Tumbling test (No. 8)	-1.01	-0.35	-0.17	+0.03	0.36	0.09	A_2 = +0.05 deg/hr		
	Op-12	1	Tumbling test (No. 9)	-1.04	-0.24	-0.70	-0.41	0.87	0.16	A_2 = +0.04 deg/hr	29.4	100°F above operating temperature
9 Sep	75	1	Mass unbalance	-0.39	-0.27	+0.19		0.16	0.08			
15-30 Sep			Test equipment checkout									Installed gyro in improved holding fixture
	75	5	Servo test 1A//E.A (No. 18)	-1.158*	+0.008	+0.342*		0.074	0.017	$B_1 - A_2$ = +0.015, B_2 = -0.051		*Assuming R = -1.158, then U_S = +0.342.
10 Sep to 2 Oct			Servo test 1A//E.A (No. 19)	-1.158*	+0.158	+0.495*		0.104	0.018	B_1 = +0.036, A_2 = +0.024	114.8	*Assuming R = -1.158, then U_S = +0.495, P_2 = -0.004
5 Oct	74	1	Mass unbalance	-1.17	-0.19	+1.33		0.32	0.10			Discrepancy in U_S may be due to frequency error in 400-cps supply
15 Oct	76	1	Cogging 1A down (No. 28)	-1.295		-0.680		0.147	0.052			For all cogging tests combined $\delta\omega_{rms}$ = 0.057 deg/hr
			Cogging 1A up (No. 29)					0.111	0.011			Average R = 1.158 deg/hr
16 Oct	Op-13	1	Cogging SRA down (No. 30)	-1.129	-1.128			0.080	0.023			
			Cogging SRA up (No. 31)					0.023	0.006			
			Cogging OA down (No. 32)	-1.046				0.018	0.004			
			Cogging OA up (No. 33)	-1.055				0.032	0.010		135.7	
19, 20 Oct	72	1	Torquer linearity (No. 34)	-0.70*		-0.49*				K_2 = 20.944 ± 0.5% deg/hr-ma to 2566 deg/hr		*Assuming R = -0.72, then U_S = -0.51; linearity is 3% of K_2
21 Oct	Op-19	2	Torquer scale factor versus gimbal angle (No. 35)							K_2 = 20.944 ± 2% to 12 deg, ω<600 deg/hr	152.7	
21 Oct	Op-2	1	Mass unbalance	-0.70	-1.62	-0.46		0.21	0.09			
5 Nov	75	1	Mass unbalance, eight position	-0.95	-1.5	-0.7						
			Vibration, sinusoidal sweeps along 1A, OA, SRA							U_r = 2.9 deg/hr-g		5-g rms, 20 to 2000 cps, 0.5 oct/min
			Mass unbalance, eight position	-0.91	-1.7	-0.5						
			Random vibration									20 to 2000 cps, 12-db rolloff 1000 to 2000 cps, 1-, 2-, and 5-g rms for 1 min each on each of 1A, OA, SRA
			Mass unbalance, eight position	-0.96	-1.3	-0.8						
			Random plus sinusoidal vibration									Random 2-g rms, sinusoidal 2-g rms swept 1 oct/min. Random and sinusoidal 20 to 2000 cps with 12-db rolloff 1000 to 2000 cps, applied along OA, 1A, SRA

Table A-2. (Continued).

Date 1959	Cool to °F x Times	Test	R, deg/hr	U_I, deg/hr-g	U_S, deg/hr-g	K, deg/hr-g^2	$\delta\omega_{spread}$, deg/hr	$\delta\omega_{rms}$, deg/hr	Scale Factors and Miscellaneous	Accumulative Running Time, hr	Remarks
5 Nov (cont.)		Mass unbalance, eight position	-1.45	-0.2	+0.2						
6 Nov	Op+30 1	Mass unbalance, eight position	-1.20	-0.6	+0.1						Gyro overheated 30°F night of 5 Nov
		Tumbling under vibration				0.0176			$\frac{K_{SI}}{2}$ = -0.0003 $\frac{K_{SI}}{2}$ = -0.0006 $\frac{K_{IO}}{2}$ = -0.0011 $\frac{K_{SO}}{2}$ = +0.0016		10-g rms, 225 cps, vibration vertical, OA//EA, total 51 min Vibration with IA at 22.5-deg intervals about OA Standard deviation = 0.0015, spread = 0.0061 All units deg/hr-g^2
		Mass unbalance, eight position	-1.49	-0.2	+0.1						
		Vibration to find K_{IS} and K_{SI}						0.011	$\frac{K_{IS}}{2}$ = -0.0003		$\frac{K_{SI}}{2}$ = -0.0003 deg/hr-g^2
		Mass unbalance, eight position	-1.36	-0.7	-0.5					168.7	
16 Nov	72 1	Mass unbalance	-1.49	+0.18	+0.17						OA up R = -1.47
17 Nov	Op-53 1	Mass unbalance	-1.57	+0.20	+0.13						OA up R = -1.36
18 Nov	Op-27 1	Mass unbalance	-1.62	+0.07	+0.17						OA up R = -1.57
19 Nov	Op-18 1	Mass unbalance	-1.37	+0.12	+0.18						OA up R = -1.36
20 Nov	Op-29 1	Mass unbalance	-1.35	+0.09	+0.21						OA up R = -1.26
23 Nov	Op-570 1	Mass unbalance	-1.36	+0.12	+0.12						OA up R = -1.26
		Stepwise tumbling	-1.327	+0.200	+0.172	+0.065	0.124	0.026	A_2 = -0.002 deg/hr		Meter readings visually averaged
24 Nov	Op+24 1	"Strong floor" investigation Room 143, Building H2								182.8	3-ft-thick concrete floor greatly reduces gyro response to floor loading and shock
27, 30 Nov	Op-27 2	Equipment checkout									
1 Dec	Op-18 1	Stepwise tumbling	-1.243	+0.442	-0.057	+0.023	0.131	0.011	A_2 = -0.011 deg/hr		Strip chart recording
		Stepwise tumbling	-1.086	+0.458	+0.056	+0.079	0.121	0.011	A_2 = -0.047 deg/hr		Strip chart recording
		Stepwise tumbling	-1.089	+0.152	+0.068	+0.069	0.162	0.014	A_2 = -0.023 deg/hr	204.9	Strip chart recording

APPENDIX B

THE GYRO AND ITS EXCITATIONS

APPENDIX B

THE GYRO AND ITS EXCITATIONS

The two gyros tested in this program were Minneapolis-Honeywell Model GG49D1 units, serial numbers K-13 and K-14. These gyros belong to the MIG class of gyros described in References 3 and 4. The GG49D1 was an early development of the MIG, intended primarily for use in platform stabilization. The gyro is characterized by a relatively low damping for an integrating gyro (having an input angle of only ±1/2 degree) which is not detrimental for its intended application. This narrow input angle, however, does limit the number of applications in which the gyro can be used. A further limitation on its application is the low rate capability of the torquer. To circumvent this limited application problem, the GG-87 gyro was developed by Minneapolis-Honeywell to provide larger input angles and higher rate capabilities, making use of paddle damping and a permanent magnet torquer. Tests on GG-87 gyros are to be made in the near future.

As the Model GG49D1 gyro is intended primarily for use in platform stabilization, the excitations listed below are representative of those encountered in such applications. They were used for all the tests described unless other indication is made.

Temperature:	Approximately 180°F (1.e., the temperature-sensing resistance kept at 780 ±0.2 ohms)
Operating heater:	28 volts dc or ac. Fast warm-up heater was not used
Spin motor:	Three phase, 26 ±0.5 volts rms line-to-line, 400 cps
Signal generator:	50 ±0.5 ma rms, 400 cps
Torque generator:	10 ±0.01 ma dc

Two sources of excitation were used, designated the "Gyro Test Set" (Figure B-1) and the " Inertial Gyro Test Facility" (Figure B-2). The fundamental differences between these two sets of electronics are as follows:

	Gyro Test Set	Inertial Gyro Test Facility
Signal generator excitation	Voltage source	Current source
Torque generator excitation	Current source	Voltage source
Heater control	Switching	Proportional
Heater voltage	28 volts dc	28 volts, 60 cps

The following descriptive data for the GG49 MIG gyro is extracted from Reference 3:

Angular momentum (H)	1.0×10^5 dyne-cm-sec
Gimbal inertia (J)	100 gm-cm^2
Damping coefficient (C)	16,700 dyne-cm-sec at 180°F
Gyro gain (H/C)	6.0
Characteristic time (J/C)	6.0×10^{-3} sec
Signal generator sensitivity	5 mv/mr at 50-ma, 400-cps excitation
Torque generator sensitivity	1.0 dyne-cm/ma^2 = 20 deg/hr-ma at 10-ma excitation
Gimbal freedom	±3 deg nominal

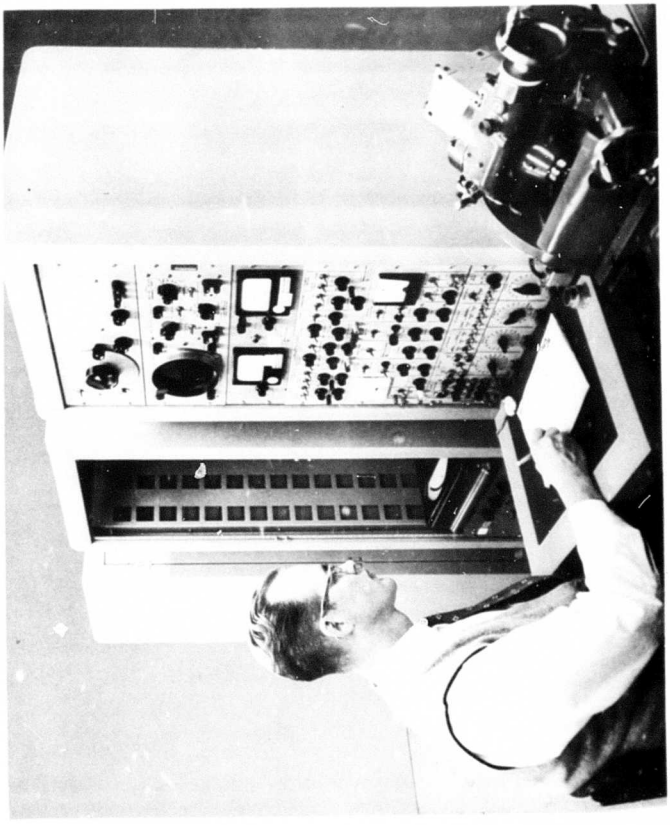

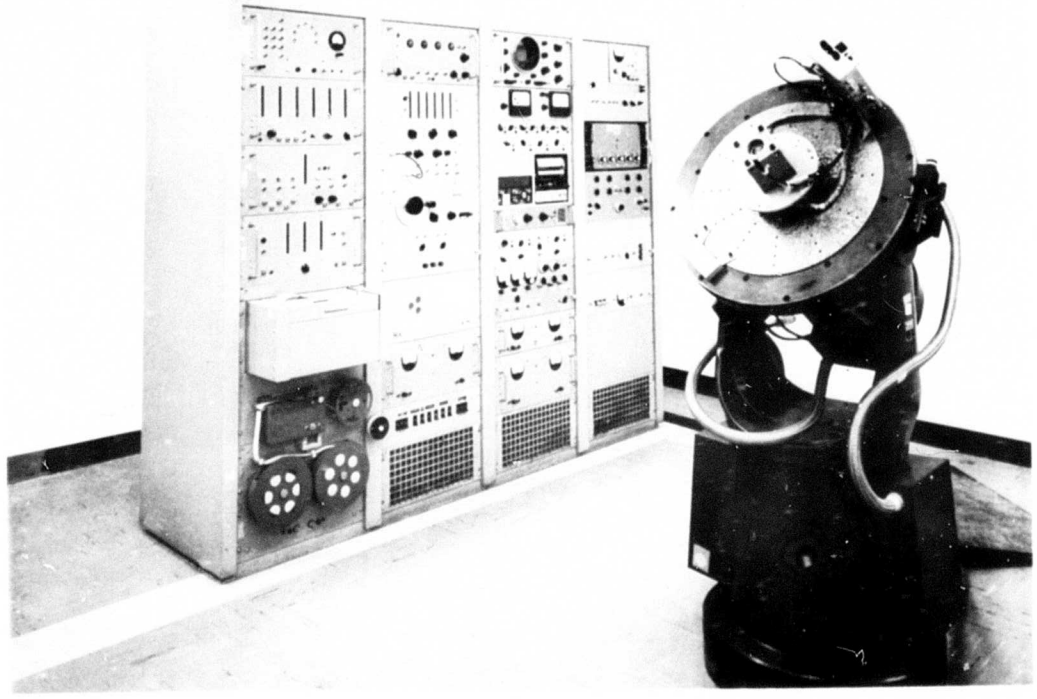

Figure B-2. Inertial Gyro Test Facility.

APPENDIX C

PRELIMINARY TESTS

APPENDIX C

PRELIMINARY TESTS

I. CONTINUITY AND IMPEDANCE

The resistance and inductance of each circuit in the gyro was measured at room temperature with an ESI impedance bridge. Results of these tests are shown in Table C-1 in comparison with the nominal values stated by Minneapolis-Honeywell.

II. POLARITY, PHASING, AND ALIGNMENT

A. Signal Generator

At operating temperature and wheel off, the gyro case was accelerated in a negative rotation about the output axis. The inertia of the gimbal causes an apparent positive rotation of the gimbal relative to the case. This motion resulted in an increasing signal secondary output voltage leading by approximately 70 degrees the signal primary excitation voltage. When the case was decelerated and stopped, the gimbal returned to its original position because of the integrating action of the viscous damping. This test confirmed the fact that a positive gimbal angle results in an output signal which is approximately in-phase.

B. Torque Generator

With the gyro at operating temperature and wheel off (the same result was obtained wheel on), positive currents of 10 milliamperes each were introduced into the torquer pattern and control windings. The signal generator output voltage was observed to proceed to the in-phase (positive) gimbal stop. Introducing negative currents into the control winding while maintaining positive current in the pattern winding caused the gimbal to move to the out-of-phase (negative) stop. This test confirmed that K_t was positive and provided a measurement of the stop voltages.

C. Spin Axis

At operating temperature and wheel on, the gyro was rotated continuously in a positive direction about the spin rotation axis, as indicated

on the case. The gimbal came to a position near null. The gyro was then rotated slightly in its mounting about the output axis to the point where rotation about the spin rotation axis kept the signal output voltage below 0.5 millivolt. When the gyro was rotated in the opposite (negative) direction, the gimbal eventually went to the stops. This procedure served to align the spin rotation axis with the mounting fixture within 0.1 milliradian, or 20 seconds of arc, as well as to establish that the direction of spin motor rotation marked on the case was correct.

D. Input Axis

At operating temperature and wheel on, the gyro was rotated about its input axis. Positive rotation resulted in an increasing in-phase signal. With the torquer servo holding the gimbal near null, a positive rotation produced a negative torquer current. This procedure was redundant, but served as a check on the preceding tests.

Table C-1. Room-Temperature Impedances of Gyro Circuits.

Gyro Circuit	Polarity (Ref. 2)	Wire Color	Connector Pin*	Ohms Nominal (Ref. 3)	Gyro K-13		Gyro K-14	
					Ohms dc	mh at 1 kc	Ohms dc	mh at 1 kc
Temperature sensor	— —	Red Orange	CC DD	625	608.4	6.4	630.1	6.8
Warm-up heater	L R	Yellow Green	D Z	124.6	123.4	5.7	122.8	8.0
Operating heater	L R	Blue Green	BB AA	31.4	31.7	0.7	31.9	0.9
Spin motor	A B C	Brown Black White	R P N	45 45 45	62.8 62.5 63.7	30.1 30.5 30.4	57.5 56.9 57.3	31.1 31.5 30.0
Signal primary	L R	Purple Grey	H E	28	32.1	6.9	31.9	7.2
Signal secondary	L R	White-Brown White-Black	J L	332	323.8	60.6	331.9	62.8
Torquer pattern	L R	White-Green White-Blue	V Y	260	243.8	43.2	245.3	44.6
Torquer control	L R	White-Red White-Yellow	S U	332	330.7	56.1	345.4	57.7
Shield ground	—	—	B	—	—	—	—	—

* Pins of connector installed by STL.

All resistances given at room temperature, 72°F. Operating temperature resistances are approximately 25 percent higher, except for heaters which change little and the temperature sensor which becomes 780 ± 0.2.

APPENDIX D

BENCH DRIFT TESTS

APPENDIX D

BENCH DRIFT TESTS*

I. NULL REPEATABILITY

With the gyro output axis vertical down, two directions (approximately east and west) were found for the input axis, in which i_c (the torquer control current) averaged zero ±0.02 milliampere. The two directions were found by rotating the gyro first in the positive direction and then in the negative direction about the output axis.

For this test it was found helpful to reduce the gain of the torquer servo to the minimum (0.1 ma/mv) and to reduce i_p (the torquer pattern current) to 1.0 milliampere. The resulting reduction in loop gain served to minimize the fluctuations in i_c and tc permit expansion of the scale on the precision (±0.1 percent) 1-milliampere meter used.

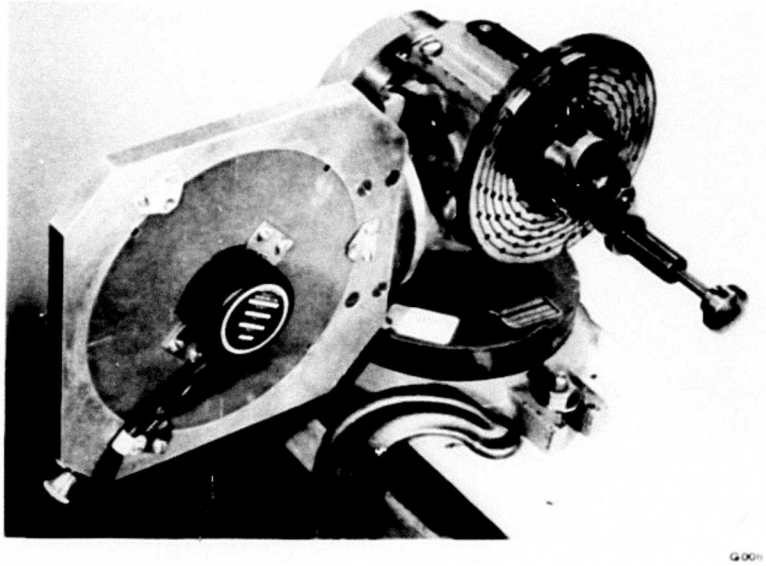

Figure D-1. Early Holding Fixture Mounted on Ellis Dividing Head.

* All bench drift tests were made using the torquer servo and with the gyro wheel on.

The scale on the vertical axis of the dividing head then in use (see Figure D-1) had 1-degree graduations from which readings of 0.1 degree could be interpolated. The angular readings at the gyro null were found to repeat within 15 minutes of arc (0.25 degree), and using 15 minutes as the least count on the angular scale each gyro repeated the angular reading on both east and west nulls. By coincidence, the table was found to be aligned with 0 degree at north, as closely as could be determined with the gyros (probably within 0.1 degree).

After the first procedure the test was run twice more, using the angular settings previously determined and measuring i_c. Results are shown in Table D-1.

In order to minimize operator error in taking an average reading, five instantaneous readings were taken on gyro K-14 at 10-second (time) intervals and the results were averaged. This technique proved difficult, because at times the meter had to be read "on the fly." The results obtained were comparable to those obtained by Minneapolis-Honeywell using a strip-chart recorder and smoothing the data by drawing an "average line" through the recorded data.

II. TORQUER CALIBRATION

The horizontal component of earth's rate was measured with the gyro output axis vertical down, and with the input axis directed first north and then south. Ten instantaneous readings were made and averaged for the i_c. The results obtained are shown in Tables A-1 and A-2, which indicate that both determinations were about 1 percent high as compared to those obtained later in torquer linearity tests. Possible reasons for this error are that the standard deviation of current-measuring uncertainty was nearly 1 percent, and there may have been an error in verticality of the output axis of as much as 0.25 degree which could have contributed 0.2 percent to the error. The test fixture shown in Figure D-1 was in use at that time.

Table D-1. Null Repeatability Data.

GYRO K-13

NULL DETERMINATION

East Null Setting	West Null Setting
CW +92°30'	CW -92°30'
CCW +92°30'	CCW -92°30'

TORQUE REPEATABILITY AT NULL SETTING

	i_c at East Null	i_c at West Null
CW	-0.010 ma	+0.015 ma
CCW	+0.010 ma	-0.010 ma
CW	-0.020 ma	+0.010 ma
CCW	-0.020 ma	-0.020 ma

These are "mentally averaged" meter readings.

i_p = 1 ma, so K_ω = 2.0 $\frac{\text{deg/hr}}{\text{ma}}$

$\delta\omega_{spread}$ = 0.070 deg/hr

$\delta\omega_{rms}$ = 0.030 deg/hr

GYRO K-14

NULL DETERMINATION

East Null Setting	West Null Setting
CW +88°15'	CW -88°15'
CCW +88°15'	CCW -88°15'

TORQUE REPEATABILITY AT NULL SETTING

	i_c at East Null					Average i_c
CW	+0.010	0.000	+0.012	+0.023	+0.023	+0.014 ma
CCW	0.000	0.000	-0.010	-0.010	-0.012	-0.006 ma
CW	-0.002	-0.008	-0.022	-0.025	-0.020	-0.015 ma
CCW	-0.003	-0.003	-0.015	-0.016	-0.015	-0.010 ma

	i_c at West Null					Average i_c
CW	+0.005	+0.010	+0.025	+0.035	+0.030	+0.021 ma
CCW	-0.020	-0.015	-0.020	-0.040	-0.050	-0.029 ma
CW	-0.030	-0.036	-0.027	-0.010	-0.005	-0.022 ma
CCW	-0.015	-0.003	-0.010	-0.005	-0.020	-0.005 ma

These are instantaneous readings.

i_p = 1 ma, so K_ω = 2.1 $\frac{\text{deg/hr}}{\text{ma}}$

$\delta\omega_{spread}$ = 0.180 deg/hr instantaneous readings

$\delta\omega_{spread}$ = 0.105 deg/hr averaged readings

$\delta\omega_{rms}$ = 0.042 deg/hr instantaneous readings

$\delta\omega_{rms}$ = 0.036 deg/hr averaged readings

III. REACTION TORQUE

With the output axis vertical down, the gyro was rotated to the true east and true west positions of the input axis. Rotation was made in alternate positive and negative directions about the output axis. Five instantaneous readings were made in each position. Results are shown in Tables A-1 and A-2.

IV. ELASTIC RESTRAINT

With the output axis vertical down and the input axis true east, i_c was measured (by taking an average of five instantaneous readings) with the gimbal at +10 milliradians and again at -10 milliradians from the null position. This procedure for determining the elastic restraint corresponds to that described in Reference 2, and includes a basic error in the measurement of restraint.

It is easily reasoned that when the gimbal is deflected from null with the gyro in the position described, a gimbal torque due to earth's rate is obtained. At the latitude of Los Angeles, making this test with the input axis east would cause an increase in apparent elastic restraint of 0.0125 $\frac{\text{deg/hr}}{\text{mr}}$. With IA west, there would be a decrease in apparent elastic restraint.

The above-described test for elastic restraint was repeated on both gyros with IA east, north, and west. The results corroborated the reasoning in the preceding paragraph, as appears in the Remarks column of Tables A-1 and A-2. If the test were performed with IA east only, it should be corrected by subtracting $0.001\omega_e \cos\beta \frac{\text{deg/hr}}{\text{mr}}$, unless the case is positioned to keep the spin axis fixed in a north-south direction during measurement.

V. GIMBAL MASS UNBALANCE

With the gyro output axis horizontal and north, i_c was measured with IA west, up, east, and down. Rotation to these positions was alternately positive and negative, and was performed four times for each position.

Meter readings were "mentally averaged" to cut down on the labor of data reduction. The process of data reduction is demonstrated in Table D-2.

This test was repeated frequently during the testing program on both gyros (see Tables A-1 and A-2), because it provides a fast (less than 1 hour) check on the mass unbalance and the reaction torque. The standard deviation of the readings obtained corroborates the initial assumption that this test can measure mass unbalance and reaction torque with an accuracy better than ±0.1 deg/hr.

Variations on this test were introduced later in the program. The eight-position mass unbalance test was used before and after vibration tests performed in the environmental testing laboratory, where there was no convenient stable pier from which to obtain a positive reference. With the output axis up, readings were made with the input axis both east and west; with the output axis down, readings were made with the input axis both east and west. Table D-3 shows data from a typical test and tabulates the eight positions. Only one reading was taken at each position, using a meter on 1 percent accuracy, so that the accuracy of the data may be no higher than ±0.2 deg/hr.

The final six mass unbalance tests on gyro K-14 included a measurement of reaction torque with OA vertical and IA west, in order to determine whether the variation in R with position was fixed or random. These tests were made on successive working days, and the gyro was never allowed to cool to room temperature during this testing period (16-23 November), as noted in Table A-2.

Table D-2. Sample Data Sheet, Gimbal Mass Unbalance Test.

Gyro: M-H (manufacturer) MIG GG19D1 (model and/or type no.) K-13 (serial no.) DATE: 31 July 1959 (day month year)

OA: (✓) horizontal and north; ( ) parallel to EA and north

Rate Sensitivity: $K_\omega = 19.9 \frac{\text{deg/hr}}{\text{ma}} = (2.064 \times 10^5/\text{H}) K_t i_p$

Torquer Sensitivity: $K_t =$ _____ dyne cm/ma^2

Torquer Primary (Pattern) Current: $i_p = 10$ ma $\pm 0.1\%$

Rotation about OA	Control Current i_c (ma) for IA directed			
	West	Up	East	Down
Positive	-0.030	-0.355	+0.040	+0.345
Negative	-0.020	-0.350	+0.040	+0.360
Positive	-0.040	-0.345	+0.050	+0.365
Negative	-0.020	-0.350	+0.045	+0.370
Total	-0.110	-1.400	+0.175	+1.440
Average	a = -0.028	b = -0.350	c = +0.044	d = +0.360
Spread	0.020	0.010	0.010	0.025

Mass Unbalance:

$$U_I = \frac{a - c}{2} K_\omega = \frac{-0.028 - 0.044}{2} (19.9) = \frac{-0.072}{2} 19.9$$

$$\boxed{U_I = -0.72 \frac{\text{deg/hr}}{\text{g}}} = \text{_____ dyne cm/g}$$

$$U_S = \frac{b - d}{2} K_\omega + \omega_e \sin\beta = \frac{-0.350 - 0.360}{2} (19.9) + 8.39 = \frac{-0.710}{2} 19.9 + 8.39$$

$$\boxed{U_S = +1.26 \frac{\text{deg/hr}}{\text{g}}} = \text{_____ dyne cm/g}$$

Reaction Torque:

$$R = -\frac{1}{4}(a + b + c + d) K_\omega = -\frac{1}{4}(-0.378 + 0.404)(19.9) = -\frac{1}{4}(+0.026) 19.9$$

$$\boxed{R = -0.13 \text{ deg/hr}} = \text{_____ dyne cm}$$

NOTES:

1. OA is assumed as the vector direction of gimbal rotation per the right hand rule for i_p and i_c positive. If this is not true, the sign of i_p should be negative in the equations.
2. IA is the input axis direction shown on the gyro name plate. If a positive rotation of the gyro about this axis per the right hand rule requires positive i_c to maintain the gimbal at null, the sign of $\omega_e \sin\beta$ should be negative in the equations.
3. Equations are written for OA horizontal and north. For OA parallel to EA and north: $U_I = \frac{a - c}{2 \cos\beta} K_\omega = \frac{a - c}{1.66} K_\omega$ and $U_S = \frac{b - d}{1.66} K_\omega$. R is unchanged.
4. β is latitude angle and components are given for STL in Los Angeles where $\beta = 33°54'53"$.

Table D-3. Typical Data for Eight-Position Gimbal Mass Unbalance Test.
Gyro K-14, 5 November 59

Reading	1	2	a	b	c	d	3	4
OA	Down	Down	North	North	North	North	Up	Up
IA	East	West	West	Up	East	Down	East	West
i_c, ma	+0.065	+0.07	-0.015	-0.40	+0.11	+0.47	+0.04	-0.025

Coefficient	U_I	U_S	R				
Orientation	SRA vertical	IA vertical	OA down	OA up	SRA vertical	IA vertical	Average of all Readings
Formula	$K_\omega \frac{a-c}{2}$	$K_\omega \frac{b-d}{2}$	$-K_\omega \frac{1+2}{2}$	$-K_\omega \frac{3+4}{2}$	$-K_\omega \frac{b+d}{2}$	$-K_\omega \frac{b+d}{2}$	
deg/hr	-1.3	-0.8	-1.4	-0.7	-1.0	-0.7	-0.96

APPENDIX E

TORQUER LINEARITY TESTS

APPENDIX E

TORQUER LINEARITY TESTS

I. LINEARITY AT NULL

For this test, the gyro was mounted on the servo table with the input axis parallel to the table axis and the table axis vertical. The servo table was slaved to the gyro, various d-c currents were applied to the torquer pattern and control windings, and the resulting table rate was determined by measuring the time, δt, required to turn the table through various angles, $\Delta\phi$. These angular intervals were selected on the basis of the table rate.

This method ("Velocity Balance") of testing linearity was used instead of the "Current Balance" method described in Section 5.1 of Reference 1, in which the gyro is rotated at a constant rate and the torquer servo control current is measured. Choice of the "Velocity Balance" method was made because of difficulties encountered in earlier tests with accurate measurements of i_c in a torquer servo loop, and because of expected uncertainties in the instantaneous angular velocity of the table.

The equation used for the data from this test, derived from equations (2) and (3) in the text, is

$$\text{Torquer error at each point} = \delta\omega = \omega_{IO} - K_\omega i_c + \omega_t + \omega_\epsilon \sin\beta$$

where ω_t is the angular velocity of the servo table relative to the earth, ω_ϵ is the angular velocity of the earth, and β is the local latitude. The torquer scale factor, K_ω, may be obtained by a least-squares fit of a straight line to the data, or

$$K_\omega = \frac{\Sigma(\omega_{IO} + \omega_t + \omega_\epsilon \sin\beta)}{\Sigma i_c} .$$

Since various combinations of torquer excitation (i_p and i_c), torquer excitation circuits (Figure E-1), and table angle ($\Delta\phi$) were used, it is necessary in the interest of clarity to tabulate these combinations. This is done for both gyros in Table E-1.

Results of the tests are shown in Figures E-2 and E-3 for maximum torquer currents i_p and i_c up to 35 milliamperes. Saturation is just becoming visible on the chart for K-13, and possible saturation is masked by a change in the test circuit at the 2500 deg/hr points on K-14. The black crosses at approximately 600 deg/hr on the top charts for both gyros represent repeatability data taken the following day as part of the rate sensitivity versus gimbal angle tests described below. Additional repeatability data for K-14 was taken a day later and is presented in Figure E-3b.

No attempt was made to determine δt over the same interval of table angle, as for example from $\phi = 0$ to $\phi = 10$ degrees. A set of special runs was made at 600 deg/hr over successive 10-degree intervals, with i_c first positive and then negative. The results (Figure E-4) show a standard deviation of 0.07 percent and a spread of 0.23 percent in both directions, with an obvious trend indicating possible eccentricity of the table angular readout. It appears then that the total of instrumentation and gyro errors can be reduced to 0.01 percent rms or less at this table speed by always measuring δt between the same table angles. The error might be further reduced by using both optical pickoffs rather than the one pickoff used in this test.

II. RATE SENSITIVITY VERSUS GIMBAL ANGLE

This test was made in a manner similar to that for the linearity test described above, with torquer pattern and control currents of +10 and $\pm$30 milliamperes, respectively, using a table angle of 10 degrees. The variable was the gyro gimbal angle, which was varied by introducing an offset voltage into the servo. In this way, the servo table maintained the gimbal angle desired. In order to keep the spin axis perpendicular to the table axis, the gyro case was rotated through a corresponding angle in the opposite direction.

Results of this test are shown in Figures E-5 and E-6, from which it appears that the torquer performance could best be approximated for a given gyro by using as a correction factor a power series in θ and i_c. Maximum errors are seen to be about 2 percent, with a maximum rate of change of error in excess of 1 percent per degree of gimbal rotation. Over the central 2 degrees of gimbal rotation, the rate of change of torquer error is approximately linear. It varies 0.40 percent per degree for K-13 and 0.84 percent per degree for K-14.

Table E-1. Torquer Linearity Test Parameters.

Gyro K-13; 21 and 22 October 1959

i_p, ma	i_c, ma	$\Delta\phi$, deg	R, ohms	L, henries	Circuit (see Figure E-1)
10	0 2 4	1	1000	25	a
	6 8 10 15 20 25 30 35	10			
15 20 25 30 35	35	360	100	1	
0 6 10	0 6 10	1 10 10	—	25	b

Gyro K-14; 19 and 20 October 1959

10	0 2 4	1	1000	25	a
	6 8 10 12 15 20 25 30 35	10			
15 20 25 30 35	35	360	100	1	

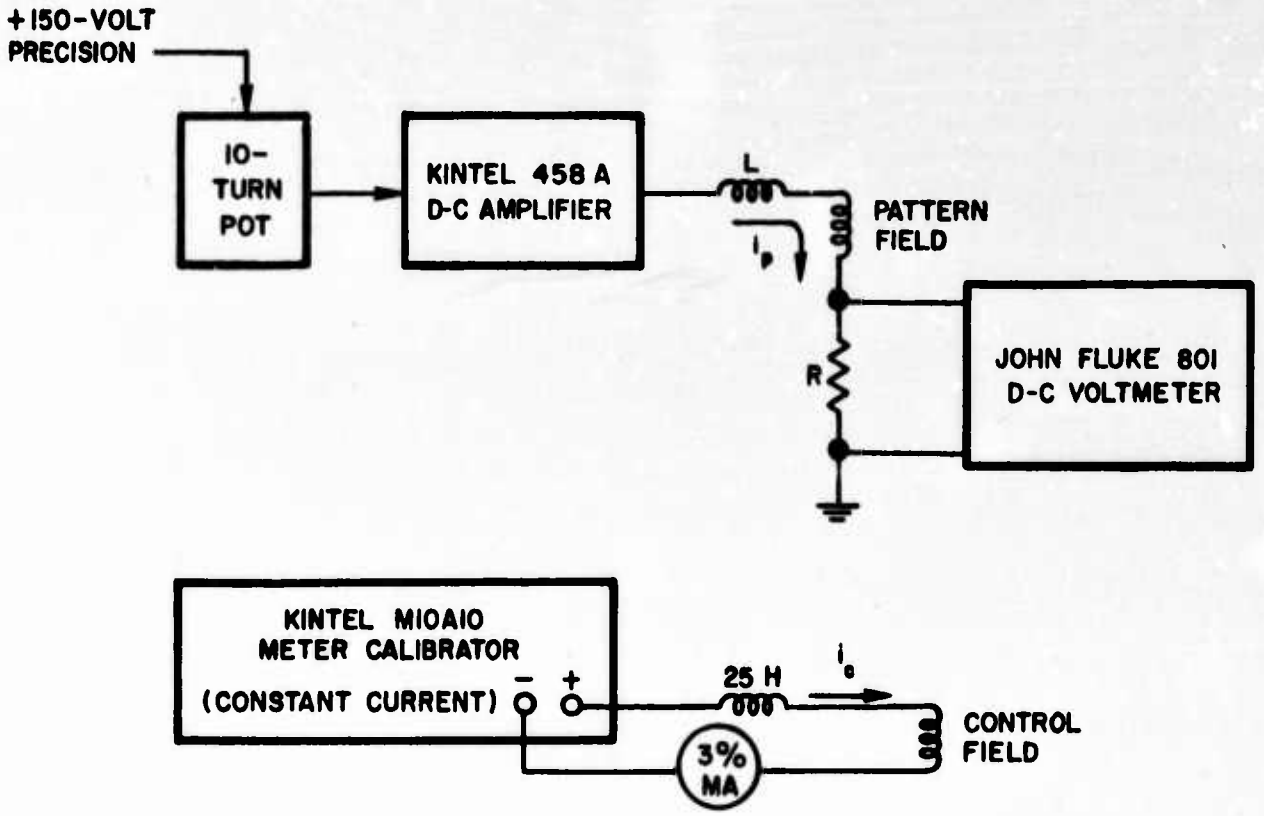

Figure E-1. Circuits for Torquer Linearity Tests.

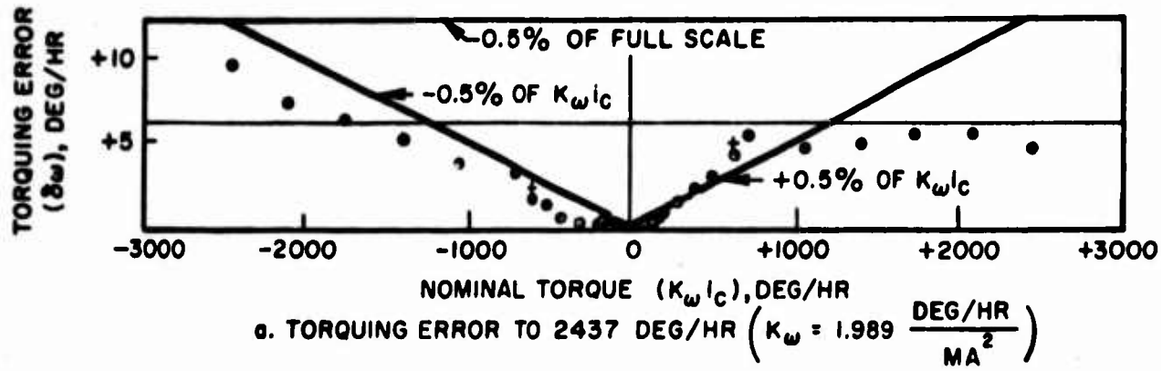

a. TORQUING ERROR TO 2437 DEG/HR $\left(K_\omega = 1.989 \frac{\text{DEG/HR}}{\text{MA}^2}\right)$

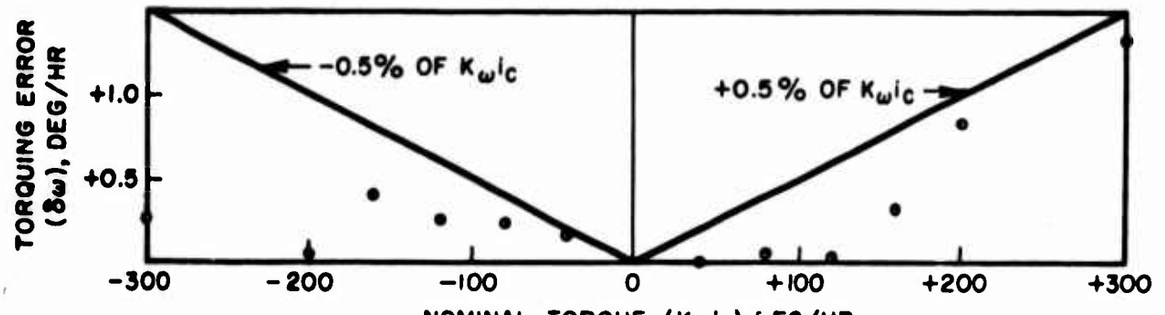

b. TORQUING ERROR TO 298 DEG/HR

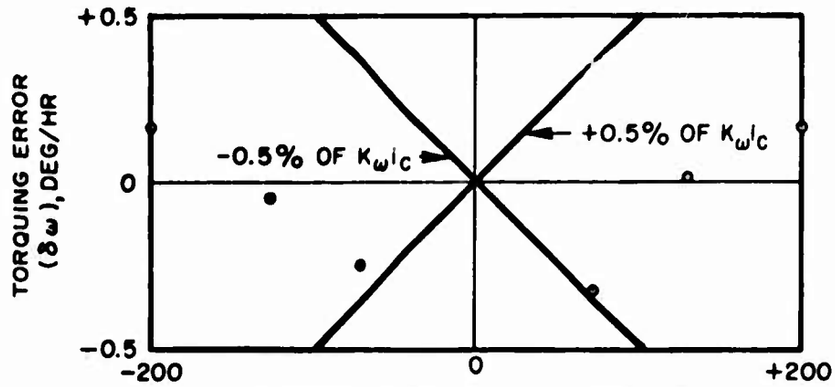

c. TORQUING ERROR TO 200 DEG/HR WITH $i_p = \pm i_c$

$\left(K_\omega = 1.9849 \frac{\text{DEG/HR}}{\text{MA}^2}\right)$

G010

Figure E-2. Torquer Linearity, Gyro K-13.

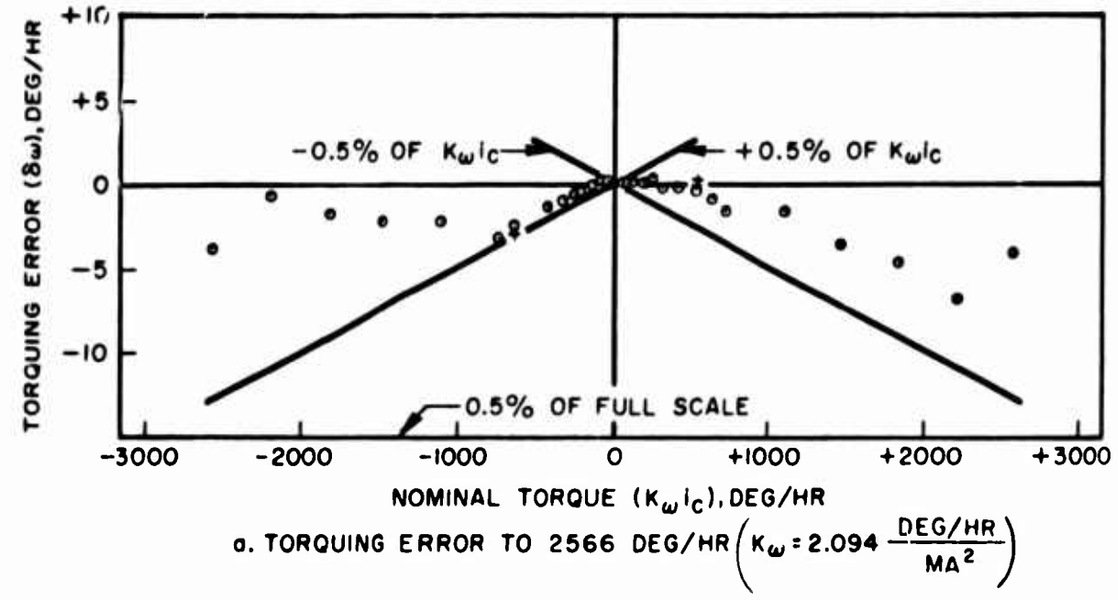

a. TORQUING ERROR TO 2566 DEG/HR $\left(K_\omega = 2.094 \frac{\text{DEG/HR}}{\text{MA}^2}\right)$

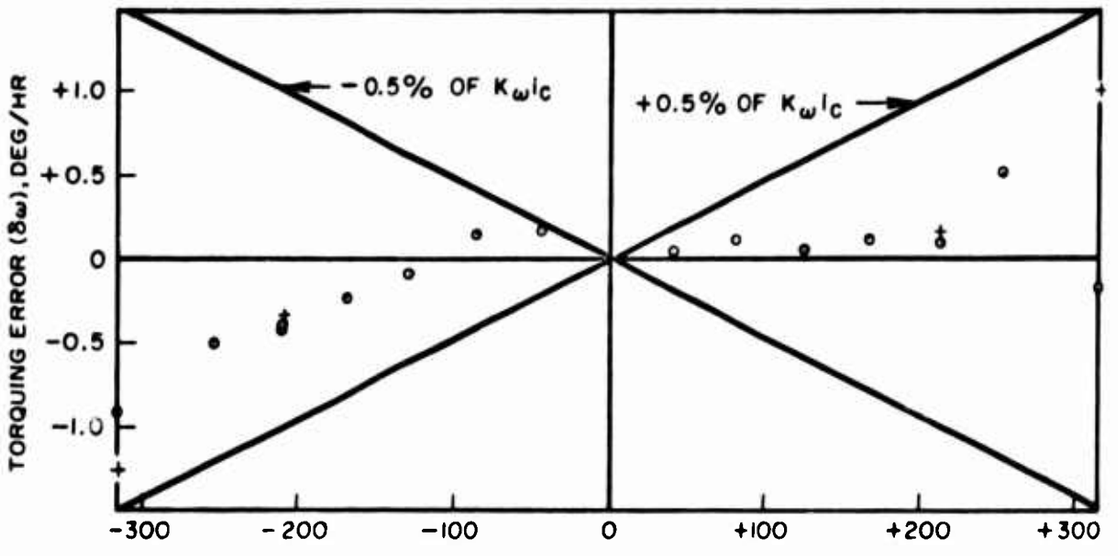

b. TORQUING ERROR TO 314 DEG/HR

Figure E-3. Torquer Linearity, Gyro K-14.

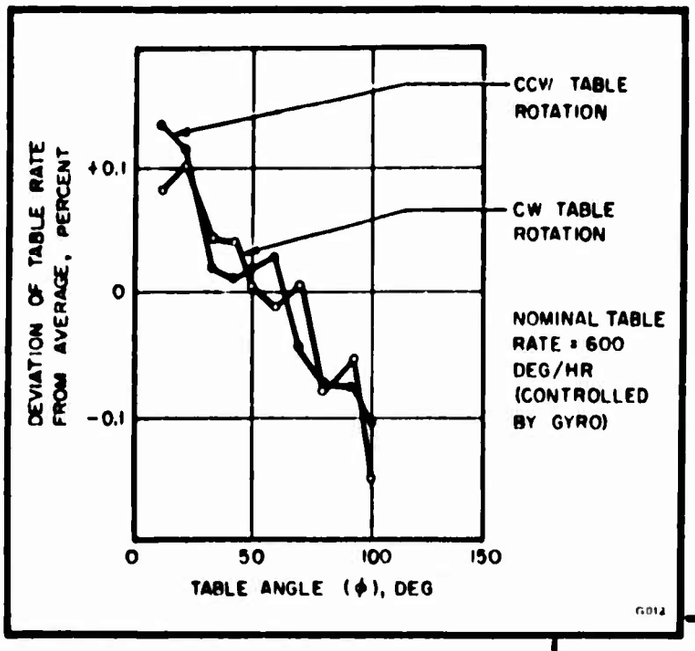

Figure E-4. Table Readout Error Versus Position.

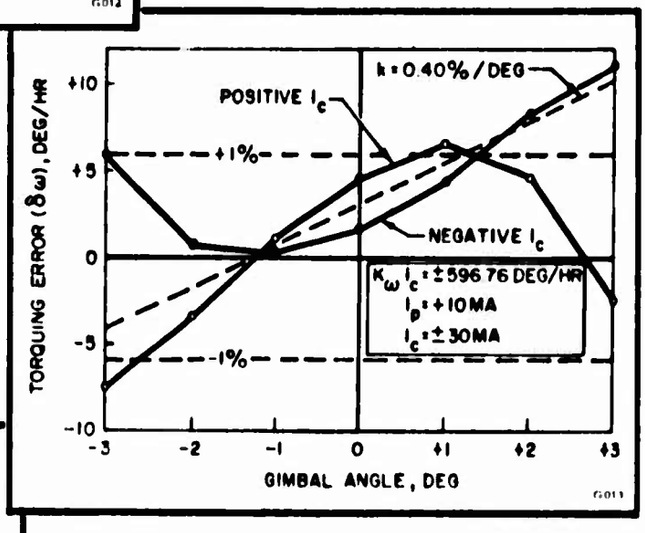

Figure E-5. Torquer Scale Factor Versus Gimbal Angle, Gyro K-13.

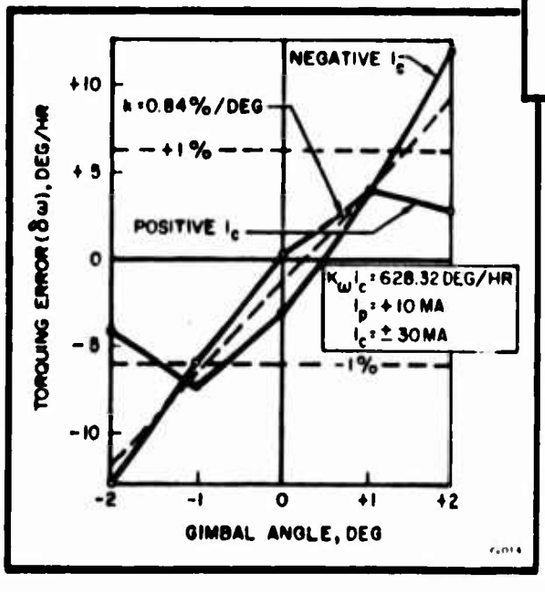

Figure E-6. Torquer Scale Factor Versus Gimbal Angle, Gyro K-14.

APPENDIX F

TUMBLING TESTS

APPENDIX F

TUMBLING TESTS

I. CONTINUOUS TUMBLING TESTS

A. Test Procedure

The tumbling tests were performed with the gyro mounted on the servo table, which was driven at a constant speed of ten times earth's rate by means of a follow-up servo referenced to a synchronous motor. The table axis and the gyro output axis were parallel to the earth's axis, so that no rotation existed about the gyro input axis.

The gyro was operated in the torquer servo mode, with i_c recorded on a strip-chart recorder. The major input to the gyro was the acceleration due to gravity. The vector of this acceleration described a wide cone about the output axis as the servo table rotated, and acted on the gimbal mass unbalance so as to produce a sinusoidal variation of i_c as a function of table position ϕ. The anisoelastic compliance of the gimbal structure produced a sinusoidal variation which was a function of 2ϕ (References 1 and 6), and the reaction torque produced a nonzero average value of i_c.

Preliminary procedures included setting the torquer servo gain to the lowest value which would maintain the signal output voltage e_o below 1 millivolt (i.e., $\theta < 0.2$ milliradian) during the test. The resulting gain was about 0.2 ma/mv for gyro K-13 and 0.1 ma/mv for K-14. This compromise was made in order to keep high-frequency noise on the strip chart at a minimum while at the same time avoiding interference from elastic restraint.

Alignment of the gyro input axis perpendicular to the table axis was accomplished by tilting the gyro about the spin axis until the difference between the torquer control currents measured at table rotations of ω_t = 2500 deg/hr and ω_t = -2500 deg/hr was less than 0.05

milliampere. These readings were made at the same table angle to minimize the effect of mass unbalance. Use of this procedure reduced input-axis misalignment to less than 0.2 milliradian.

Four revolutions of the servo table were made for the tumbling test on each gyro. For the first and third revolutions, the gyro was maintained at its proper operating temperature. For the second revolution, the operating temperature was lowered about 10°F by maintaining the temperature-sensing resistance at 765 ohms; for the fourth revolution, the temperature was raised about 10°F above normal by maintaining the temperature-sensing resistance at 795 ohms.

Figures F-1 and F-2 show two typical records obtained from tumbling tests. The sinusoidal waveform is clear in Figure F-1, showing results for gyro K-13 which has the greater mass unbalance. The 1 deg/hr reaction torque of gyro K-14 appears clearly in Figure F-2 as a zero offset. The various frequency components of gyro uncertainty and servo noise are evident, particularly some large discontinuities which appear to be pivot friction. These large deviations from a smooth sinusoid also appear in both gyros when they are not at nominal operating temperature.

B. Data Processing

Gyro drift coefficients were computed from tumbling test data by the following procedure: The average i_c was measured from the strip-chart recording at 10-degree increments of table angle ϕ. The inputs to the gyro were

$$\omega_{IA} = 0$$

$$\omega_{OA} = 0$$

$$a_S = -g \cos\beta \cos\phi$$

$$a_I = -g \cos\beta \sin\phi .$$

Substituting these values into the performance equation (2) of Section IV, we obtain

$$-\omega_{IO} = -K_\omega i_c = R - U_I g \cos\beta \cos\phi + U_S g \cos\beta \sin\phi + Kg^2 \cos^2\beta \sin 2\phi + \delta\omega .$$

The raw data from the strip-chart recording (i_c versus ϕ) was fitted by Fourier analysis to the equation

$$-K_\omega i_c = A_o - A_1 \cos\phi - B_1 \sin\phi - A_2 \cos 2\phi - B_2 \sin 2\phi - \text{residual.}$$

Comparing these equations, it can be seen that

$$R = +A_0$$

$$U_I = \frac{-A_1}{g \cos\beta}$$

$$U_S = \frac{+B_1}{g \cos\beta}$$

$$K = \frac{+B_2}{g^2 \cos\beta}$$

$$\delta\omega = A_2 \cos 2\phi + \text{residual.}$$

In this report the customary practice was followed of not including $A_2 \cos 2\phi$ in $\delta\omega$. Thus, in the data for tumbling tests

$\delta\omega_{spread}$ = maximum residual - minimum residual, and

$\delta\omega_{rms}$ = rms of residuals

A sample Fourier analysis is shown in Table F-1. This form of analysis is a least-squares fit, minimizing the rms of the residuals. A summary of the data obtained from continuous tumbling tests is shown in Figures F-3 and F-4.

BLANK PAGE

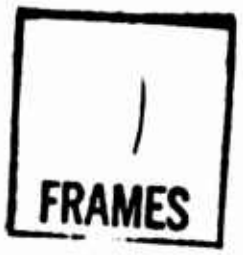

NOTES: 1. Data, column (2) or (3), must appear in equal increments of ϕ with no missed points
2. $\Sigma(6)$ and $\Sigma(20)$ must each be less than n/2000. $\Sigma(15)$, $\Sigma(16)$, $\Sigma(17)$, and $\Sigma(18)$ must each
3. $\Sigma(19)$ must equal $\Sigma(5) \pm n/2000$.

(1)	(2)	(3)	(4)	(5)	(6)	(7)	(8)	(9)	(10
	Tumbling Data	Servo Data	$3600\,\delta\phi/(3)$	$-K_\omega i_p(2)$ or C - (4)	(5) - A_0		(6) (7)		(6) (
ϕ, deg	i_c, ma	δt, sec	ϕ, deg/hr	$-\omega_{IO}$, deg/hr	$-\omega_{IO}-A_0$, deg/hr	cos ϕ	$(-\omega_{IO}-A_0)$ cos ϕ	sin ϕ	$(-\omega_{IO}$ sin
0	-0.160			+3.216	+2.569	+1.000	+2.569	0	
10	-0.130			+2.613	+1.966	+0.985	+1.937	+0.174	+0.3
20	-0.112			+2.251	+1.604	+0.940	+1.508	+0.342	+0.5
30	-0.087			+1.749	+1.102	+0.866	+0.954	+0.500	+0.5
40	-0.082			+1.648	+1.001	+0.766	+0.767	+0.643	+0.6
50	-0.062			+1.246	+0.599	+0.643	+0.385	+0.766	+0.4
60	-0.037			+0.744	+0.097	+0.500	+0.049	+0.866	+0.0
70	-0.012			+0.241	-0.406	+0.342	-0.139	+0.940	-0.3
80	+0.007			-0.141	-0.788	+0.174	-0.137	+0.985	-0.7
90	+0.032			-0.643	-1.290	0	0	+1.000	-1.2
100	+0.047			-0.945	-1.592	-0.174	+0.277	+0.985	-1.5
110	+0.057			-1.146	-1.793	-0.342	+0.613	+0.940	-1.6
120	+0.067			-1.347	-1.994	-0.500	+0.997	+0.866	-1.7
130	+0.075			-1.508	-2.155	-0.643	+1.386	+0.766	-1.6
140	+0.095			-1.910	-2.557	-0.766	+1.959	+0.643	-1.6
150	+0.100			-2.010	-2.657	-0.866	+2.301	+0.500	-1.3
160	+0.085			-1.709	-2.356	-0.940	+2.215	+0.342	-0.8
170	+0.085			-1.709	-2.356	-0.985	+2.321	+0.174	-0.4
180	+0.077			-1.548	-2.195	-1.000	+2.195	0	
190	+0.075			-1.508	-2.155	-0.985	+2.123	-0.174	+0.3
200	+0.055			-1.106	-1.753	-0.940	+1.648	-0.342	+0.6
210	+0.040			-0.804	-1.451	-0.866	+1.257	-0.500	+0.7
220	+0.012			-0.241	-0.888	-0.766	+0.680	-0.643	+0.
230	+0.002			-0.040	-0.687	-0.643	+0.442	-0.766	+0.4
240	-0.020			+0.402	-0.245	-0.500	+0.123	-0.866	+0.2
250	-0.045			+0.905	+0.258	-0.342	-0.088	-0.940	-0.2
260	-0.060			+1.206	+0.559	-0.174	-0.097	-0.985	-0.5
270	-0.085			+1.709	+1.062	0	0	-1.000	-1.0
280	-0.105			+2.111	+1.464	+0.174	+0.255	-0.985	-1.4
290	-0.135			+2.714	+2.067	+0.342	+0.707	-0.940	-1.9
300	-0.145			+2.915	+2.268	+0.500	+1.134	-0.866	-1.9
310	-0.155			+3.116	+2.469	+0.643	+1.588	-0.766	-1.8
320	-0.160			+3.216	+2.569	+0.766	+1.968	-0.643	-1.6
330	-0.165			+3.317	+2.670	+0.866	+2.312	-0.500	-1.3
340	-0.157			+3.156	+2.509	+0.940	+2.358	-0.342	-0.8
350	-0.155			+3.116	+2.469	+0.985	+2.432	-0.174	-0.4
				$\Sigma(5)$ = +23.276	$\Sigma(6)$ = -0.016		$\Sigma(8)$ = +40.999		$\Sigma(10$ -21.0

ω_{IO} = Gyro Drift Rate, $-\omega_{IO} = A_0 + A_1 \cos\phi + B_1 \sin\phi + A_2 \cos 2\phi + B_2 \sin 2\phi$ + residual

$A_0 = \frac{1}{n}\Sigma(5) = +0.647$, $A_1 = \frac{2}{n}\Sigma(8) = 2.278$, $B_1 = \frac{2}{n}\Sigma(10) = -1.168$, $A_2 = \frac{2}{n}\Sigma(12) = +0.029$, $B_2 = \frac{2}{n}\Sigma$

n = no. of equally spaced, nonrepeated data points.
n = 36 for ϕ every 10 deg
n = 12 for ϕ every 30 deg

Tumbling Test
$-\omega_{IO} = -1\ \omega\ ^1c$
$K_\omega = 20.1 \frac{\text{deg/hr}}{\text{ma}}$
$i_p = 10\ \text{ma}_1{}^1c$ in (2)

Servo Test $-\omega_{IO} = -\overline{IA} \times \bar{\omega}_\epsilon - 3600\,\delta\phi$
$\delta\phi =$ _____ deg
δt ☐ sidereal, ☐ solar
list δt versus ϕ in (3)

IA‖TA oriented

C = $-\overline{IA} \times \bar{\omega}_\epsilon$	δt sidere
	δt solar

Table F-1. Sample Fourier Analysis of Tumbling Data for Gyro K-13.

nts.
ch equal 0.

(10)	(11)	(12)	(13)	(14)	(15)	(16)	(17)	(18)	(19)	(20)	(21)
) (9)		(6) (11)		(6) (13)	A_1 (7)	B_1(9)	A_2(11)	B_2(13)	A_0+(15)+(16)+(17)+(18)	(5)-(19)	$(20)^2$
$\omega_{IO}-A_0$) in ϕ	cos 2ϕ	$(-\omega_{IO}-A_0)$ cos 2ϕ	sin 2ϕ	$(-\omega_{IO}-A_0)$ sin 2ϕ	A_1 cos ϕ	B_1 sin ϕ	A_2 cos 2ϕ	B_2 sin 2ϕ	$-\omega_{IO}$- Res., deg/hr	Residual, deg/hr	$(Res)^2$
0	+1.000	+2.569	0	0	+2.278	0	+0.029	0	+2.954	+0.262	0.0682
.342	-0.940	+1.848	+0.342	+0.672	+2.244	-0.203	+0.027	-0.030	+2.685	-0.072	0.0053
.549	+0.766	+1.229	+0.643	+1.031	+2.141	-0.399	+0.022	-0.057	+2.354	-0.103	0.0106
.551	+0.500	+0.551	+0.866	+0.954	+1.973	-0.584	+0.015	-0.076	+1.975	-0.226	0.0510
.644	+0.174	+0.174	+0.985	+0.986	+1.745	-0.751	+0.005	-0.087	+1.559	+0.089	0.0080
.459	-0.174	-0.104	+0.985	+0.590	+1.465	-0.895	-0.005	-0.087	+1.125	+0.121	0.0146
.084	-0.500	-0.049	+0.866	+0.084	+1.139	-1.011	0.015	-0.076	+0.684	+0.060	0.0036
.382	-0.766	+0.311	+0.643	-0.261	+0.779	-1.098	-0.022	-0.057	+0.249	-0.008	0.0001
.776	-0.940	+0.741	+0.342	-0.269	+0.396	-1.150	-0.027	-0.030	-0.164	+0.023	0.0005
.290	-1.000	+1.290	0	0	0	-1.168	-0.029	0	-0.550	-0.093	0.0086
.568	-0.940	+1.496	-0.342	+0.544	-0.396	-1.150	-0.027	+0.030	-0.896	-0.049	0.0024
.685	-0.766	+1.373	-0.643	+1.153	-0.779	-1.098	-0.022	+0.057	-1.195	+0.049	0.0024
.727	-0.500	+0.997	-0.866	+1.727	-1.139	-1.011	-0.015	+0.076	-1.442	+0.095	0.0090
.651	-0.174	+0.375	-0.985	+2.123	-1.465	-0.895	-0.005	+0.087	-1.631	+0.123	0.0151
.644	+0.174	-0.445	-0.985	+2.519	-1.745	-0.751	+0.005	+0.087	-1.757	-0.153	0.0234
.329	+0.500	-1.329	-0.866	+2.301	-1.973	-0.584	+0.015	+0.076	-1.819	-0.191	0.0365
.806	+0.766	-1.805	-0.643	+1.515	-2.141	-0.399	+0.022	+0.057	-1.814	+0.105	0.0110
.410	+0.940	-2.215	-0.342	+0.806	-2.244	-0.203	+0.027	+0.030	-1.743	+0.034	0.0012
0	+1.000	-2.195	0	0	-2.278	0	+0.029	0	-1.602	+0.054	0.0024
.375	+0.940	-2.026	+0.342	-0.737	-2.244	+0.203	+0.027	-0.030	-1.397	-0.111	0.0123
.600	+0.766	-1.343	+0.643	-1.127	-2.141	+0.399	+0.022	-0.057	-1.130	+0.024	0.0006
.726	+0.500	-0.726	+0.866	-1.257	-1.973	+0.584	+0.015	-0.076	-0.803	-0.001	0
.571	+0.174	-0.155	+0.985	-0.875	-1.745	+0.751	+0.005	-0.087	-0.429	+0.188	0.0353
.496	-0.174	+0.120	+0.985	-0.677	-1.465	+0.895	-0.005	-0.087	-0.015	-0.025	0.0006
.212	-0.500	+0.123	+0.866	-0.212	-1.139	+1.011	-0.015	-0.076	+0.428	-0.026	0.0007
.243	-0.766	-0.198	+0.643	+0.166	-0.779	+1.098	-0.022	-0.057	+0.887	+0.018	0.0003
.551	-0.940	-0.525	+0.342	+0.191	-0.396	+1.150	-0.027	-0.030	+1.344	-0.138	0.0190
.062	-1.000	-1.062	0	0	0	+1.168	-0.029	0	+1.786	-0.077	0.0059
.442	-0.940	-1.376	-0.342	-0.501	+0.396	+1.150	-0.027	+0.030	+2.196	-0.085	0.0072
.943	-0.766	-1.583	-0.643	-1.329	+0.779	+1.098	-0.022	+0.057	+2.559	+0.155	0.0240
.964	-0.500	-1.134	-0.866	-1.964	+1.139	+1.011	-0.015	+0.076	+2.858	+0.057	0.0032
.891	-0.174	-0.430	-0.985	-2.432	+1.465	+0.895	-0.005	+0.087	+3.089	+0.027	0.0007
.652	+0.174	+0.447	-0.985	-2.530	+1.745	+0.751	+0.005	+0.087	+3.235	-0.019	0.0004
.335	+0.500	+1.335	-0.866	-2.312	+1.973	+0.584	+0.015	+0.076	+3.295	+0.022	0.0005
.858	+0.766	+1.922	-0.643	-1.613	+2.141	+0.399	+0.022	+0.057	+3.266	-0.110	0.0121
.430	+0.940	+2.321	-0.342	-0.844	+2.244	+0.203	+0.027	+0.030	+3.151	-0.035	0.0012
(10) = 030		Σ(12) = +0.522		Σ(14) = -1.578	Σ(15) = 0	Σ(16) = 0	Σ(17) = 0	Σ(18) = 0	Σ(19) = +23.292	Σ(20) = -0.016	Σ(21) = 0.3984

$\Sigma(14) = -0.088$, $\sigma = \sqrt{\Sigma(21)/n} = +0.11$

$\delta\phi/\delta t$

d	EA, south	Vertical, down	Horizontal, south	Horizontal, E-W
real	15.000	8.369	12.448	0
r	15.041	8.392	12.482	0

C. Results

The outstanding characteristic of gyro performance during tumbling tests was the large, long-duration drift excursions appearing clearly in tumbling tests 1, 2, 3, 7, and 9 and to a lesser extent in all remaining tumbling tests. The view that this phenomenon results from pivot friction is borne out by the fact that it was intensified at low operating temperatures on both gyros.

The record of gyro K-13 indicates that its operating temperature is about $10^{\circ}F$ below the temperature for proper flotation, which might occur if the padding resistor on the temperature-sensing winding were chosen to adjust the damping constant C rather than the flotation temperature. This phenomenon was not discovered in the mass unbalance test, the cogging test, or in any other standard production test performed by Minneapolis-Honeywell on MIG gyros.

The accuracy of measurement of the drift coefficients R, U_I, and U_S is probably well within ±0.10 deg/hr where the friction is small, as in tests 4, 6, and 8. The value of R may be influenced by the output impedances of the source of excitation, in this case of the servo table electronics. The anisoelastic coefficient K is largely masked by the random drift, even on the best of the test runs. The value of the Fourier coefficient A_2, which has little meaning,* is often of greater magnitude than B_2. $\delta\omega_{rms}$ might be interpreted as a short-term (4-minute) random drift rate where A_2 is small or included.

II. STEPWISE TUMBLING TESTS

The discontinuous behavior shown, especially by gyro K-13, during tumbling tests did not appear in the bench drift tests. On the supposition that tumbling-test phenomenon resulted from the slow, steady rotation of the table (causing side loading of the OA pivots as well as a rotating

*A_2 is a measure of $K_{SI} + K_{IS}$, both of which were found during vibration tests to be very small.

gravity vector), it was decided that a new type of tumbling test would be performed in which the gyro would be rotated about the OA in 10-degree steps and the measurement of i_c would be made with the gyro at rest. The advantages of such a procedure are:

a. The test can be performed on a machinist's dividing head or other simple fixture; a rate table is not required.

b. The test can be completed in a much shorter period of time than can a continuous tumbling test, since the gyro can be moved rapidly from step to step.

c. Side loading on the OA pivots is reduced about ten times,* greatly reducing pivot friction.

d. The acceleration and deceleration of the gyro about the output axis should eliminate any tendency to stiction.

It was expected that the stepwise tumbling test would produce a better measurement of mass unbalance and reaction torque than the continuous tumbling tests and in a shorter period of time. It was hoped that a significant measurement of the anisoelastic coefficient might also be obtained with this procedure.

The stepwise tumbling tests were performed with the output axis parallel to earth's axis, using instrumentation similar to that of the continuous tumbling tests except that the gyro was excited by the gyro test set and was mounted in a Hauser dividing head, as shown in Figure F-5. A typical strip-chart recording of the torquer current for this test is shown in Figure F-6. Data reduction was performed as for the continuous tumbling tests.

Figure F-7 shows the data obtained for gyro K-14. The test of 23 November used a milliameter for data readout. Test 1 of 1 December was run at a higher torquer servo gain than tests 2 and 3, and this higher gain may have interacted with the recorder to cause an error in measurement of reaction torque.

---

*The residual side loading results from earth's rate, which is still present.

An interesting conjecture is suggested by the waveforms of $\delta\omega$ versus ϕ for tests 1 and 3 of 1 December. Figure F-8 shows some of the waveforms which might be expected if the plastic ball separators used in the spin-axis bearings were loose and shifted axially as the spin axis approached the horizontal, or shifted radially as the spin axis approached the vertical. Using an estimate of 50 milligrams for the total weight of the separators, we find that a shift of 0.001 inch would cause a mass unbalance shift of about 0.25 deg/hr. Such a shift could easily account for a large portion of the observed uncertainty. If the separator were free to move in any direction with no friction, the shift would not be detectable; however, this hypothesis appears most unlikely.

A further observation of interest is the somewhat greater settling time appearing in Figure F-6 for table angles as the spin axis approaches the horizontal. This characteristic appeared only in the stepwise tumbling tests.

Figure F-9 makes a point-by-point comparison of the three stepwise tumbling tests performed on gyro K-14 on 1 December. It corroborates strongly the changes in reaction torque and mass unbalance determined by harmonic analysis.

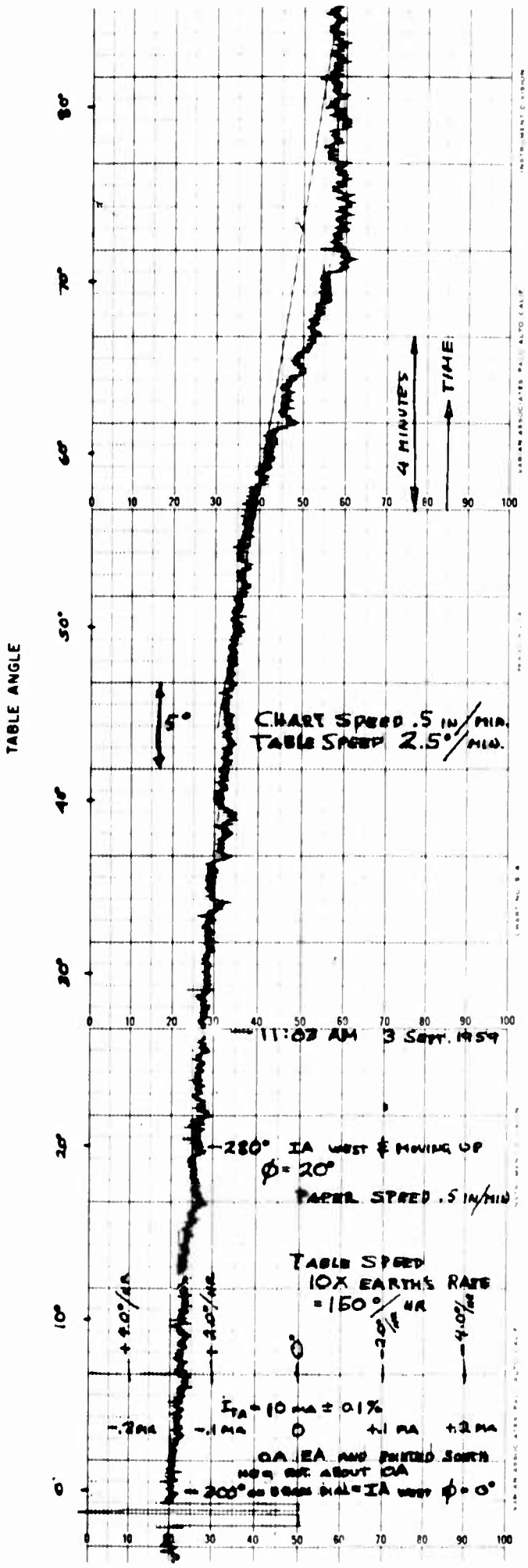

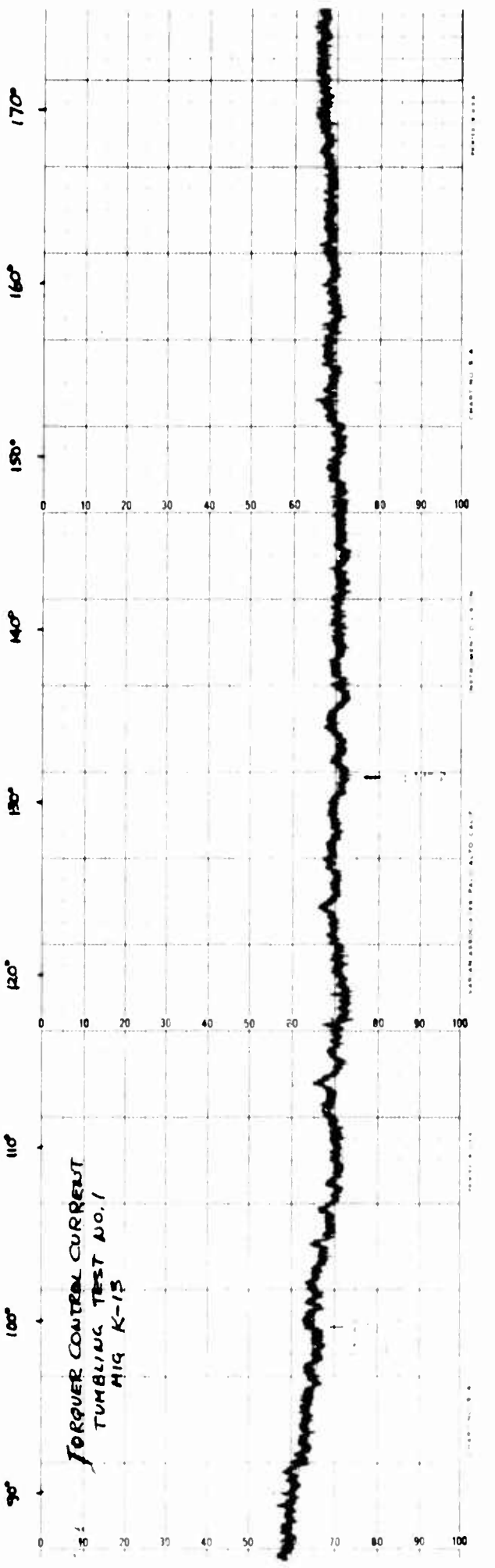

Figure F-1. Strip-Chart Recording of Tumbling Test 1, Gyro K-13.

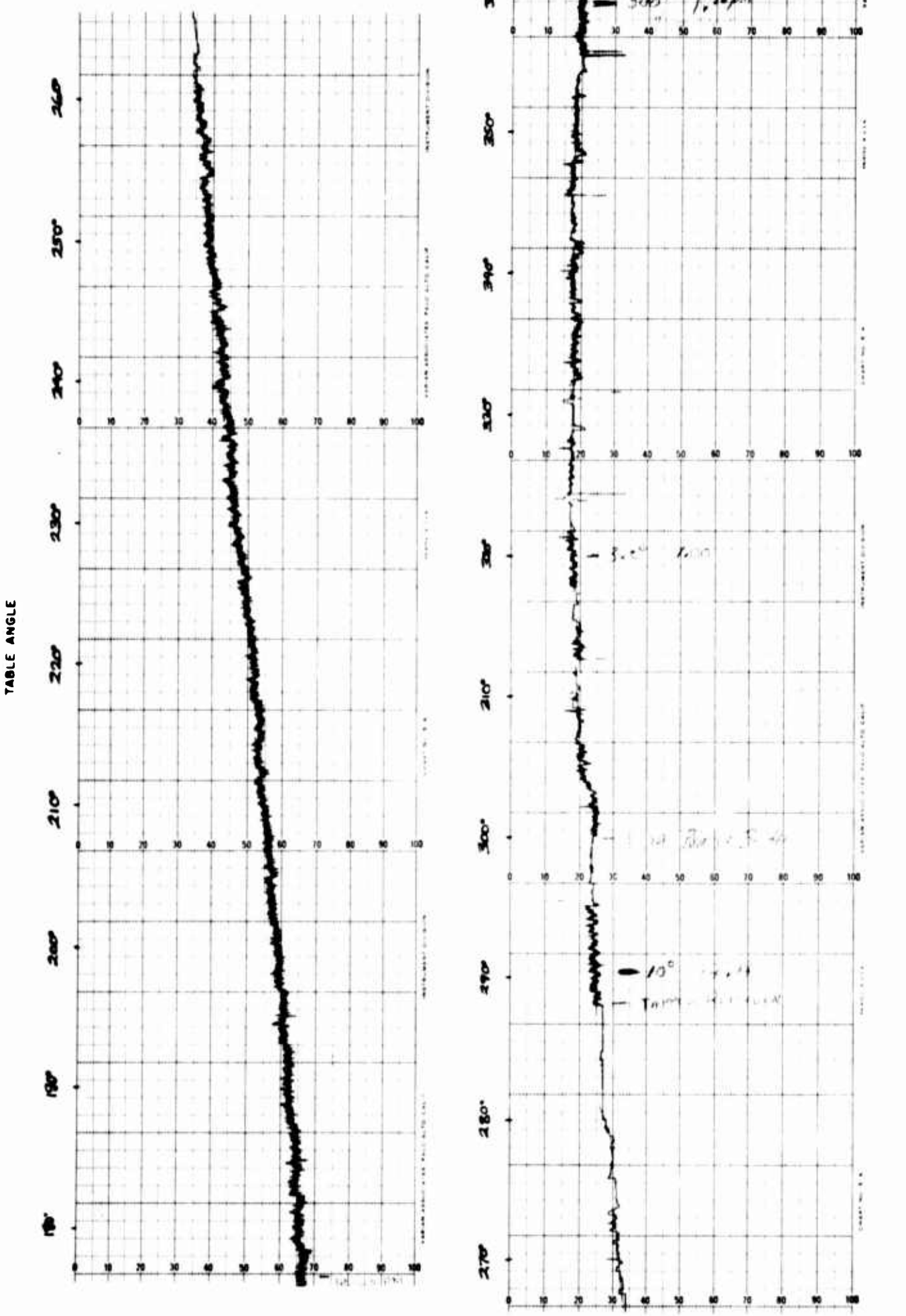

Figure F-1. (Continued).

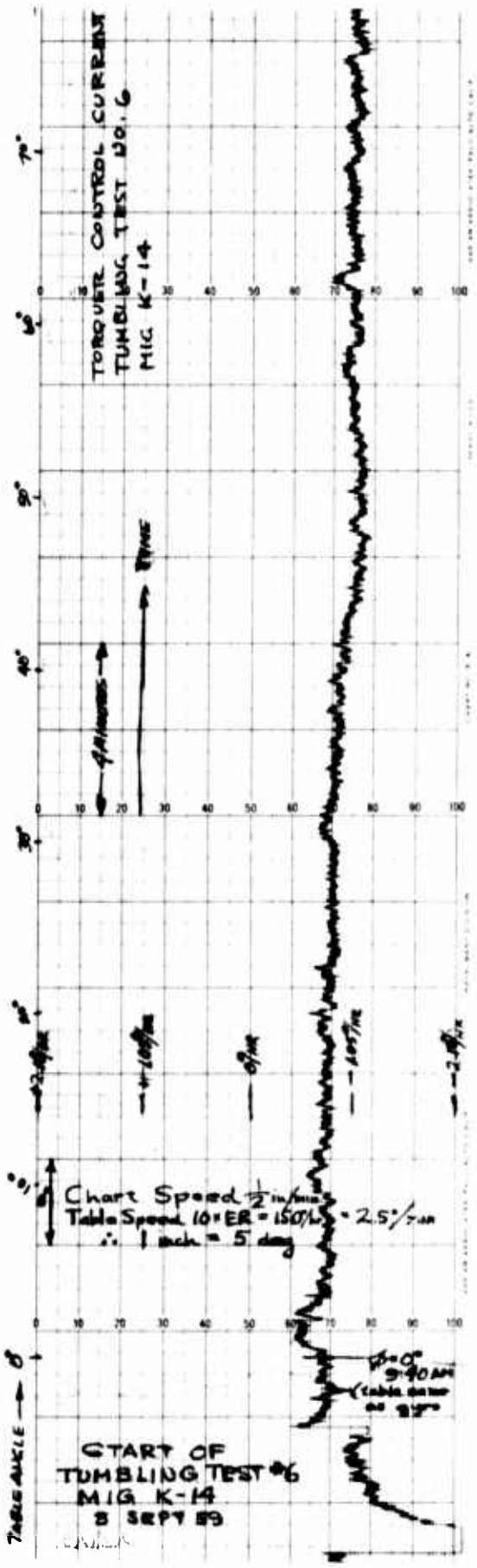

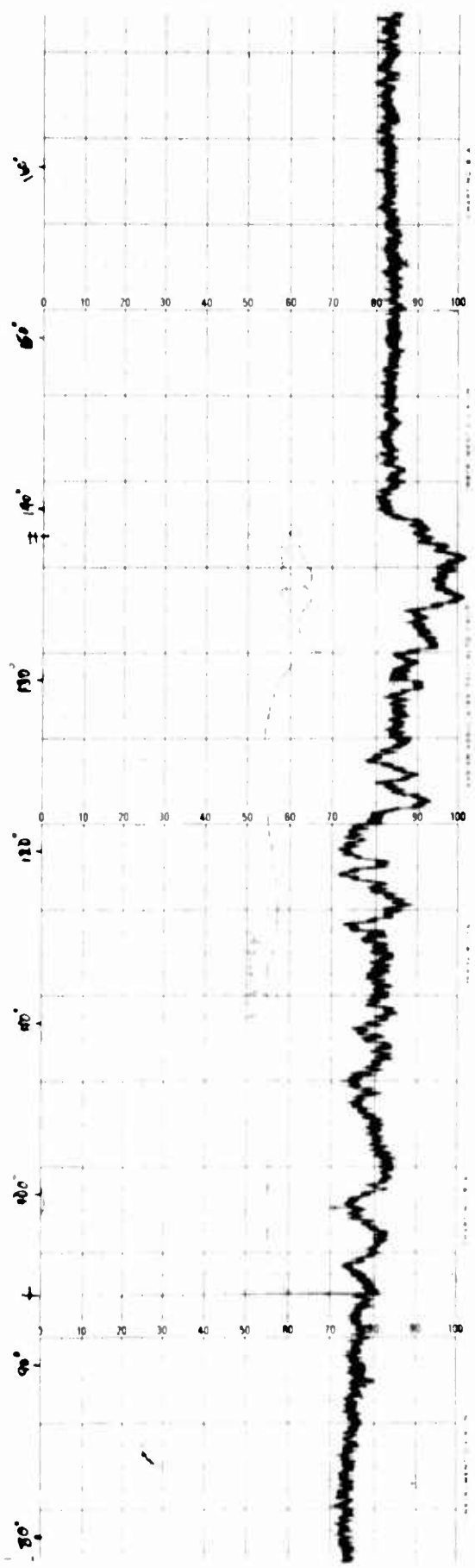

Figure F-2. Strip-Chart Recording of Tumbling Test 6, Gyro K-14.

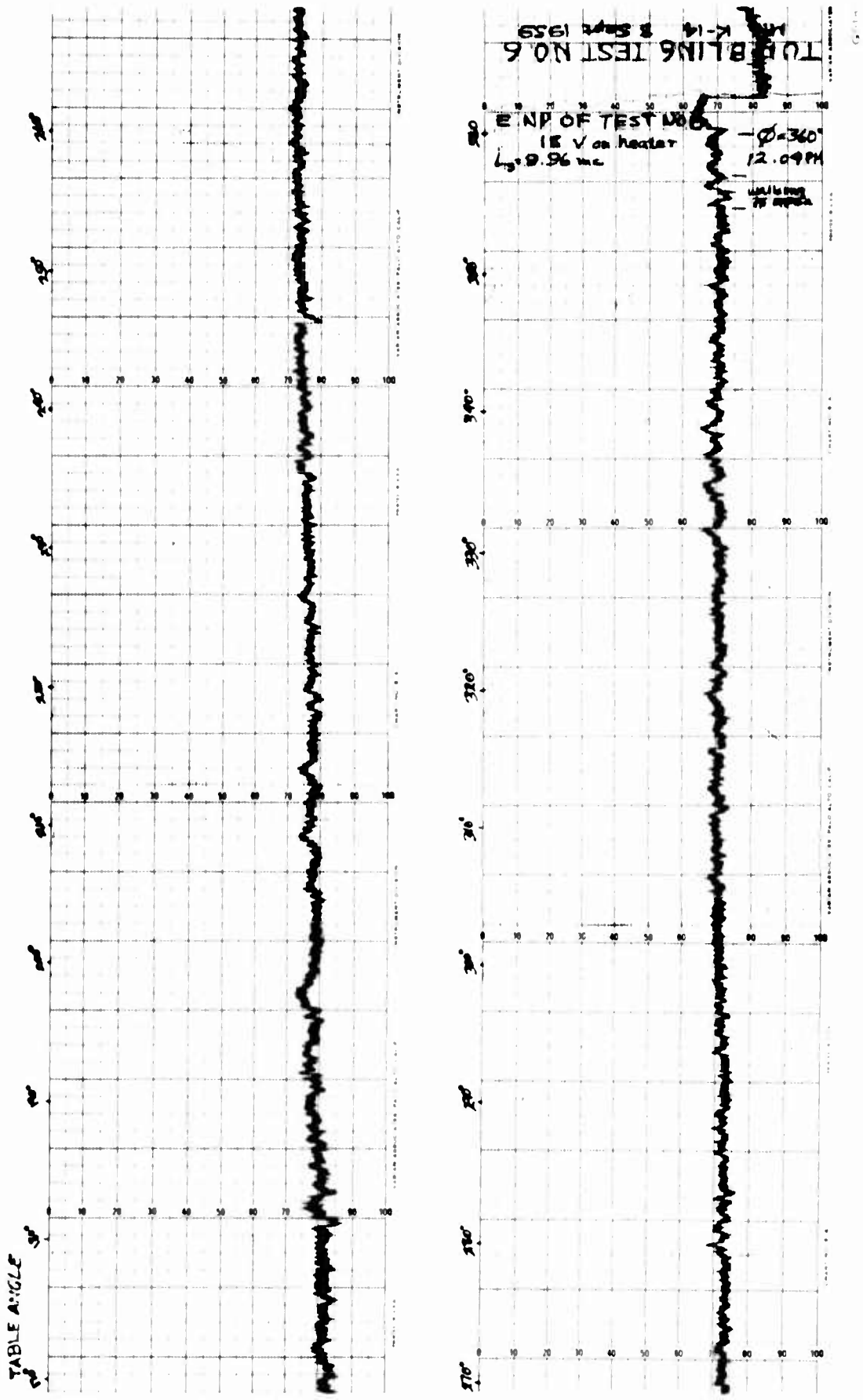

Figure F-2. (Continued).

TUMBLING TEST 1

3 SEP 1959

−OA PARALLEL TO EA

STANDARD EXCITATIONS

$R = +0.59$ DEG/HR

$U_I = +2.80 \frac{\text{DEG/HR}}{G}$

$U_S = +1.61 \frac{\text{DEG/HR}}{G}$

$K = +0.21 \frac{\text{DEG/HR}}{G^2}$

$A_2 = +0.06$ DEG/HR

$\delta\omega_{RMS} = 0.23$ DEG/HR

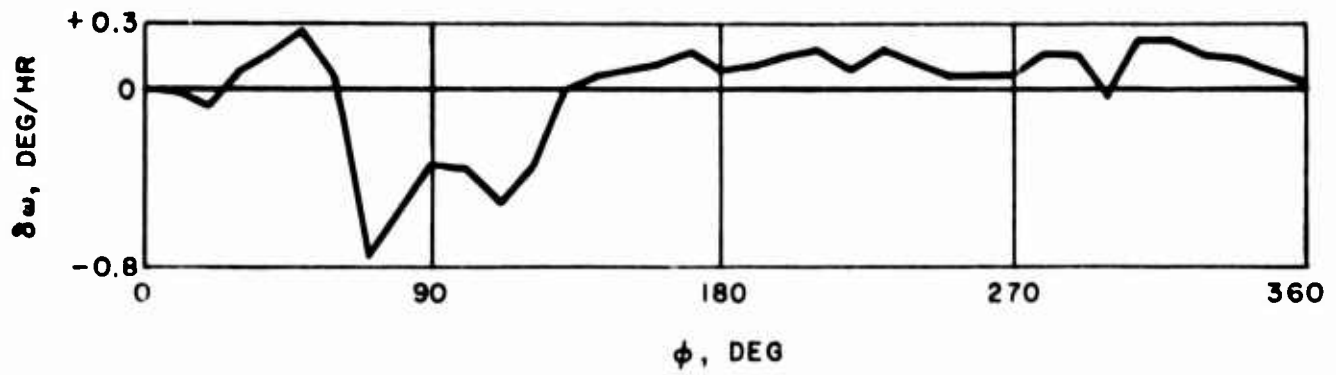

TUMBLING TEST 3

4 SEP 1959

−OA PARALLEL TO EA

STANDARD EXCITATIONS

$R = +0.55$ DEG/HR

$U_I = +2.92 \frac{\text{DEG/HR}}{G}$

$U_S = +1.85 \frac{\text{DEG/HR}}{G}$

$K = +0.22 \frac{\text{DEG/HR}}{G^2}$

$A_2 = +0.36$ DEG/HR

$\delta\omega_{RMS} = 0.20$ DEG/HR

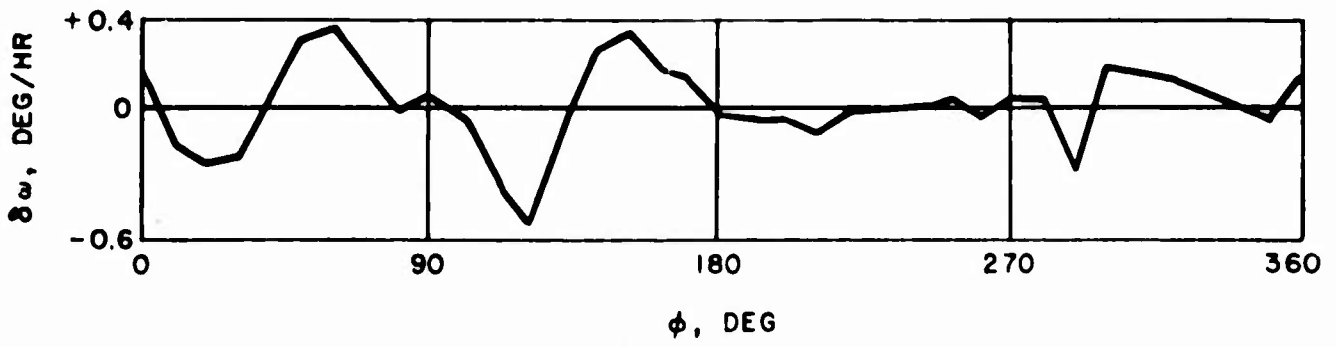

a. NOMINAL OPERATING TEMPERATURE

Figure F-3. Tumbling Test Data Summary, Gyro K-13.

TUMBLING TEST 2

3 SEP 1959

- OA PARALLEL TO EA

OPERATING TEMPERATURE 10°F LOW

$R = +0.51$ DEG/HR

$U_I = +2.67 \frac{\text{DEG/HR}}{G}$

$U_S = +1.85 \frac{\text{DEG/HR}}{G}$

$K = +0.21 \frac{\text{DEG/HR}}{G^2}$

$A_2 = +0.30$ DEG/HR

$\delta\omega_{RMS} = 0.37$ DEG/HR

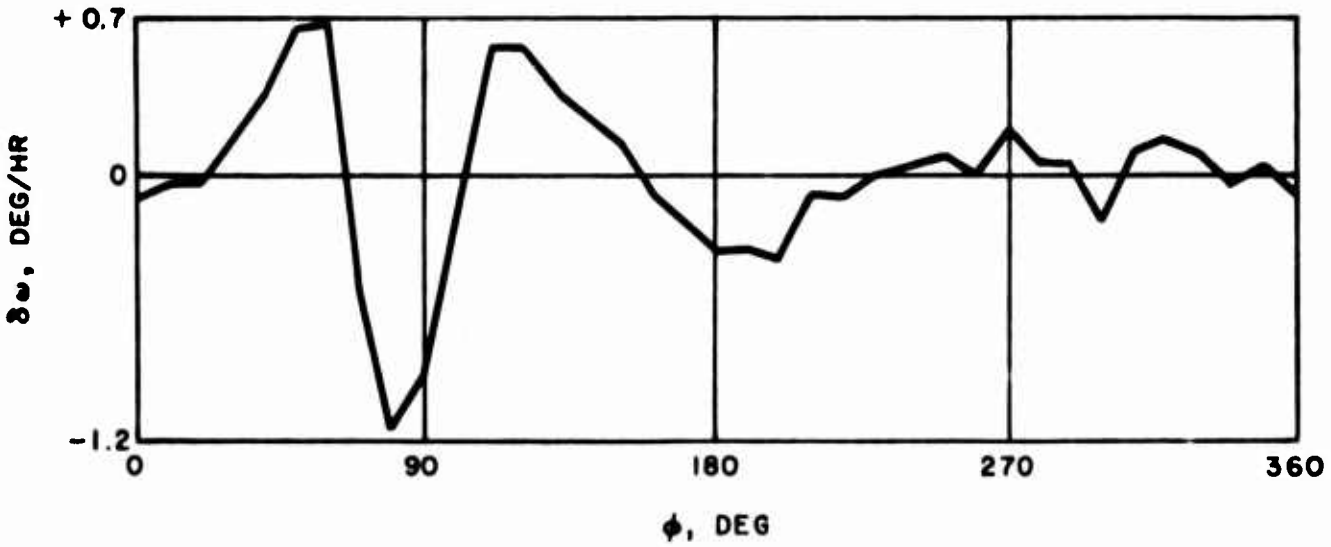

TUMBLING TEST 4

4 SEP 1959

- OA PARALLEL TO EA

OPERATING TEMPERATURE 10°F HIGH

$R = +0.65$ DEG/HR

$U_I = +2.75 \frac{\text{DEG/HR}}{G}$

$U_S = +1.41 \frac{\text{DEG/HR}}{G}$

$K = -0.13 \frac{\text{DEG/HR}}{G^2}$

$A_2 = +0.03$ DEG/HR

$\delta\omega_{RMS} = 0.11$ DEG/HR

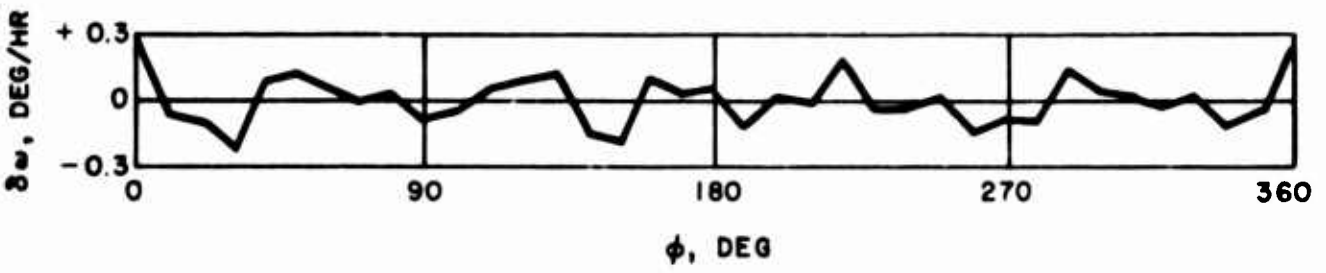

b. NON-NOMINAL OPERATING TEMPERATURE

Figure F-3. (Continued).

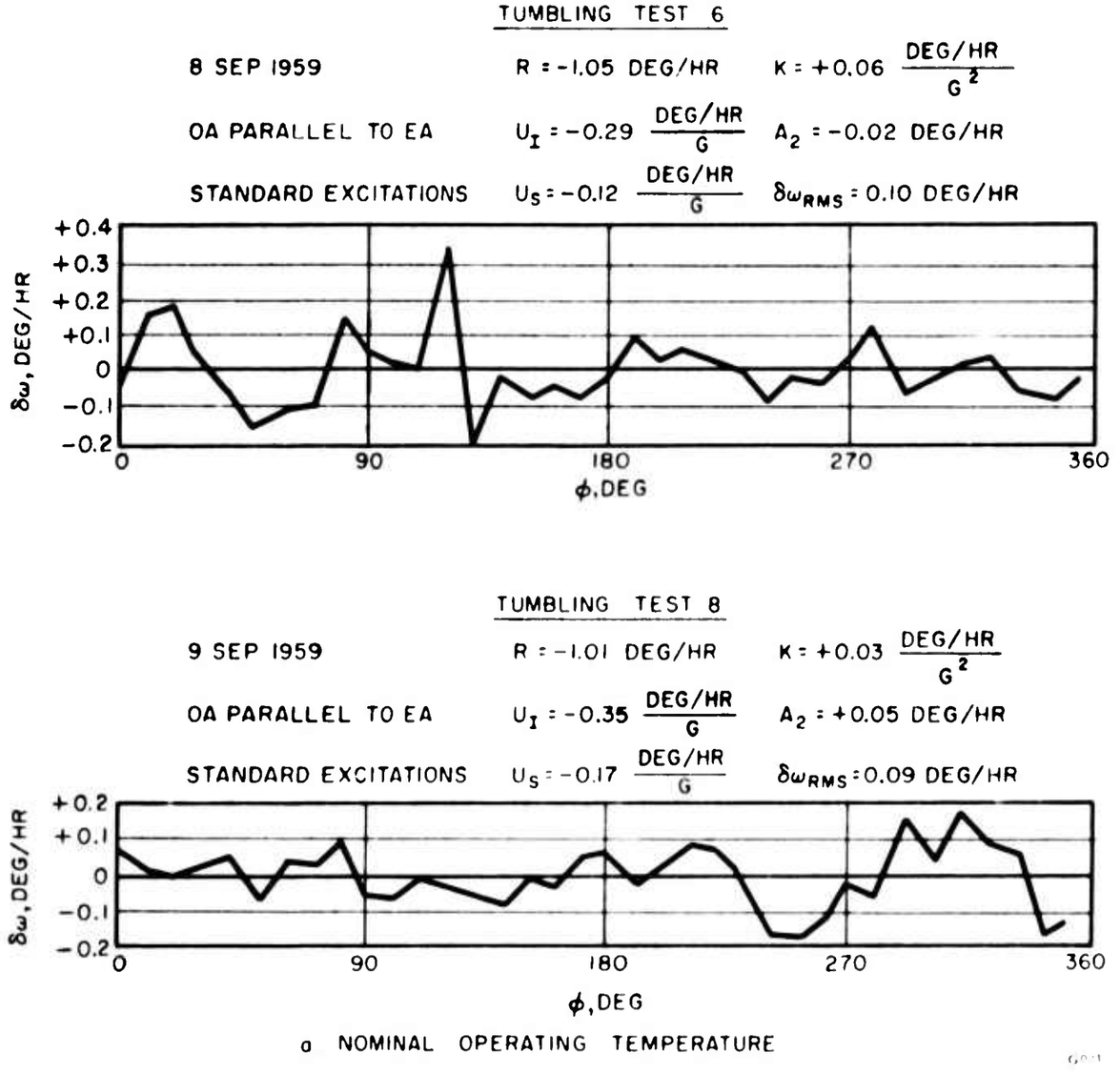

Figure F-4. Tumbling Test Data Summary, Gyro K-14.

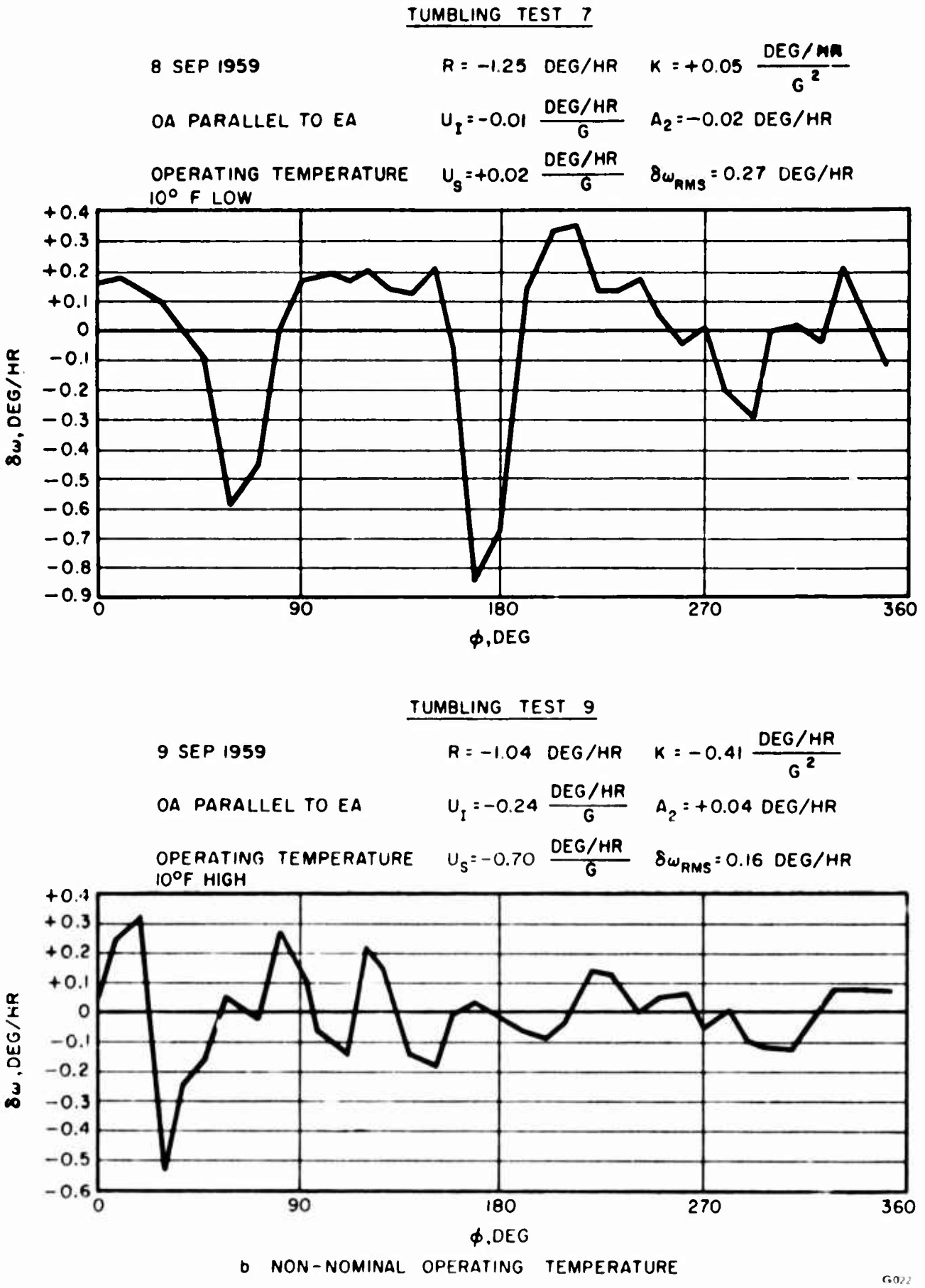

b NON-NOMINAL OPERATING TEMPERATURE

G022

Figure F-4. (Continued)

Figure F-5. Improved Holding Fixture Mounted on Hauser Dividing Head.

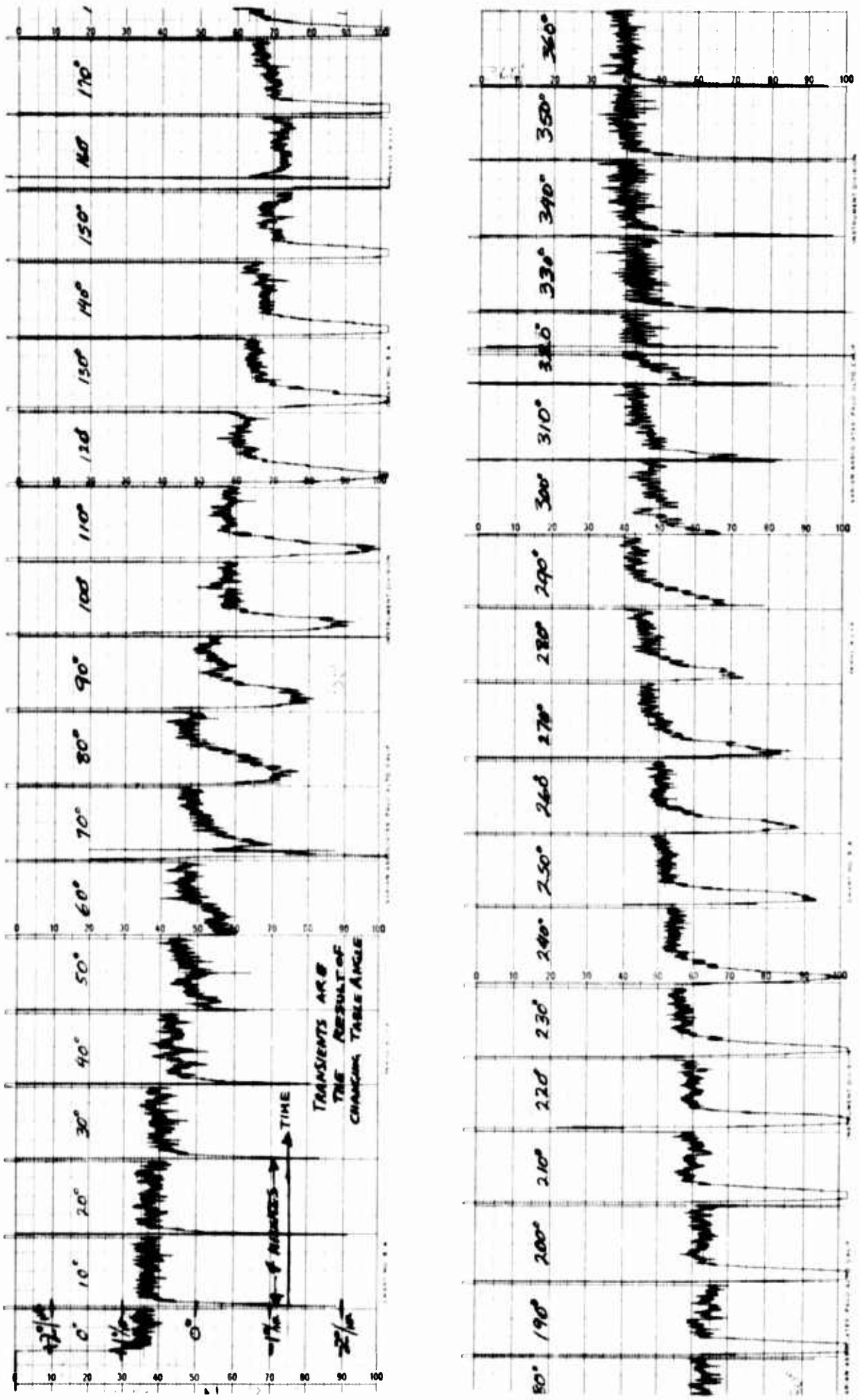

Figure F-6. Typical Strip-Chart Recording of Stepwise Tumbling Test.

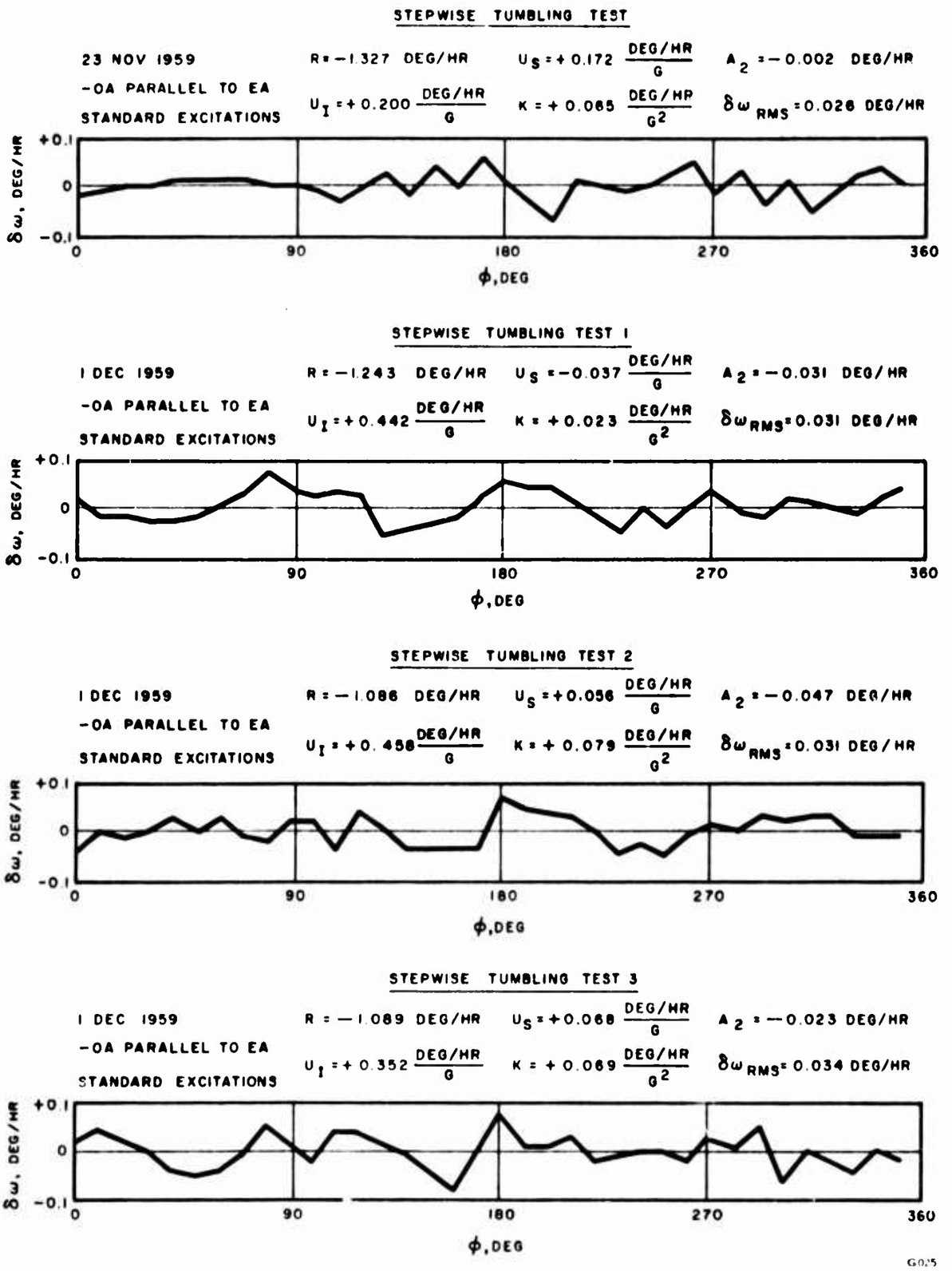

Figure F-7. Stepwise Tumbling Test Data Summary, Gyro K-14.

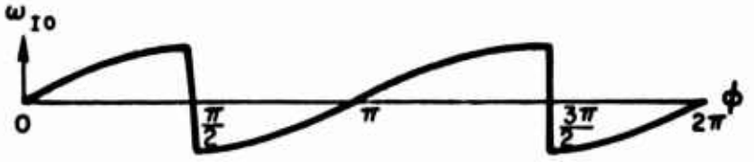

a. DRIFT DUE TO AXIAL MASS SHIFT WHEN SPIN AXIS IS HORIZONTAL; ASSUME TUMBLING TEST WITH $-OA$ PARALLEL TO EA, ROTATION NEGATIVE ABOUT OA, AS IN STEPWISE TUMBLING TESTS

b. BEST FIT, SECOND HARMONIC CORRECTION AS DETERMINED BY FOURIER ANALYSIS

c. FORM OF RESIDUALS ($c = a - b$) FOR AXIAL MASS SHIFT; SEE PLOTS OF $\delta\omega$ VERSUS ϕ FOR STEPWISE TUMBLING TESTS 1 AND 3 ON 1 DECEMBER 1959

d. DRIFT DUE TO RADIAL MASS SHIFT WHEN SPIN AXIS IS VERTICAL UNDER SAME CONDITIONS

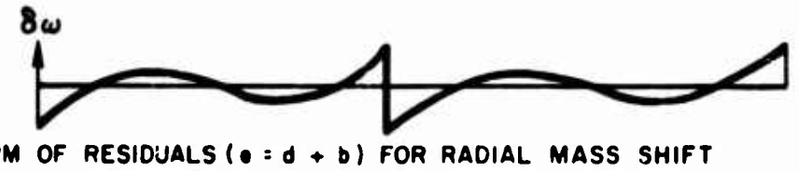

e. FORM OF RESIDUALS ($e = d + b$) FOR RADIAL MASS SHIFT

f. FORM OF RESIDUALS ($\delta\omega$) FOR EQUAL AXIAL AND RADIAL MASS SHIFTS; THIS IS $a + d$; SECOND HARMONIC OR B_2 TERM IS ZERO, BUT FOURTH AND HIGHER HARMONICS ARE PRESENT

G027

Figure F-8. Waveforms of Residuals Which Might be Caused by Bearing Retainer Mass Shift.

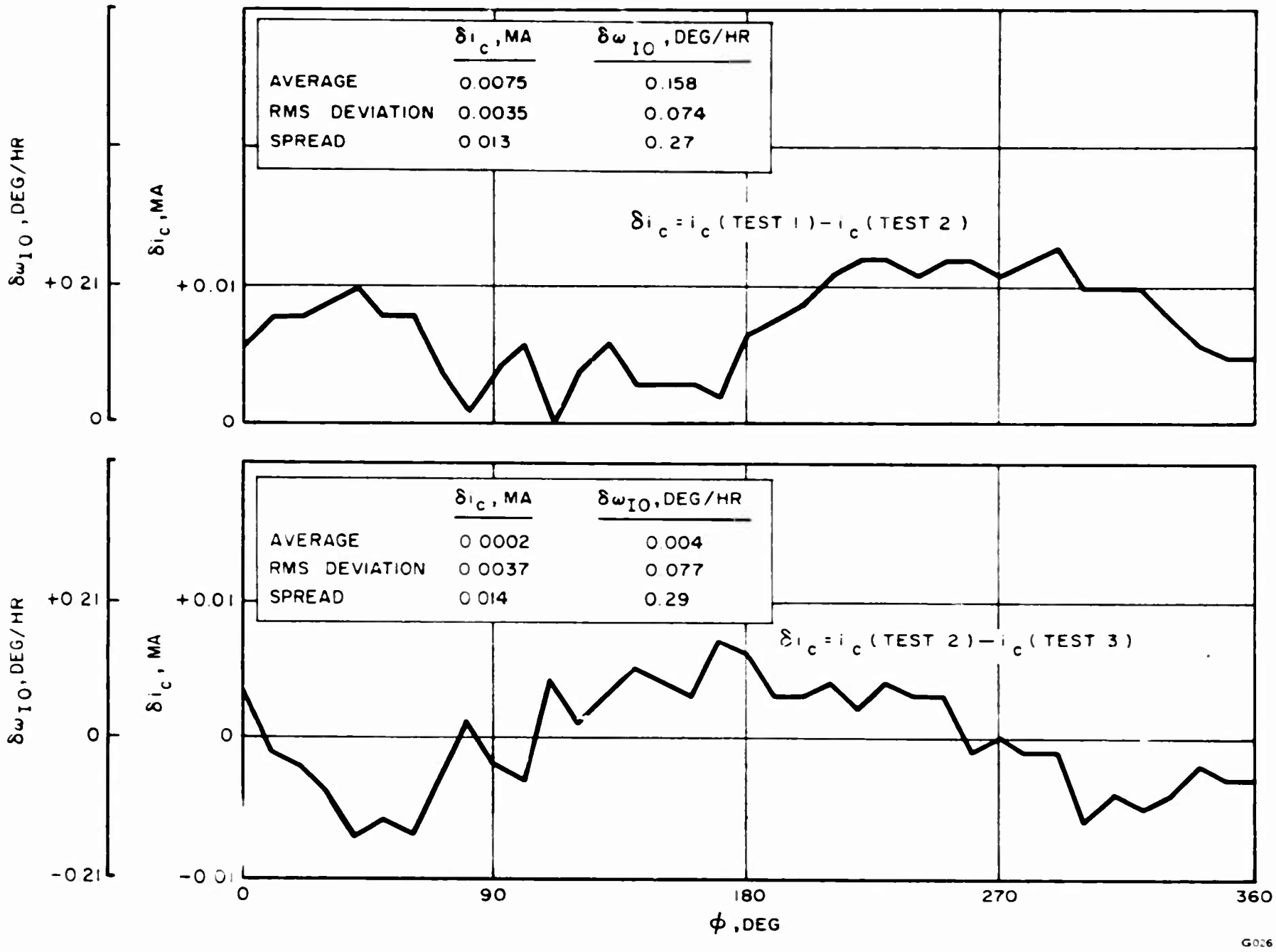

Figure F-9. Point-by-Point Comparison of Stepwise Tumbling Tests, Gyro K-14, 1 December 1959.

APP. NDIX G

SERVO AND COGGING TESTS

APPENDIX G

SERVO AND COGGING TESTS

I. SERVO TESTS

In servo tests the gyro is used to stabilize the servo table in inertial space in the same manner as it would stabilize one axis of a stable platform. The apparent rate of rotation of the table with respect to the earth is then $-\omega_e \cos \psi$, where ψ is the angle between the gyro input axis and the earth's polar axis. Any drift of the gyro results in a departure from this rate.

The gyro input axis was made parallel to the table axis and no torquer control current was applied, so the equation of table rate becomes $\omega_t = \omega_{IO} - \omega_e \cos \psi$.

The servo test was run with the gyro input axis in three orientations: parallel to negative earth's axis, horizontal and south, and vertical down. With gravity inputs to the gyro evaluated in the same manner as for the tumbling tests, the test equations become for IA parallel to -EA:

$$-\omega_{IO} = 15 - \omega_t = -\omega_{IA} = R - U_S g \sin \beta$$

$$+ (-U_I g \cos \beta + K g^2 \sin 2\beta) \cos \varphi + \delta\omega \quad ;$$

for IA horizontal:

$$-\omega_{IO} = 12.448 - \omega_t = -\omega_{IA} = R - U_I g \cos \varphi + \delta\omega \quad ;$$

and for IA vertical:

$$-\omega_{IO} = 8.369 - \omega_t = -\omega_{IA} = R + U_S g + \delta\omega \quad .$$

These equations assume a sidereal time base and Los Angeles lattitude, and neglect minor compliances. $\delta\omega$ is the residual obtained from a Fourier analysis of the data. Table rotation rate ω_t was measured as $\delta\phi/\delta t$ and computed for each 10 degrees of table rotation.

The test data was fitted by Fourier analysis to obtain A_0, A_1, B_1, A_2, B_2, and residuals, as in the tumbling tests. Results of the analysis are shown in Figures G-1 and G-2. It will be noted that the servo test data for gyro K-13 shows the same "friction" phenomenon appearing in the tumbling tests. This uncertainty does not result from faulty operation of the automatic data printout equipment, which was continuously checked by strip-chart records of the table-tracking microsyn.* Additional evidence indicating that the phenomenon was characteristic of the gyro rather than of the test instrumentation is that gyro K-14 showed the same behavior, but not to a significant degree.

While the servo test is not particularly useful for determination of drift coefficients, it does simulate the behavior of the gyro as a stabilization device in a space-fixed coordinate system over long periods. For such an application, the gyro can be compensated as indicated by its previous performance. Figures G-3 and G-4 show the results of such "compensation" by comparing consecutive rotations of the servo test for each of the gyros. The figures show plots of the accumulated drift angle for a given number of hours from one run to the next, assuming that on the second run the gyro was perfectly compensated in accordance with the results of the first run. Although the figures indicate that K-13, while exhibiting greater randomness, is a better long-term space reference, it would not be safe to draw any such conclusions on the basis of a single set of servo tests.

This "compensated" servo data presented in Figures G-3 and G-4 is of primarily academic interest. Such compensation is much discussed but

*A microsyn rotor driven synchronously at counter earth's rate, thus permitting continuous comparison of the servo table position (microsyn stator) with the table-tracking rotor.

seldom applied, and has probably never been applied to MIG gyros. Results of gyro tests are presented in this form using the standard test procedure developed by MIT, and such data is therefore important for comparison of the performance of various gyros.

The time-consuming tests with IA vertical and IA horizontal were eliminated for gyro K-14 because of the lack of significant data from these tests on K-13.

II. COGGING TESTS

The cogging test is very similar to the servo test in that the gyro is used to control the servo table. In the cogging test, however, as the gyro and table rotate under the influence of earth's rate plus gyro errors, the time required for a rotation of 1 degree is accurately measured. The table is then torqued back to its starting position and allowed to drift through the same 1-degree angle while the time is measured once more. This process is repeated many times, and the results are compared. The time required for a rotation of 1 degree under the influence of earth's rate alone is known, so that the influence of gyro errors can readily be determined.

In the cogging tests for the MIG gyros, the 1-degree interval was timed 15 times for each of six different gyro positions. Tests were made with each axis vertical up and vertical down. ω_t was computed as the average of the 15 determinations of $3600/\delta t$. As was the case for the servo tests, $\omega_{IO} = \frac{+\omega_t}{-\omega_t} + \omega_\epsilon \cos \psi$, and since a_S and a_I are known the reaction torque and mass unbalance can be computed. Deviations from the average ω_t in each position are used to obtain $\delta\omega_{spread}$ and $\delta\omega_{rms}$.

The numerical results of the cogging tests are shown in Tables A-1 and A-2. Point-by-point plots of $\delta\omega$ are shown in Figures G-5 and G-6 from which it can be seen that the random drift is much greater for both gyros when the spin axis is horizontal (IA vertical). It can also be seen that $\delta\omega_{rms}$ is comparable for the two gyros and is consistently very low.

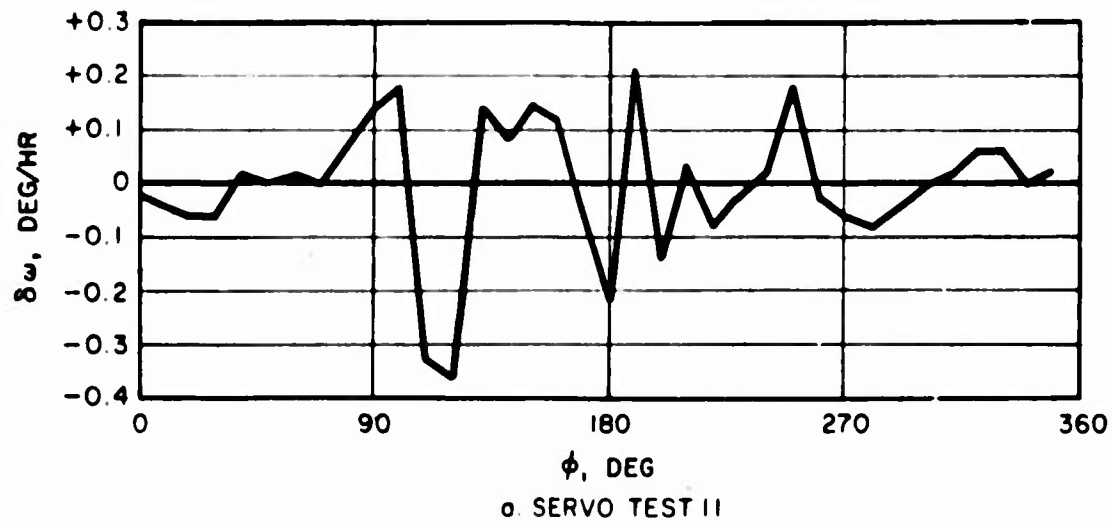

Figure G-1. Servo Test Data, Gyro K-13.

24 SEP 1959
IA HORIZONTAL
STANDARD EXCITATION

$A_0 - \omega_\epsilon \cos \beta = -0.02$ DEG/HR
$A_1 = -2.38$ DEG/HR
$B_1 = -0.09$ DEG/HR

$A_2 = -0.04$ DEG/HR
$B_2 = +0.27$ DEG/HR
$\delta\omega_{RMS} = 0.51$ DEG/HR

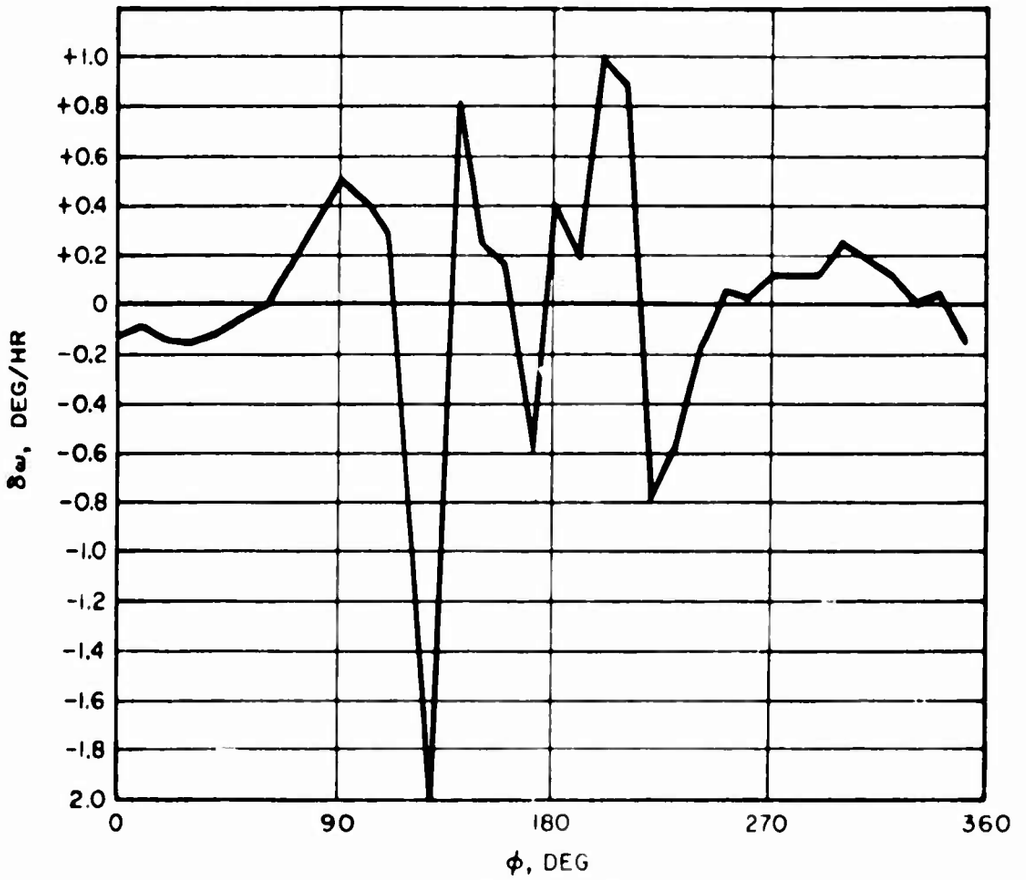

c SERVO TEST 13

24 SEPT 1959
IA VERTICAL
STANDARD EXCITATION

$A_0 - \omega_\epsilon \sin \beta = +2.54$ DEG/HR
$A_1 = +0.04$ DEG/HR
$B_1 = +0.22$ DEG/HR

$A_2 = +0.00$ DEG/HR
$B_2 = +0.01$ DEG/HR
$\delta\omega_{RMS} = +0.07$ DEG/HR

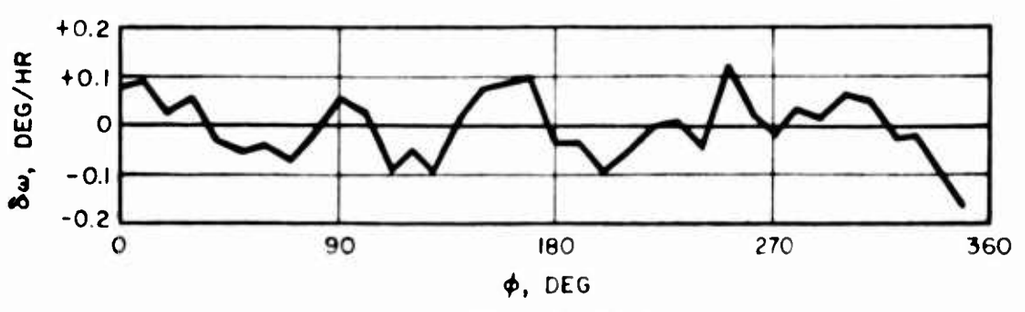

d. SERVO TEST 14

G0.29

Figure G-1. (Continued).

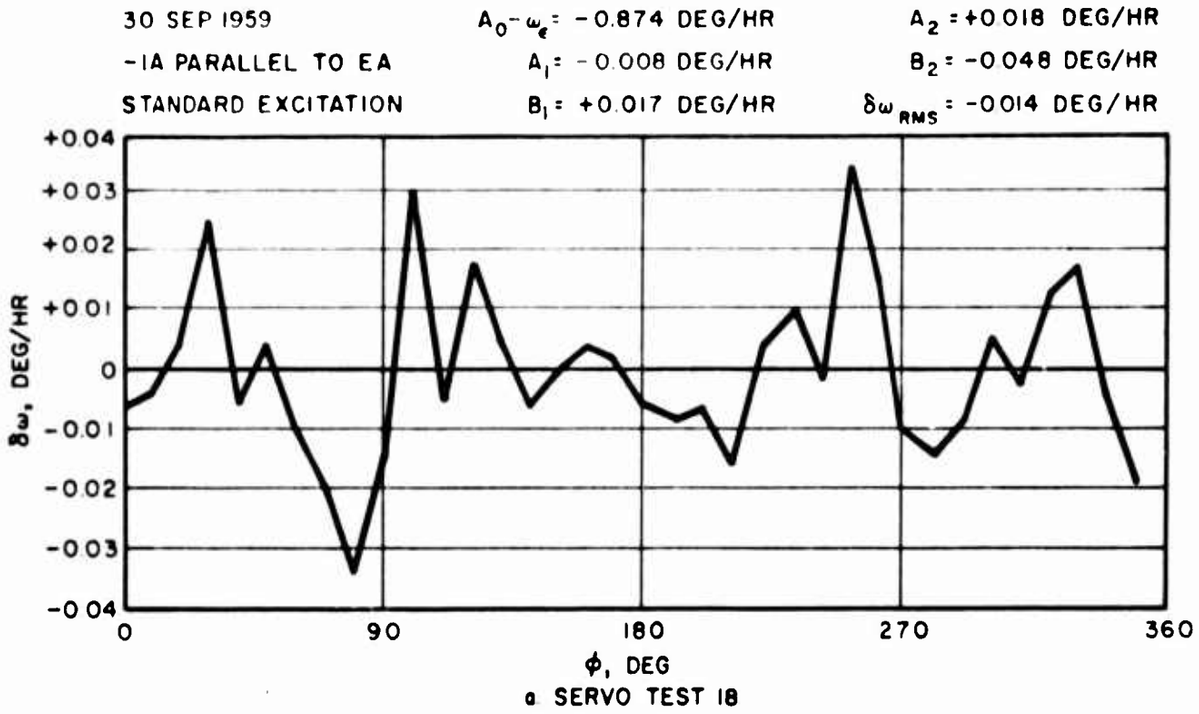

a. SERVO TEST 18

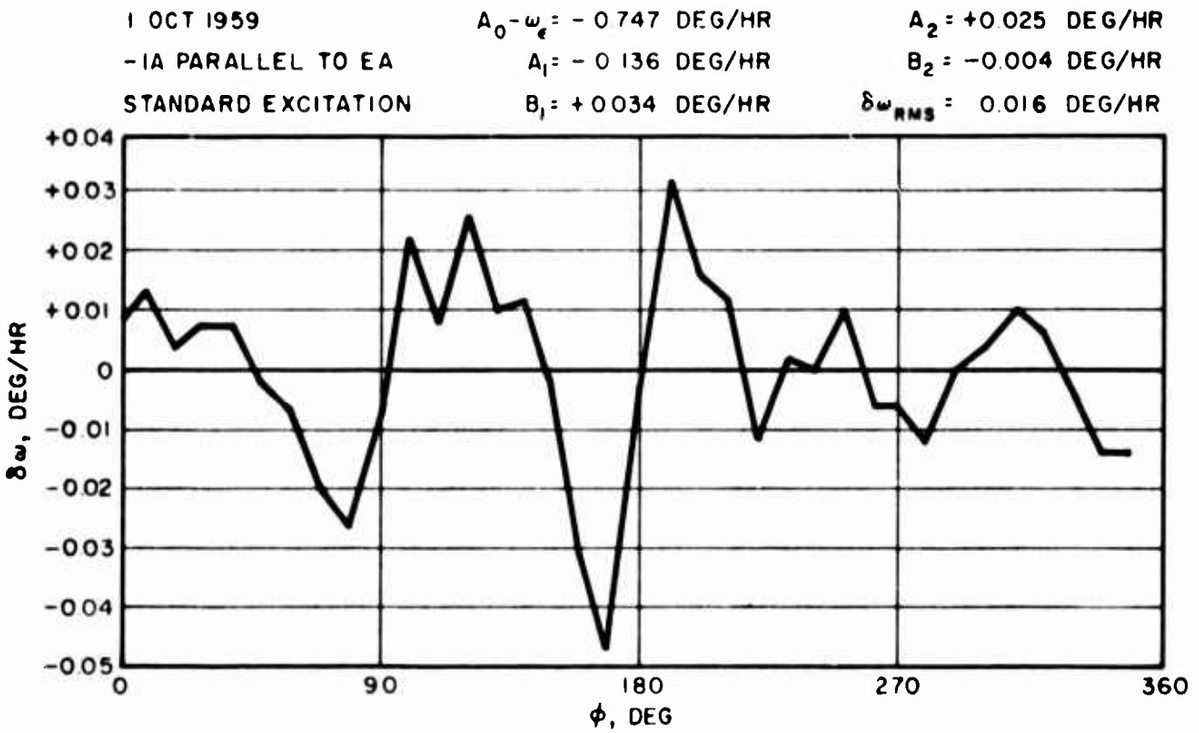

b. SERVO TEST 19

G030

Figure G-2. Servo Test Data, Gyro K-14.

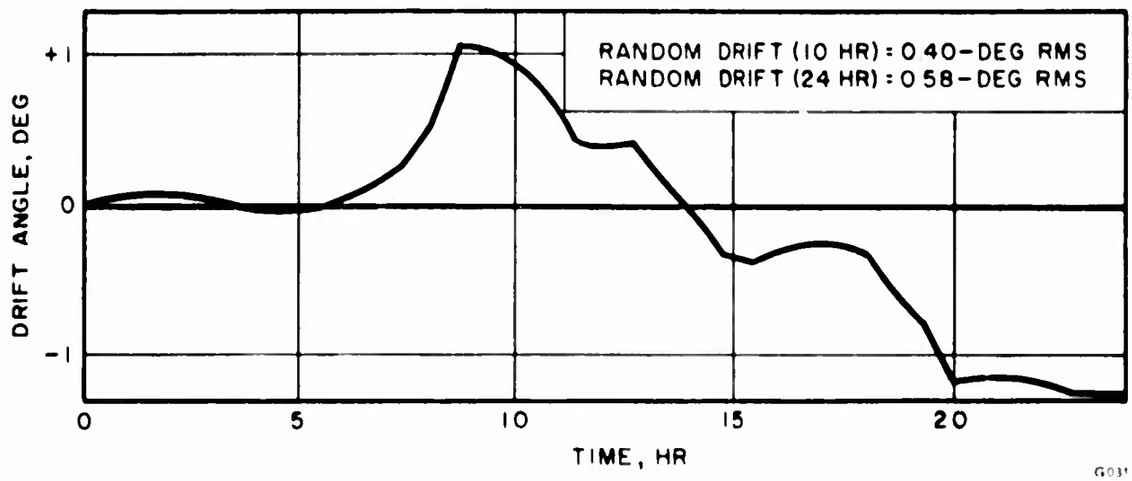

Figure G-3. Compensated Accumulated Drift Angle From Comparison of Servo Tests, Gyro K-13.

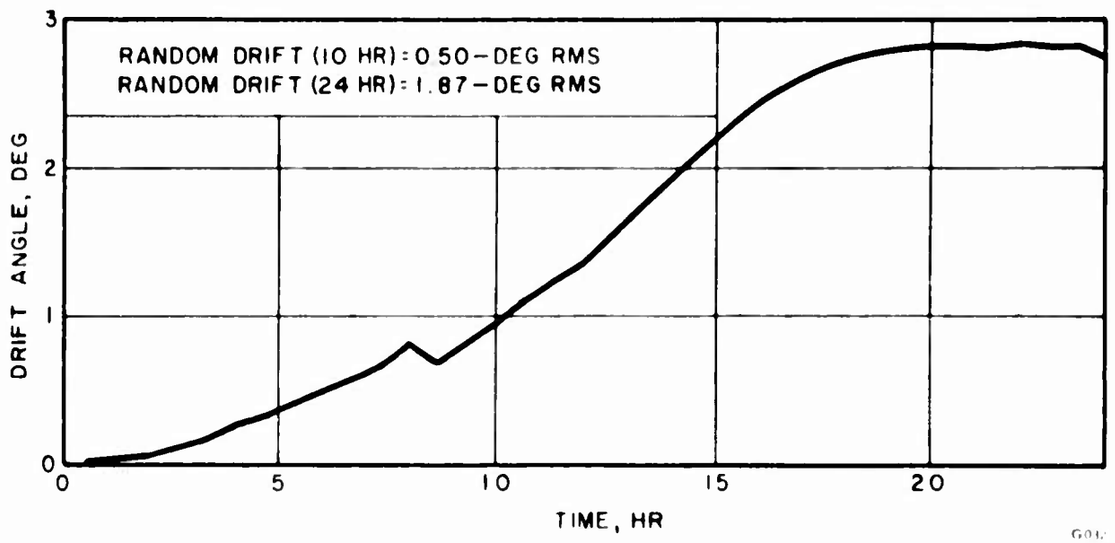

Figure G-4. Compensated Accumulated Drift Angle From Comparison of Servo Tests, Gyro K-14.

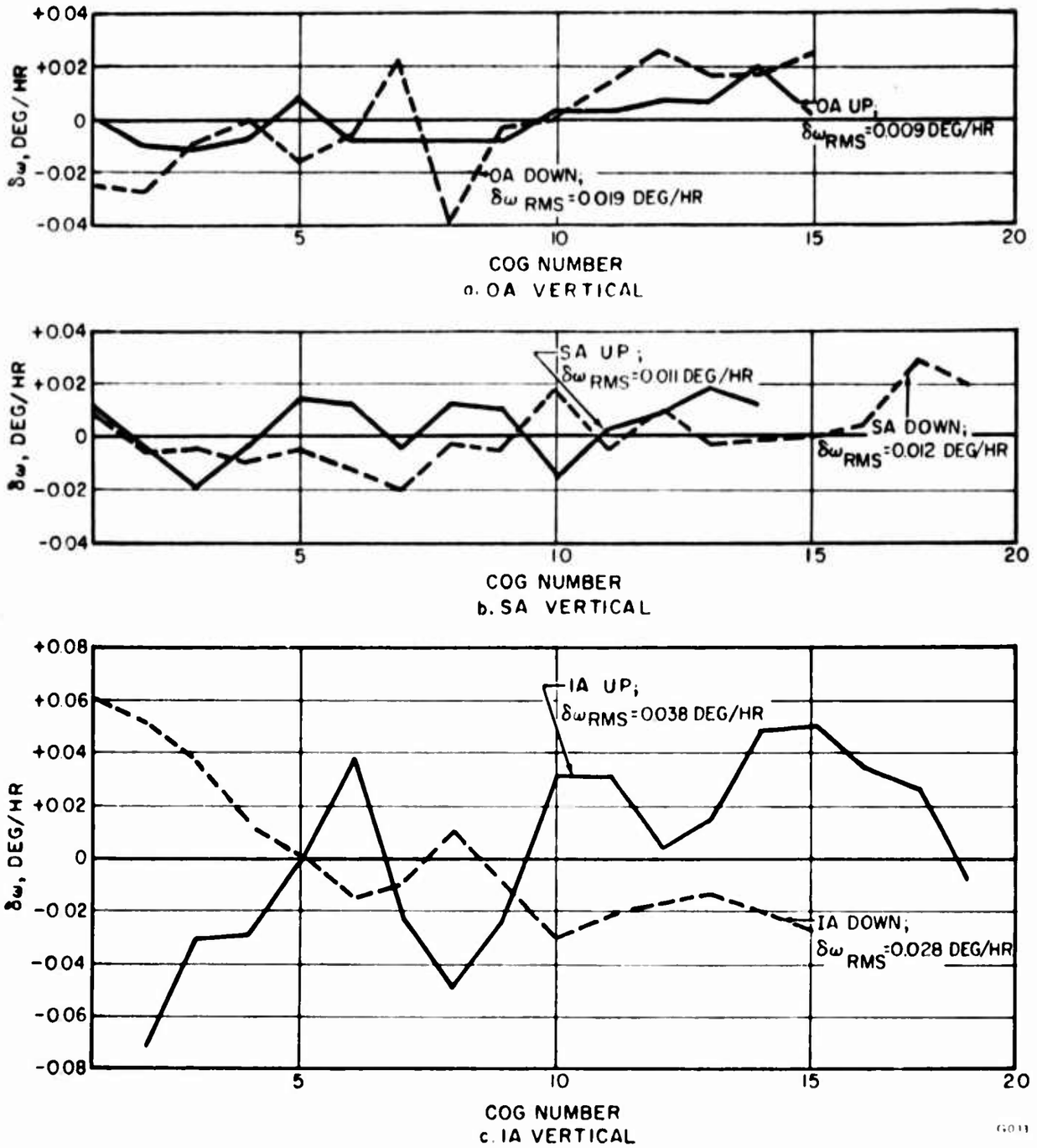

Figure G-5. Cogging Test Data, Gyro K-13.

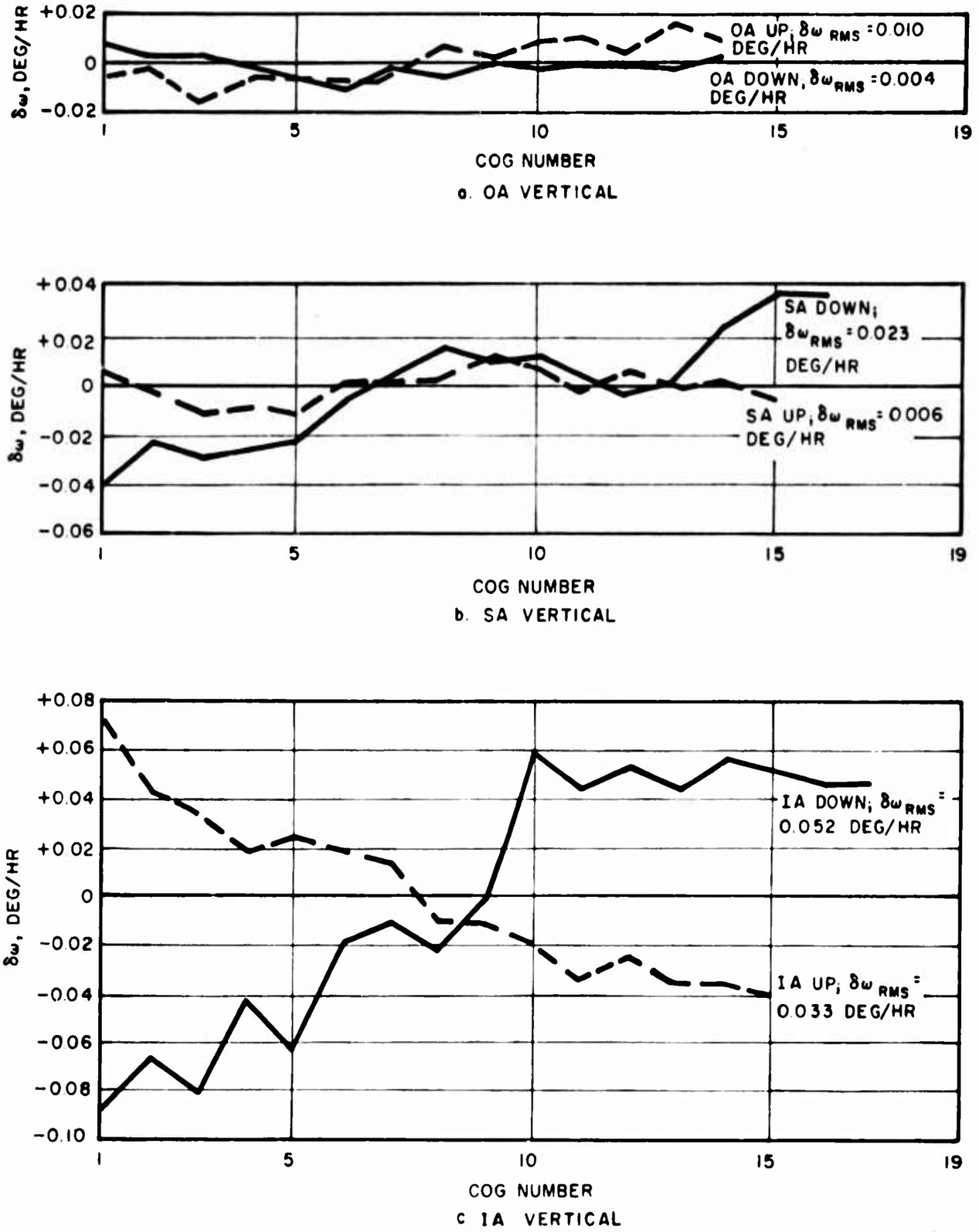

Figure G-6. Cogging Test Data, Gyro K-14.

APPENDIX H

VIBRATION TESTS

APPENDIX H

VIBRATION TESTS

I. TEST CONDITIONS

Excitation for all vibration tests was provided by the gyro test set.* The gyros were operated in torquer servo mode, with the acceleration along each axis monitored with an Endevco accelerometer and recorded on a Visicorder together with the torquer control current. The vibration exciter was an M-B model C-25H with Ling electronic drive. Unless otherwise noted, the direction of vibration was vertical.

II. SEARCH FOR RESONANCES

The resonance tests were similar to acceptance tests. A 5-g rms (limited to 0.4-inch double amplitude) sinusoidal vibration was applied along each axis (IA, OA, and SA). Frequencies from 8 to 2000 cps were swept for gyro K-13, and frequencies from 20 to 2000 cps were swept for gyro K-14. The sweep rate was 0.5 oct/min, resulting in a time of about 15 minutes for each sweep.

This test was made on gyro K-13 early in the test program, utilizing the three-axis holding fixture shown in Figure H-1. The Visicorder record of the test is reproduced in Figure H-2, from which the following observations can be made:

a. Wide excursions of i_c occurred at frequencies below 20 cps. The most likely explanation for the excursions is angular accelerations (wobbling) of the vibration exciter table.

b. Fixture resonances caused, at frequencies above 1000 cps, an apparent increase in the gyro anisoelastic drift.

---

*See Appendix B.

c. No significant gyro internal resonances were observed, except for the spin-motor rotor radial mass unbalance which was measured by slowing the sweep in the vicinity of 400 cps. Since

$$U_r = \frac{\sqrt{2}\, K_\omega\, \delta i_c}{a_S} = 2.3 \frac{\text{deg/hr}}{g} \quad ,$$

this radial unbalance could cause an uncertainty of this magnitude during wheel-off tests. Wheel-off tests are, chiefly for this reason, not useful.

d. External disturbances, such as closing the door of the shaker room, walking near the vibration exciter, or especially touching the exciter, appear clearly in the gyro output.

Large changes in gyro mass unbalance occurred during the test, causing K-13 to be out of specification (see Table A-1) on 19 August.

There were some changes in test techniques when the resonance test was performed on gyro K-14. The improved holding fixture shown in Figure H-3 was used (without the angle block). The servo gain was kept low to minimize noise on the recording of i_c. Recording and data reduction were simplified by recording demodulated accelerometer outputs. The frequency sweeps were started at 20 cps in order to eliminate the punishing excursions of the gimbal which probably caused the mass shift in gyro K-13.

Figure H-4 shows two sample sections of the Visicorder recording of the test of K-14. Because of the changes in technique, this test was much more satisfactory than that of K-13. Fixture resonances were small except for some peaks near 1300 cps (see Figure H-4), which were probably due to the long tie-down bolts through the holding fixture. The figures shown in Table A-2 for 5 November show that the gyro drift coefficients repeated within the expected accuracy of the eight-position mass unbalance tests conducted before and after the sinusoidal vibration sweeps.

III. RANDOM-FREQUENCY VIBRATION

Random-frequency vibration was applied to both gyros, using the improved holding fixture and the techniques described above for the sinusoidal vibration test of K-14. The specification was for a 20 to 2000-cps band of Gaussian noise, rolled off at 12 db/oct above 1000 cps. This vibration was to be applied to each axis at 1-, 2- and 5-g rms, with durations sufficient to allow the gyro to settle to its steady-state performance under the given acceleration. Exciter equalization was reached in 45 minutes at 1-g rms, as shown in Figure H-5.

Response of the gyros to random vibration was slight. The test at each amplitude for each axis was limited to 1 minute. Without vibration, the excursions of i_c were approximately 0.2 deg/hr peak-to-peak, increasing when vibration was applied. These excursions were somewhat greater for vibration along the spin rotation axis, reaching in one instance 2.3 deg/hr peak-to-peak, but with no average offset. The entries in Tables A-1 and A-2 for 4 and 5 November show that mass unbalance and reaction torques changed little as a result of this test.

IV. RANDOM PLUS SINUSOIDAL VIBRATION

With the improved holding fixture, the reduced torquer servo gain, and the same equalization as for the random vibration test, the gyros were vibrated at 2-g rms random plus 2-g sinusoid, swept at 1 oct/min. Vibration was applied along each of the gyro axes.

As in the previous tests, there were no significant resonances except for the spin-motor rotor mass unbalance. Otherwise the maximum excursion was about 3 deg/hr peak-to-peak in the vicinity of 20 cps, resulting probably from table wobble rather than from internal or servo resonances. The entries in Tables A-1 and A-2 for 5 November show that while K-13 was not much affected by this test, the mass unbalances on K-14 were considerably and permanently reduced, to the extent of over 1 deg/hr total change.

V. DETERMINING ANISOELASTIC COEFFICIENTS

A. Tumbling Under Vibration

The procedure for this test is outlined in Reference 1, and is an elaboration of a test conducted earlier by MIT. In brief, the gyro is placed with OA parallel to the earth's axis and rotated 360 degrees about OA in 15-degree increments. At each of the steps, the gyro is vibrated at a constant frequency and amplitude. This test has the unique capability of measuring separately all the anisoelastic coefficients while eliminating earth's rate torque from the data.

The test was performed on gyro K-13 at a vibration level of 10-g rms at 230 cps, using the fixture shown in Figure H-1. Torquer servo gain was low. High-speed recordings were made of i_c, a_S, a_I, and a_O, in order that instantaneous measurements might be made. Recordings were made at each increment with both the standard 10-g vibration and zero vibration.

The data was reduced by using a straightedge to draw an average line through the data points on the strip chart. The average of several such determinations was used for any one point. The quantity $K_\omega \delta i_c / a_{SI}^2$ was then subjected to a harmonic analysis versus the angle of rotation about OA (φ).

The results of this test on gyro K-13, appearing in Table A-1 under 16-21 September, were discouraging. The standard deviation and spread in terms of deg/hr-g^2 swamp the measured anisoelastic coefficients and render them worthless. Several factors contributed to the failure of this test:

1. It was run on three separate days with three complete shut-downs, and was further interrupted by some failures of laboratory circuit breakers.

2. The data was taken at high recording speed, so that only a few seconds of data could be sampled

3. Only one vibration amplitude was used at each increment of rotation.

4. i_c was recorded only before and during vibration, but not afterward.

5. The recorder factor for i_c was too low (2 in./ma).

6. The three-axis holding fixture may not have been sufficiently rigid.

7. The source for i_p was a transistorized constant current source which was not adequately stable or ripple-free.

8. Gyro K-13's previously noted characteristic friction was exhibited.

9. Of perhaps the greatest importance, there was no shielding to protect the gyro from the stray magnetic field of the vibration exciter.

The measurement of the K coefficients, described separately in sections B and C below, was successfully carried out on gyro K-13, reviving hope that a meaningful tumbling test could be made. The test plan was accordingly modified, and careful preparations made for the testing of K-14. The improved holding fixture (Figure H-3) was used, mounted on a solid block and protected by a 0.030-inch-thick-mu-metal shield. Figure H-6 shows the orientation of the gyro axes for this test. A Kintel M10 A 10 meter calibrator was used as a current source for i_p. The recording speed was reduced to 24 in./min and the scale factor to 10 in./ma. Accelerometer outputs were demodulated. Recordings were made for 1 minute at each g level, beginning with 0 g and proceeding to 6 g, 8 g, 10 g, and back to 0 g for each increment of ϕ. These increments were made 22.5 degrees, as dictated by the spacing of inserts on the angle block. All data was taken on the same day.

Figure H-7a shows sections of the strip-chart recording taken from the points where the vibration g level was changed, thus illustrating the variations resulting from the change in acceleration. Reduction of the data was performed. First, the data points from the Visicorder

recording were tabulated, the g^2 sensitivity computed and a least-squares fit made. A sample tabulation and computation for the data at ϕ = 22.5 degrees is shown in Figure H-7b. The slope of the straight line obtained was then harmonically analyzed according to the formula given on page 21 of Reference 1 in order to obtain the anisoelastic coefficients.

A graphic illustration of the test results appears in Figure H-7c, where a few of the measurements obtained for various angles of ϕ are plotted.

The coefficients determined in this way show a remarkable consistency, as indicated by the entries in Table A-2 for 6 November. The standard deviation of 0.0015 deg/hr-g^2 is less than 1/10 of the measured value of K, and of the same order of magnitude as the minor compliances $K_{SI}/2$, $K_{IS}/2$, and $K_{SO}/2$. A second technique for measuring $K_{SI}/2$ and $K_{IS}/2$, described in section C below, substantially confirms the values obtained in this test.

B. Measurement of $\frac{K_{SS} - K_{II}}{2}$

This test was performed on gyro K-13 only, using the improved holding fixture and techniques described in section A above. The method used is described in Reference 1 as Method II and is the commonly accepted method of measuring K under vibration (see References 3, 4, 9, and 10). The direction of vibration is at right angles to OA and at 45 degrees to IA and SRA. Vibration is applied at levels of 0-, 4-, 6-, 8-, and 10-g rms. A frequency of 230 cps was used for the test of K-13.

In reduction of the data, the slope of the best line for $K_\omega \delta i_c$ versus a_{SI}^2 is equal to

$$K + \frac{(K_{SI} - K_{IS})}{2} .$$

The latter factor is usually considered negligible. The method of least squares of $\delta\omega$ was used to fit a line to $K_\omega \delta i_c$ versus a_{SI}^2, as shown in Figure H-8. The test data was consistent and meaningful, yielding results which showed the gyro to be within specification, as indicated in Table A-1 under 21 September.

C. Measurement of $\frac{K_{IS}}{2}$ and $\frac{K_{SI}}{2}$

This test, described in Reference 1 (pp. 23-25), consists of vibrating the gyro in a horizontal direction parallel to IA and then parallel to SRA, with OA vertical in both cases. The test was performed for K-14 only, making use of the horizontal vibration facility of the environmental laboratory and otherwise using the same improved fixtures and techniques described in section A above. The horizontal vibration facility consists of a low concrete pier with a leveled metal top on which an aluminum slab is supported by a film of oil. The vibration exciters can be tilted to a horizontal position and connected to the aluminum slab which serves as the vibrating table.

For this test, the gyro holding fixture was attached to the slab, which was vibrated by the M-B C-10 vibration exciter. Recordings of i_c were made at levels of 0-, 6-, 8-, 10-, and 0-g rms for 40 seconds at each level. The vibration frequency was 225 cps

The slope of the resulting line was computed, as in the preceding test, for a least-squares fit of $\delta\omega$. The formulas of Reference 1 were used to compute $K_{IS}/2$ and $K_{SI}/2$. Results are shown in Table A-2 under 6 November. They corroborate the results obtained with the tumbling tests under vibration and show an rms drift for the 10 measurements, which is the lowest encountered in the entire test program except for cogging tests.

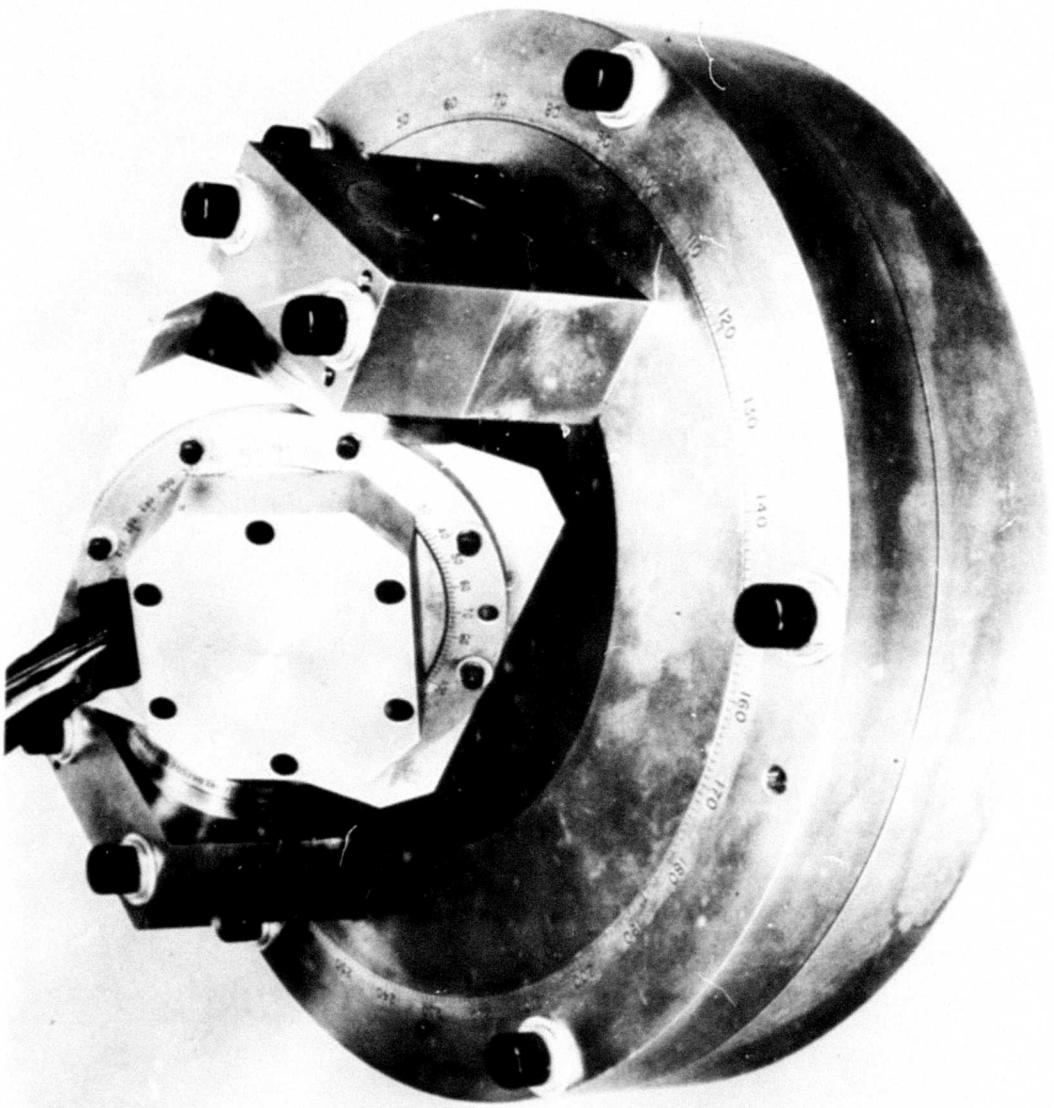

Figure H-1. Three-Axis Holding Fixture for Environmental Testing.

BLANK PAGE

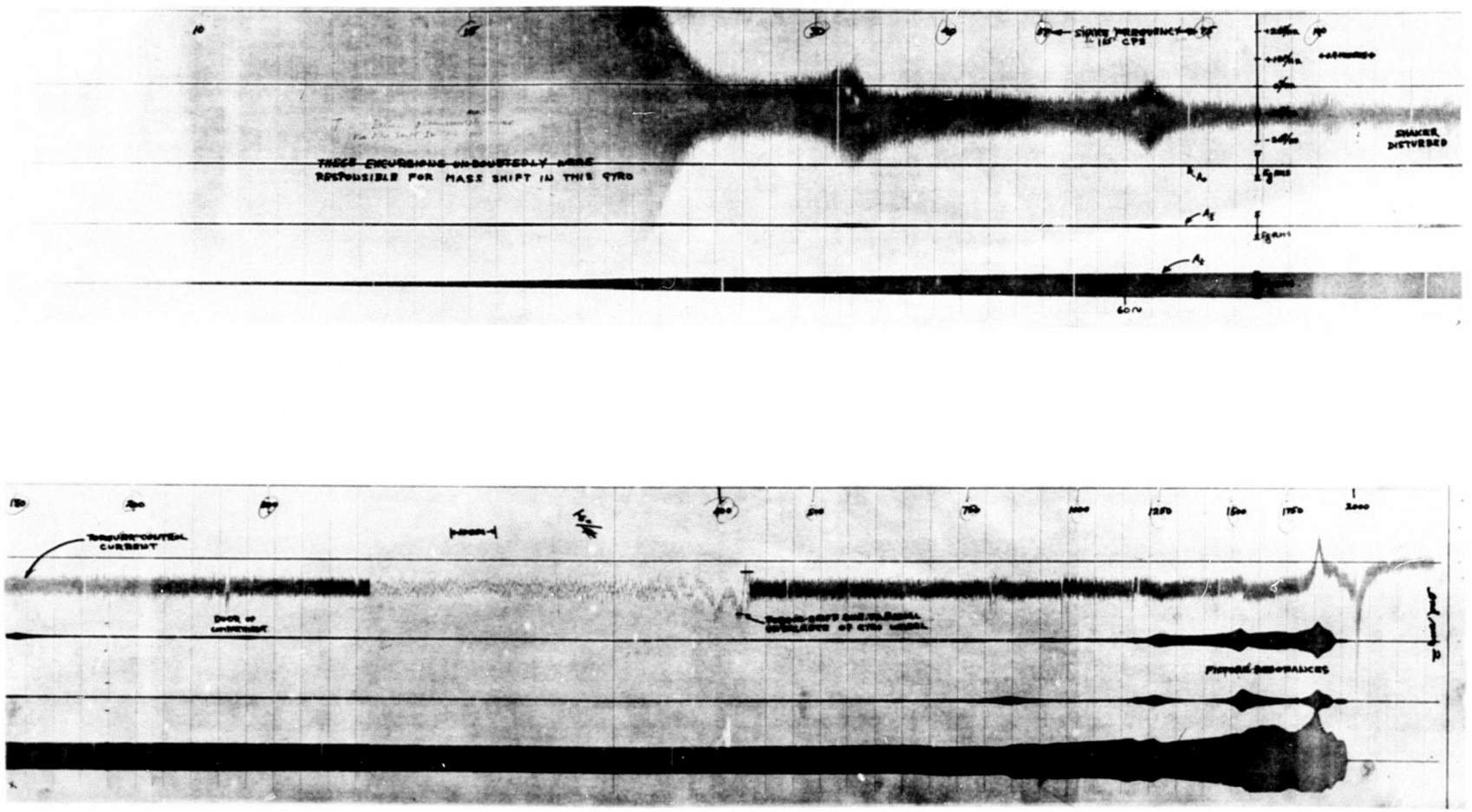

Figure H-2. Environmental Testing Torquer Control Current and Acceleration Versus Frequency, Gyro K-13.

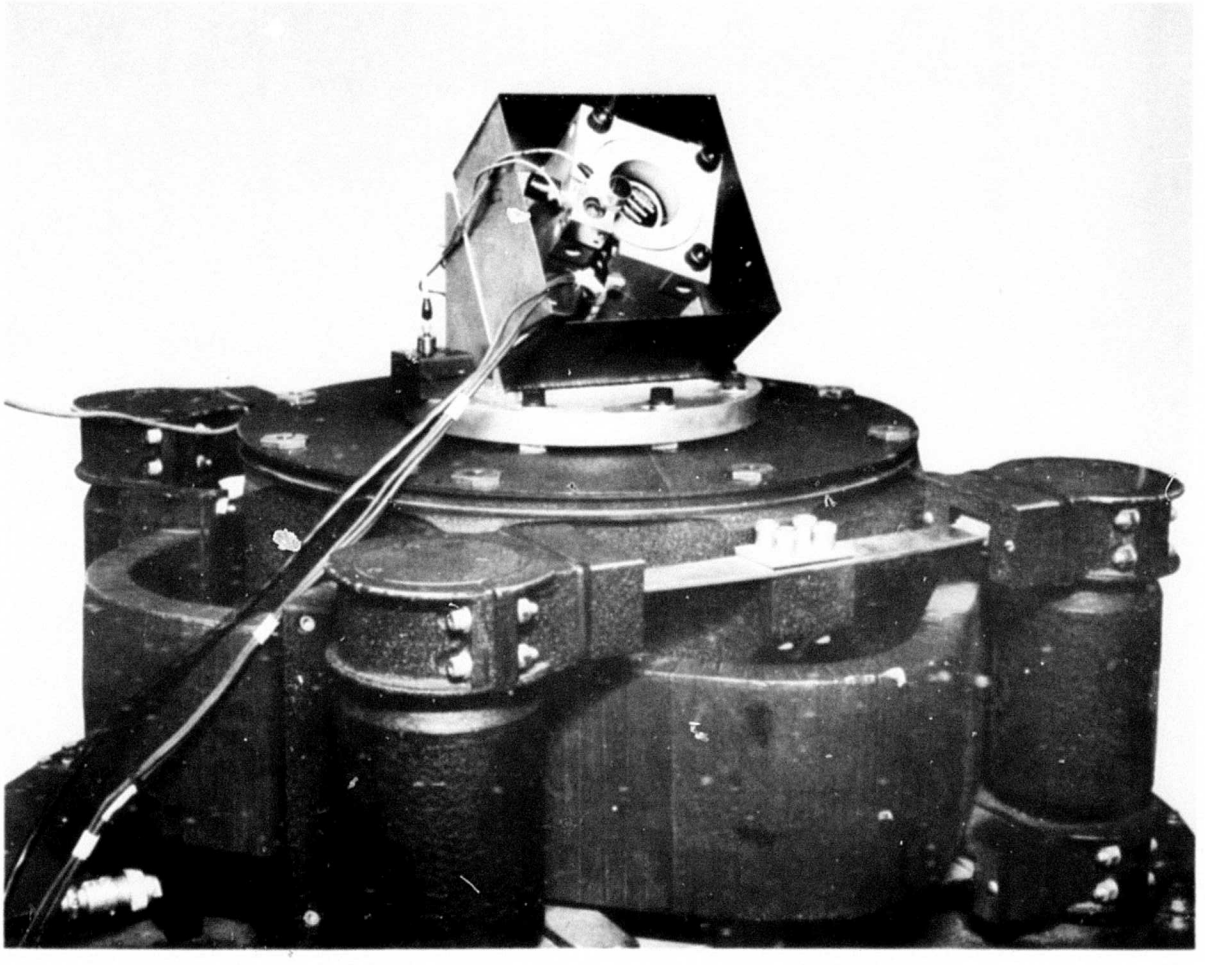

Figure H-3. MIG Gyro Mounted on C25H Vibration Exciter.

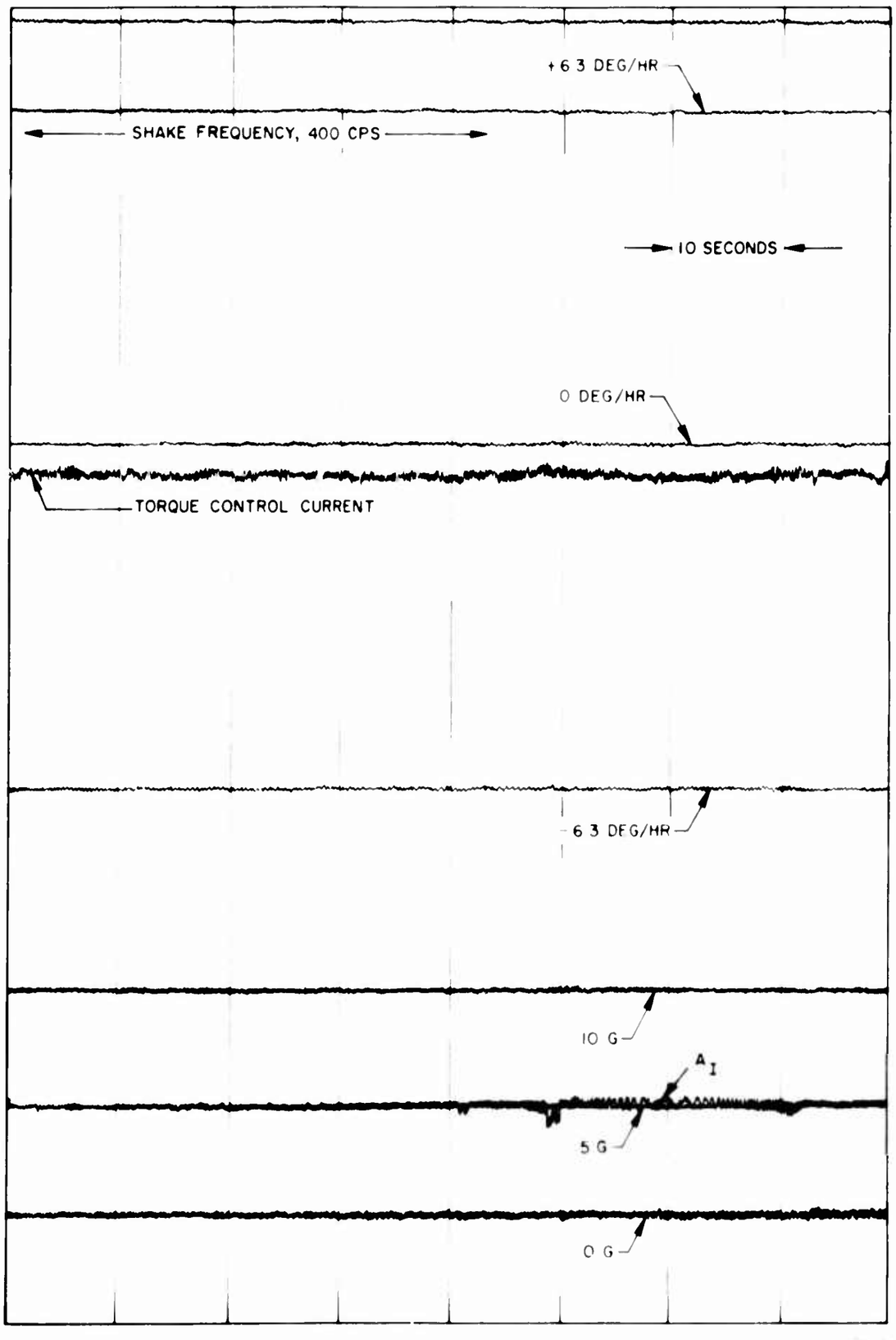

Figure H-4. Environmental Testing Torquer Control Current and Acceleration Versus Frequency, Gyro K-14.

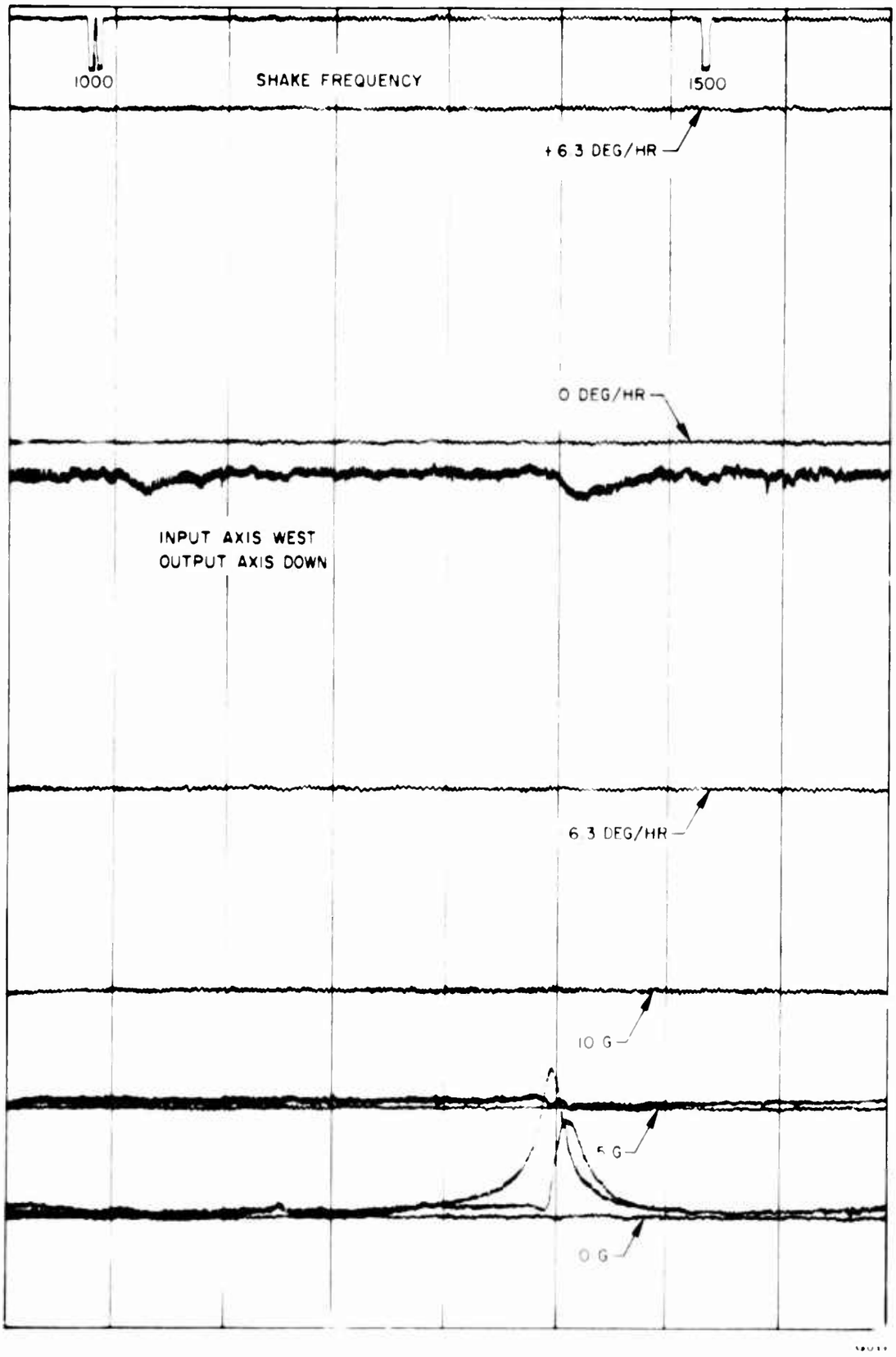

Figure H-4. (Continued).

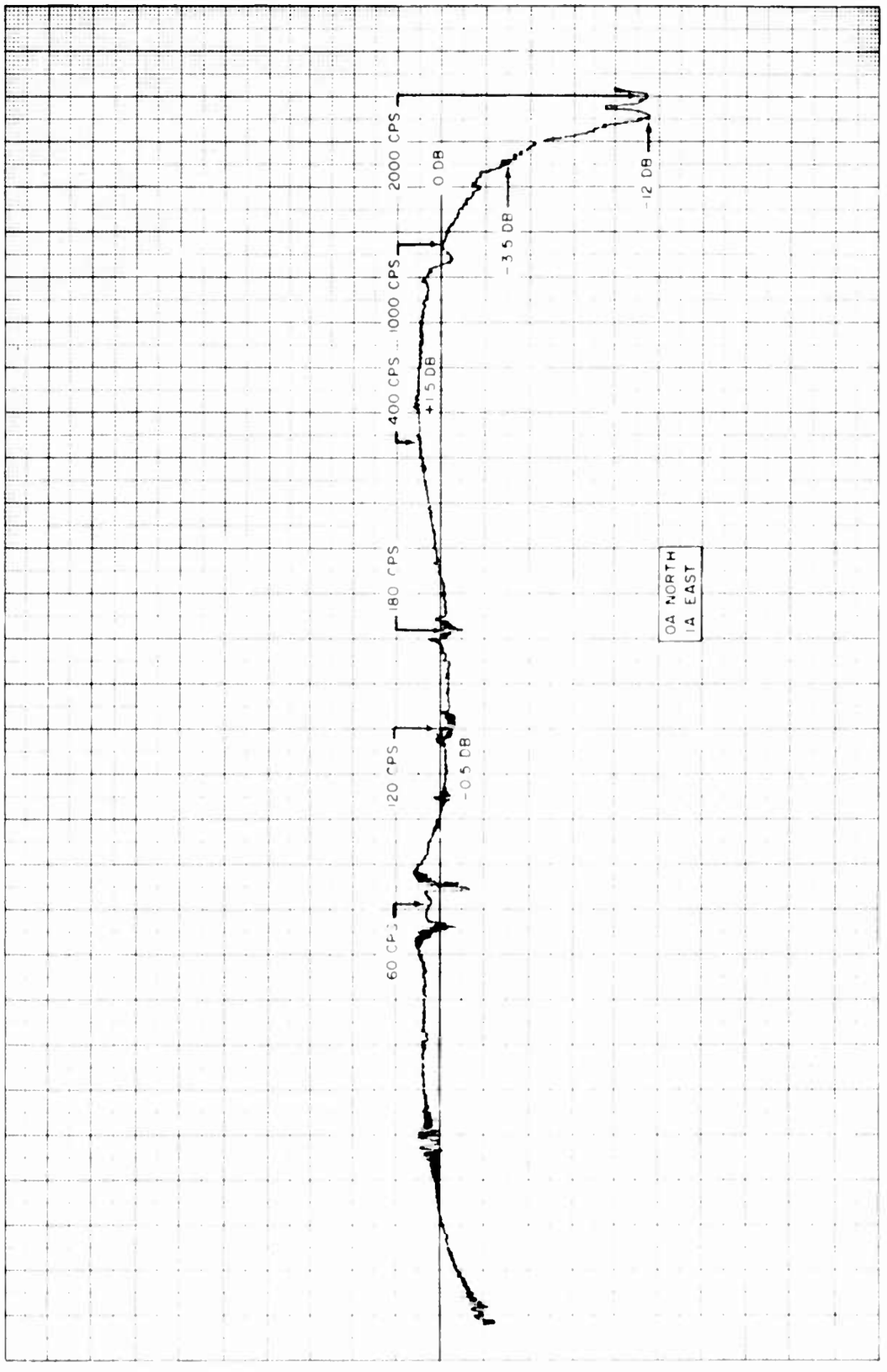

Figure H-5. Vibration Exciter Equalization for Random Vibration Tests, Gyro K-13.

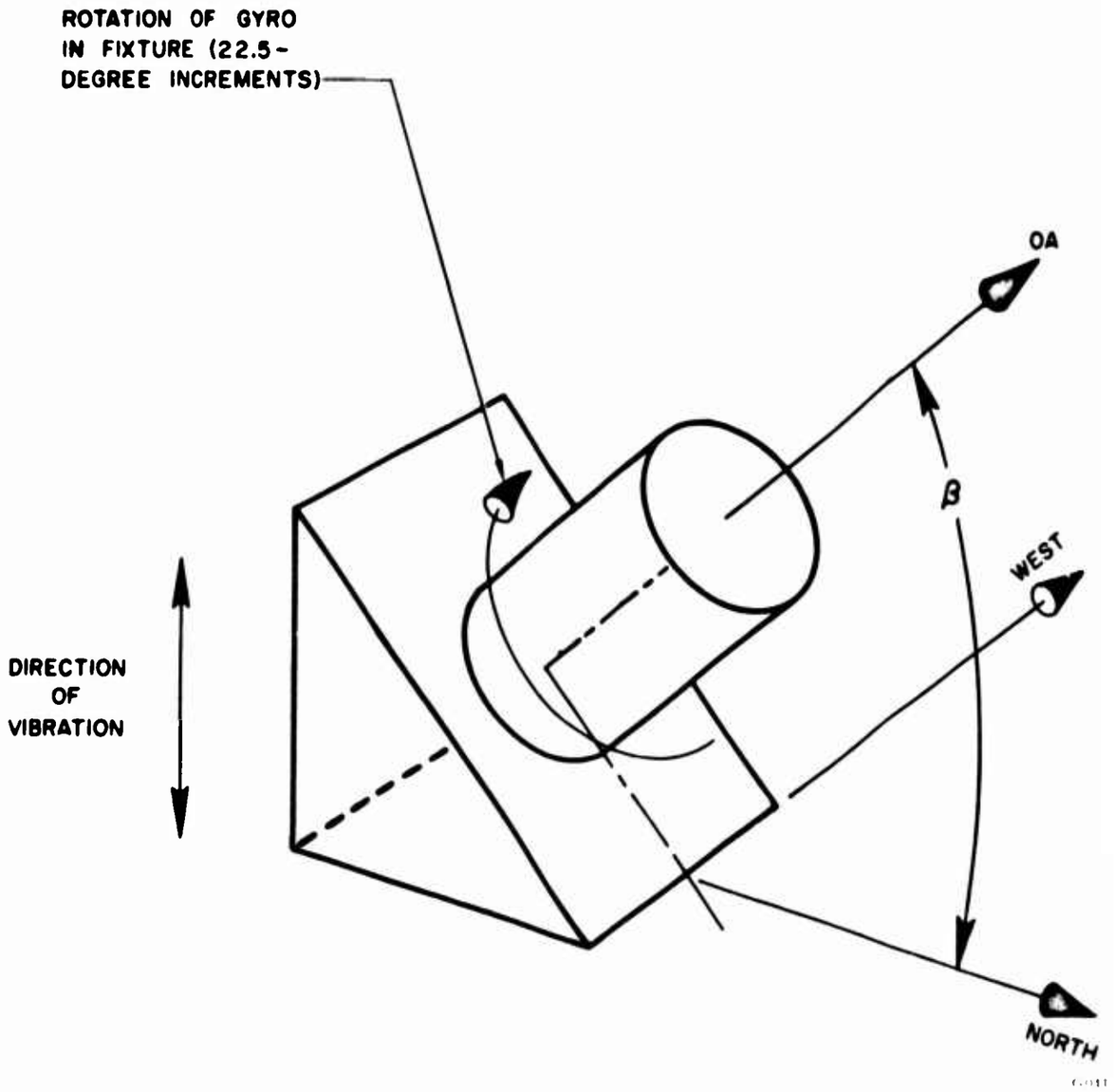

Figure H-6. Orientation of Gyro Axes for Vibration Tests.

112
98

BLANK PAGE

FRAMES

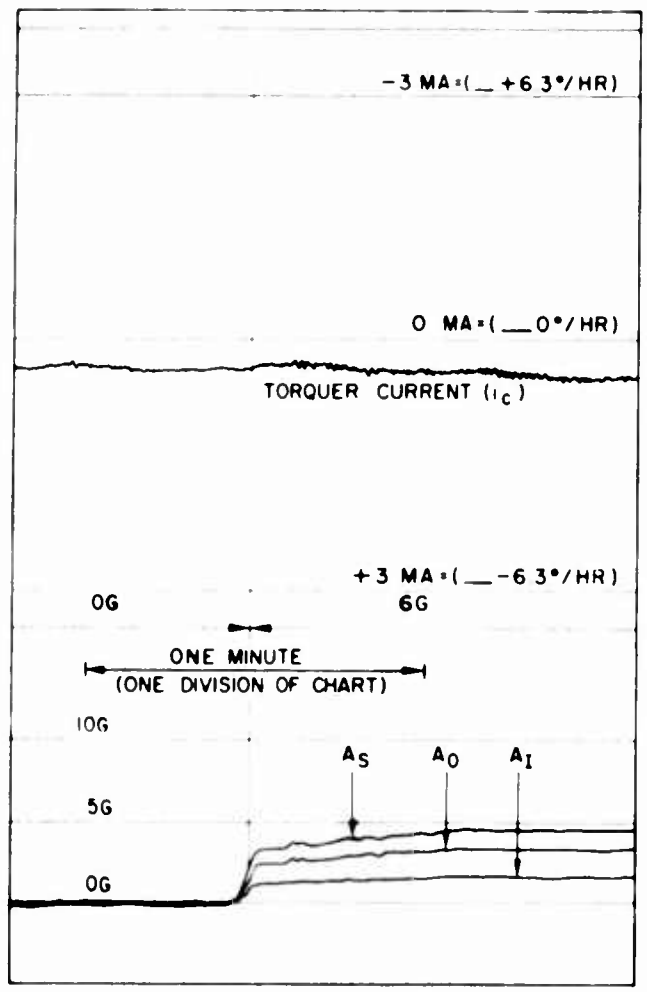

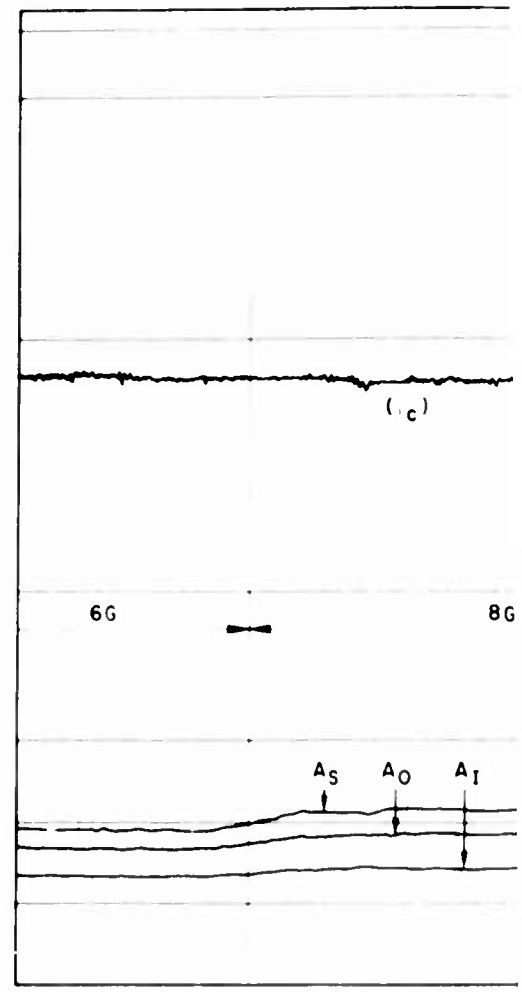

a SECTIONS FRON

a,G	a_S,G	a_I,G	$a^2_{\ ,}$,G^2	i_c,MA	δi_c,MA	$\delta\omega$,DEG/HR	$\frac{\delta\omega}{a^2_{SI}}$
0	—	—	—	+0 033	—	—	
6	4.6	1.7	24.1	+0 046	+0 013	−0 272	C
8	5.9	2 2	39 6	+0 055	+0 022	−0 460	C
10	7 6	2 8	65 6	+0 068	+0 035	−0 731	C
0	—	—	—	+0 033	—	—	

NOTE 0 0113 $\frac{\text{DEG / HR}}{G^2}$ WAS I OF I6 DATA POINTS TO WHICH

b SAMPLE DATA REDUCTION

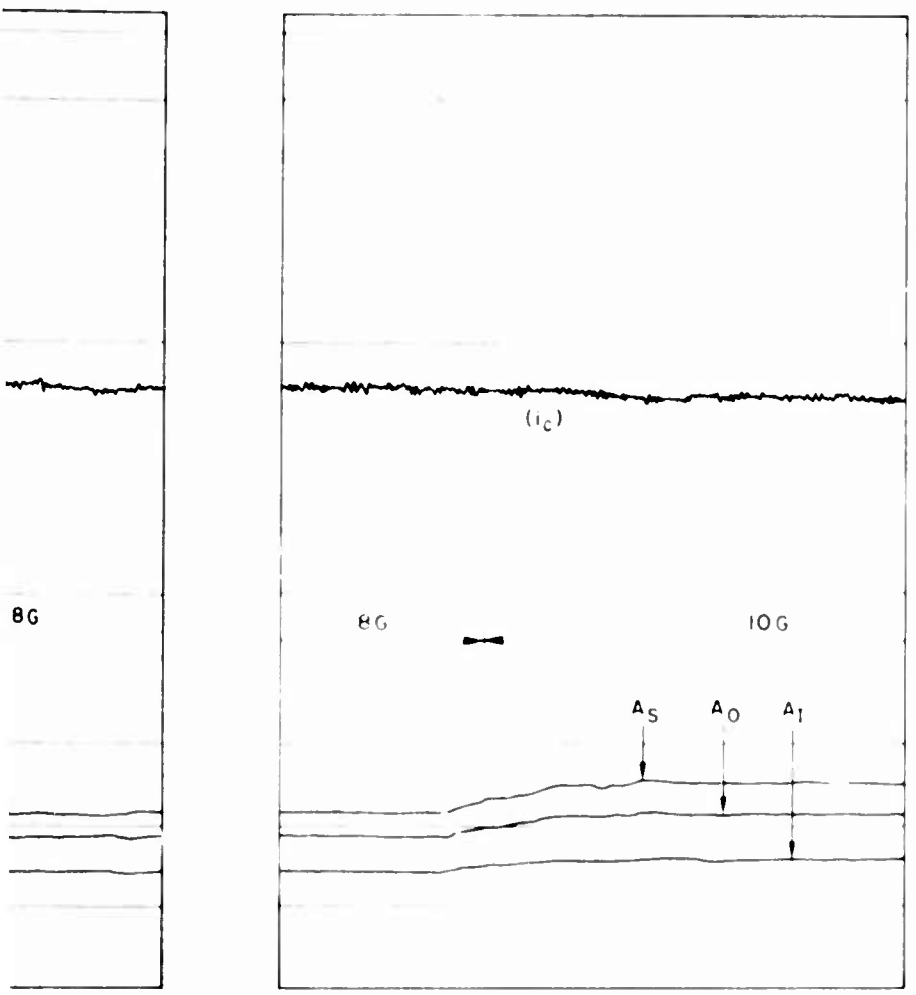

ROM STRIP – CHART RECORDING OF VIBRATION TEST

$\delta\omega$, DEG/HR / G^2	$\frac{\delta\omega}{\sigma_{SI}^2}$, LEAST SQUARES
—	
0.0113	
0.0116	0.0113 $\frac{\text{DEG/HR}}{G^2}$
0.0111	
—	

CH A FOURIER SERIES WAS FIT

ON

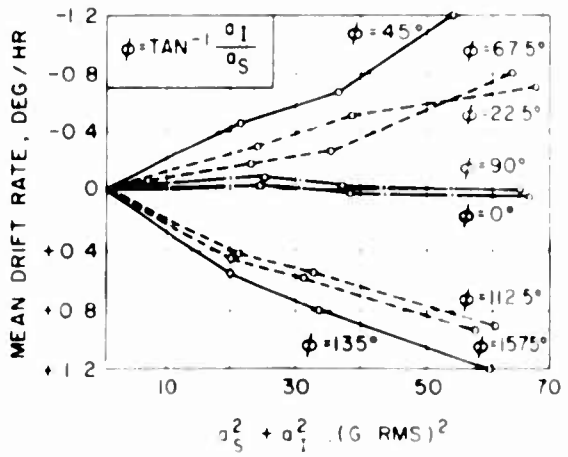

c PLOTS OF TEST RESULTS

Figure H-7. Typical Vibra
Results, Gyro F

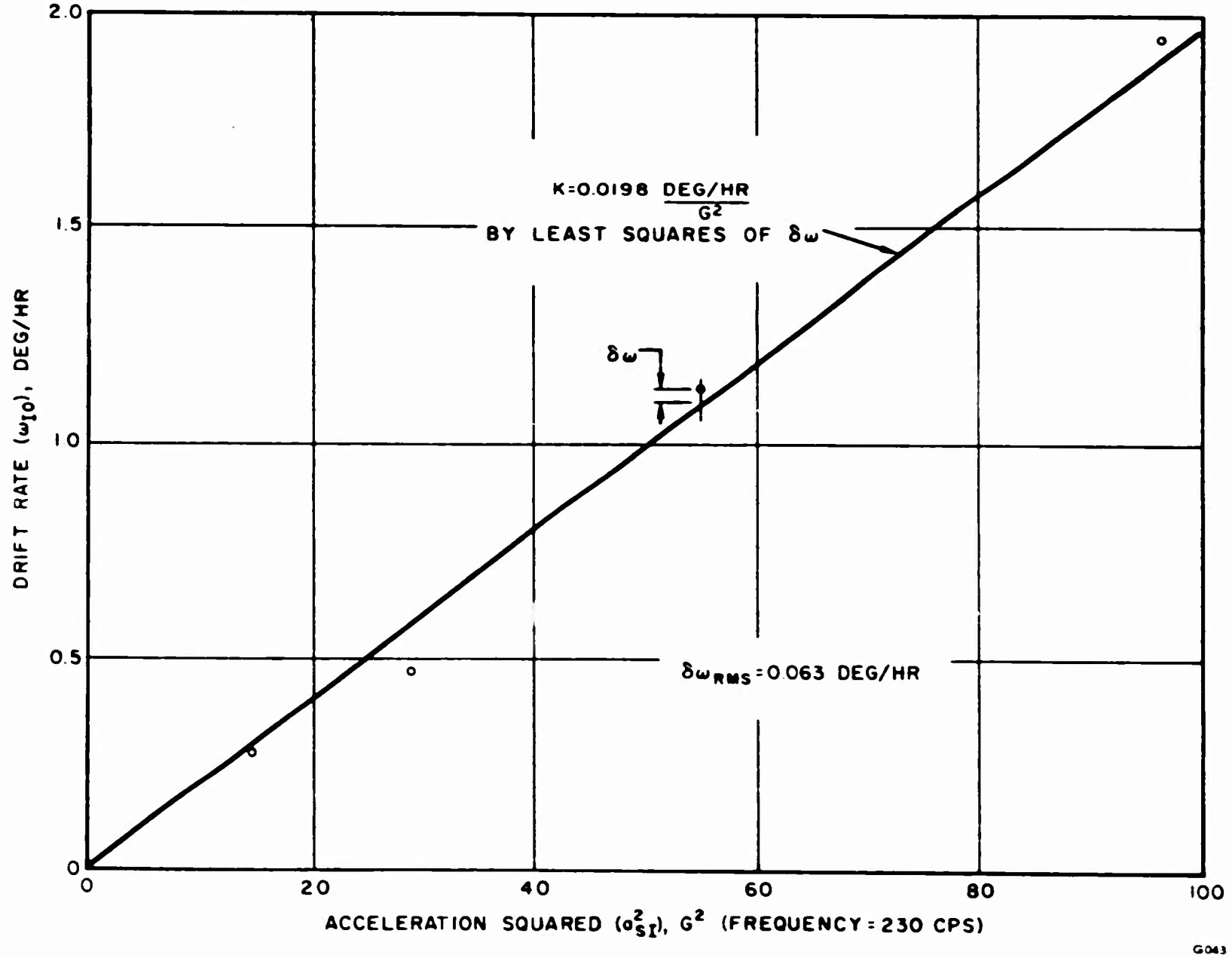

Figure H-8. Drift Rate Due to Vibration at 45 Degrees to IA and SRA, Gyro K-13.

REFERENCES

1. Evans, B. H. "Inertial Laboratory Test Plan No. 6. MIG Test Plan." Space Technology Laboratories, Inc., GM 43.8-396, 17 August 1959.

2. Roberts, H. A., et al. "A Guide for Testing the Miniature Integrating Gyro (MIG) GG49." Minneapolis-Honeywell Aeronautical Division, Document U-ED9788, 24 January 1958.

3. Durkee, R. P. "Descriptive Material, Miniature Integrating Gyro (MIG)." Minneapolis-Honeywell Aeronautical Division, Document U-ED9789," 14 February 1958.

4. Durkee, R. P., et al. "Preliminary Descriptive Material, Miniature Integrating Gyro Family." Minneapolis-Honeywell Aeronautical Division, Document U-ED9804, 17 December 1958.

5. Denhard, W. G. "Laboratory Testing of a Floated, Single-Degree-of-Freedom, Integrating, Inertial Gyro." Massachusetts Institute of Technology, Report R-105, Parts I, II, and III, September 1956. (C)

6. Eiselen, E. T. "Equations for Evaluation of SDF Gyro Drifts During Vibration and Acceleration." Space Technology Laboratories, Inc., 12 September 1958.

7. Grubin, C. "Three Dimensional Rotational Dynamics of the Single Axis, Floated, Integrating Gyroscope." Space Technology Laboratories, Inc., TM-59-0000-00408, November 1959.

8. Clark, R. B "A Survey of Current Gyro Testing Practices as Applicable to Inertial Guidance for Ballistic Missiles." Space Technology Laboratories, Inc., unpublished, 17 June 1959.

9. "Military Specification, Gyroscope, Inertial, Testing Procedures For." MIL-G-26369, 23 May 1958.

10. Scoville, A. "Vibration Test of MIT HIG-4 Unit." Massachusetts Institute of Technology, Report E-513, 1 December 1955.

11. Baxter, A. "A Method for Evaluating Floated Rate Integrating Gyros." Gyrodynamics Division, Kearfott Company, Inc.

12. Denhard, W. G., et al. "Annual Progress Report of the Inertial Gyro Group for October 1, 1957 to September 30, 1958." Massachusetts Institute of Technology, Report R-184, 30 September 1958. (S)

REFERENCES (Continued)

13. Fellows, W. E. "Vibration Effects on Gyroscopes and Accelerometers." Minneapolis-Honeywell Aeronautical Division, Document R-ED29004-1A, 31 October 1958.

14. "Jet Propulsion Laboratory Detail Specification Miniature Integrating Gyroscope." Jet Propulsion Laboratory, Specification No. 14030 Change B, 15 April 1958. (C)

15. "The M-2516 Floated Rate Integrating Gyro." Gyrodynamics Division, Kearfott Company, Inc., Technical Product Description GTO-10630, June 1959.

16. "A Handbook on Floated Integrating Gyros." Reeves Instrument Corporation, RICO 207 6583M, 1958.

17. "Sperry Floated Integrating Gyro SYG-500." Air Armament Division, Sperry Gyroscope Company, Publication No. CA-60-0001, 3M, November 1959.

DISTRIBUTION

STL

B.R. Ackerson
N.S. Bers
H. Brady
D.W. Brotemarkle
R.C. Brown
J.R. Burnett
R.C. Carden
W.J. Clark
J.C. Clegg
B.H. Evans (10)
T.A. Fuhrman
R.L. Gates
A.B. Graybill
R.G. Halliday
G.A. Harter
J. Heilfron
J. Hinsley
I.M. Holliday
L.K. Jensen (10)
J.A. Joseph
H.R. Judge
R.D. Kennedy
F.P. Klein
J.H. Koontz
H.A. Lassen
H.D. Lakin
T.W. Layton
L.K. Lee
H. Low
R.W. McKeand
G.R. Mohler
D.F. Meronek
R.C. Peters
E.I. Reeves
E.J. Robb
A. Robinson
W.T. Russell
C.W. Sarture
B. Spanier
W.J. Tallon, Jr.
F.C. Thurston
D. Vrabec
D.T. Wallace
D.W. Whitcombe
R.K. Whitford
H.Y. Wong
STL Library (5)
STL Corporate File

AFBMD

Lt Col F.M. Box
Lt Col R.A. Duffy
Maj H.S. Croyts
Maj W.W. Martin
Maj R.B. Savage
Capt W.J. Delaney
Capt R.W. Mitchell
Capt R.R. Rath

Space Technology Laboratories, Inc., P.O. Box 95001, L.A. 45, Calif. PERFORMANCE EVALUATION OF THE MIG GYRO FOR BALLISTIC MISSILE APPLICATIONS, by R.B. Clark and B.H. Evans. 117 p. illus. tables (Project Plan; ______) (STL/TN-60-0000-09112; ______) (Contract AF 04(647)-309)

Unclassified Report

This report describes a series of tests performed on two Minneapolis-Honeywell MIG gyros. Performance of the gyros during the tests is given in detail, and the philosophy, procedures, and merits of each type of test are discussed. The test program had two objectives: to evaluate the gyros themselves, and to study and compare the various types of tests used in the program.

Both of the tested gyros performed within the manufacturer's specifications during the entire program, with the exception of a mass shift occurring in one gyro as a result of excessive vibration applied dur-
(over)

UNCLASSIFIED

UNCLASSIFIED

Space Technology Laboratories, Inc., P.O. Box 95001, L.A. 45, Calif. PERFORMANCE EVALUATION OF THE MIG GYRO FOR BALLISTIC MISSILE APPLICATIONS, by R.B. Clark and B.H. Evans. 117 p. illus. tables (Project Plan; ______) (STL/TN-60-0000-09112; ______) (Contract AF 04(647)-309)

Unclassified Report

This report describes a series of tests performed on two Minneapolis-Honeywell MIG gyros. Performance of the gyros during the tests is given in detail, and the philosophy, procedures, and merits of each type of test are discussed. The test program had two objectives: to evaluate the gyros themselves, and to study and compare the various types of tests used in the program.

Both of the tested gyros performed within the manufacturer's specifications during the entire program, with the exception of a mass shift occurring in one gyro as a result of excessive vibration applied dur-
(over)

UNCLASSIFIED

UNCLASSIFIED

Space Technology Laboratories, Inc., P.O. Box 95001, L.A. 45, Calif. PERFORMANCE EVALUATION OF THE MIG GYRO FOR BALLISTIC MISSILE APPLICATIONS, by R.B. Clark and B.H. Evans. 117 p. illus. tables (Project Plan; ______) (STL/TN-60-0000-09112; ______) (Contract AF 04(647)-309)

Unclassified Report

This report describes a series of tests performed on two Minneapolis-Honeywell MIG gyros. Performance of the gyros during the tests is given in detail, and the philosophy, procedures, and merits of each type of test are discussed. The test program had two objectives: to evaluate the gyros themselves, and to study and compare the various types of tests used in the program.

Both of the tested gyros performed within the manufacturer's specifications during the entire program, with the exception of a mass shift occurring in one gyro as a result of excessive vibration applied dur-
(over)

UNCLASSIFIED

UNCLASSIFIED

Space Technology Laboratories, Inc., P.O. Box 95001, L.A. 45, Calif. PERFORMANCE EVALUATION OF THE MIG GYRO FOR BALLISTIC MISSILE APPLICATIONS, by R.B. Clark and B.H. Evans. 117 p. illus. tables (Project Plan; ______) (STL/TN-60-0000-09112; ______) (Contract AF 04(647)-309)

Unclassified Report

This report describes a series of tests performed on two Minneapolis-Honeywell MIG gyros. Performance of the gyros during the tests is given in detail, and the philosophy, procedures, and merits of each type of test are discussed. The test program had two objectives: to evaluate the gyros themselves, and to study and compare the various types of tests used in the program.

Both of the tested gyros performed within the manufacturer's specifications during the entire program, with the exception of a mass shift occurring in one gyro as a result of excessive vibration applied dur-
(over)

UNCLASSIFIED

UNCLASSIFIED

Unclassified Report

ing a **test.** Results of different tests of the same gyro characteristics correlated within the expected consistency of gyro performance, indicating satisfactory reliability of the test procedures and equipment.

UNCLASSIFIED

UNCLASSIFIED

Unclassified Report

ing a **test.** Results of different tests of the same gyro characteristics correlated within the expected consistency of gyro performance, indicating satisfactory reliability of the test procedures and equipment.

UNCLASSIFIED

UNCLASSIFIED

Unclassified Report

ing a **test.** Results of different tests of the same gyro characteristics correlated within the expected consistency of gyro performance, indicating satisfactory reliability of the test procedures and equipment.

UNCLASSIFIED

UNCLASSIFIED

Unclassified Report

ing a **test.** Results of different tests of the same gyro characteristics correlated within the expected consistency of gyro performance, indicating satisfactory reliability of the test procedures and equipment.

UNCLASSIFIED

UNCLASSIFIED